https://dspace.org/

Definition of the Halogen Bond IUPAC Recommendations 2013 A Revisit

Pradeep Varadwaj; A Varadwaj; Helder Marques; K Yamashita

https://hdl.handle.net/10539/42220
WOS

Downloaded from a DSpace repository. https://dspace.org/

CRYSTAL GROWTH & DESIGN

pubs.acs.org/crystal

Article

Definition of the Halogen Bond (IUPAC Recommendations 2013): A Revisit

Pradeep R. Varadwaj,* Arpita Varadwaj, Helder M. Marques, and Koichi Yamashita

Cite This: *Cryst. Growth Des.* 2024, 24, 5494−5525

Read Online

ACCESS | Metrics & More | Article Recommendations

ABSTRACT: This Article revisits the "Definition of the Halogen Bond (IUPAC Recommendations 2013)" [Desiraju, G. R. et al. *Pure Appl. Chem.* **2013**, *85* (8), 1711−1713], recommendations that fail to include the fundamental, underlying concept of (electrophilic) σ- and p-/π-hole theory and orbital-based charge transfer interactions that accompany halogen bond formation. An electrophilic σ-hole, or p-/π-hole, is an electron-density-deficient region of positive polarity (and positive potential) on the electrostatic surface on the side of halogen along, or orthogonal to, a covalently bonded halogen in a molecular entity that leads to the development of a noncovalent interaction—a halogen bond—when in close proximity to an electron-density-rich nucleophilic region on the same or another identical or different molecular entity, with which it interacts. This Article re-examines the characteristic features of the halogen bond and lists a wide variety of donors and acceptors that participate in halogen bonding. We add caveats that are essential for identifying halogen bonding in chemical systems, necessary for the appropriate use of the terminologies involved. Illustrative examples of chemical systems that feature inter- and intramolecular halogen bonds and other noncovalent interactions in the crystalline phase are given, together with a case study of some dimer systems using first-principles calculations. We also point out that the π-hole/belt (or p-hole/belt) that may develop on the surface of a halogen derivative in halogenated molecules may be prone to forming a π-hole/belt (or p-hole/belt) halogen bond when in close proximity to nucleophiles on another similar or different molecular entity.

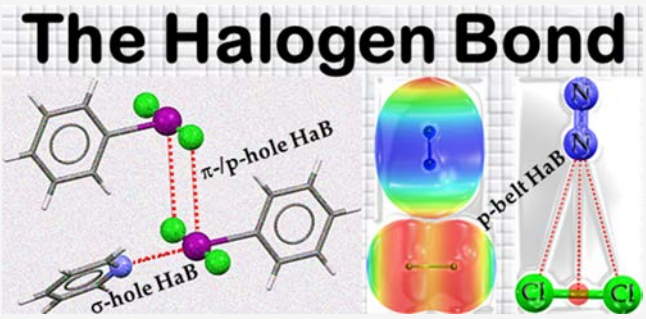

Downloaded via UNIV OF THE WITWATERSRAND on July 4, 2024 at 11:42:23 (UTC).
See https://pubs.acs.org/sharingguidelines for options on how to legitimately share published articles.

■ INTRODUCTION

Noncovalent interactions are a broad family of attractive interactions that occur locally in many chemical systems.[1−8] They are important in the supramolecular assembly and shaping of crystals in the solid state and are categorized into different flavors based on their character and the identity of the chemical elements that participate in their formation. These interactions are chemical synthons of variable strength, from very weak to a strength comparable to that of a coordinate bond, or indeed a covalent bond.[9−14] Their strength is determined based on the nature of the participating electron-density-donating and electron-density-accepting molecules/fragments/atoms.[15] They are players in the formation of dimers, trimers, tetramers, oligomers, and supramolecular systems. They often feature directional properties, but not (always) when they are the forced consequence of a true (primary) interaction(s).

Weak noncovalent interactions are weak forces that typically occur between neutral molecular entities, while stronger interactions appear when one of the participating sites (electron density donor) has a negative charge (a polarity opposite to that of the electron density acceptor). The former interactions in the gas-phase have been investigated using a variety of spectroscopic techniques (*e.g.*, rotational,[16,17] vibrational,[18,19] and anion photoelectron spectroscopy[20] and mass spectrometry[21]), whereas strongly bonded interactions are ion−molecule or ion-pair adducts that have been reported primarily in the crystalline phase. Although chemical reactions are widely understood as a result of the making and breaking of chemical bonds,[22] noncovalent interactions, while generally weaker than covalent bonds, also develop during the course of a chemical reaction. They cause the assembly of molecular entities at surfaces, leading to the formation of stable materials with applications in optoelectronics, catalysis, and sensing.[23]

The recently proposed definition of a pnictogen bond (PnB)[24] states that these are "*weak attractive interactions* between an electrophilic region on a pnictogen atom in a molecular entity (wherein the pnictogen is involved in other stronger bonds) and a nucleophilic region in another, or the

Received: February 15, 2024
Revised: May 18, 2024
Accepted: May 20, 2024
Published: June 24, 2024

ACS Publications © 2024 American Chemical Society

same, molecular entity". (A molecular entity is defined as "any constitutionally or isotopically distinct atom, molecule, ion, ion-pair, radical, radical ion, complex, conformer, etc., identifiable as a separately distinguishable entity"[25]). This definition is misleading given that PnBs are not and cannot always be regarded as "*weak attractive interactions*", since they can be of the van der Waals type, weak, strong, or even very strong depending on the energy strength of the interaction.[9] For example, the pnictogen bond in [$X_3Sb\cdots F^-$ (X = F, Cl, Br)] should not be regarded as a weak interaction given it comprises an appreciable amount of covalency.[9] This is applicable to halogen bonds as well,[12,15] considering that they feature a variety of bond strengths.

The experimental and computational recognition of inter- and/or intramolecular noncovalent interactions formed by elements of groups 14−17 of the periodic table in chemical systems, especially when they behave as electrophiles, has gained significant momentum over the past decade. Revised definitions, characteristic features, footnotes, and illustrative examples containing electron density donors and acceptors have been proposed. These noncovalent attractive interactions have been termed tetrel bonds (TtBs), group 14;[10,26,27] pnictogen bonds (PnBs), group 15;[28−30] chalcogen bonds (ChBs), group 16;[31−33] and halogen bonds (XBs), group 17.[2,34,35] This classification is useful to identify how an element of a particular group behaves in maintaining an attractive engagement but with a specific name, as unambiguously demonstrated by Cavallo and workers in their unique piece "Naming interaction from the electrophilic site".[36] Clearly, integrating all types of noncovalent interactions into three classes (σ-hole interactions,[37−39] π-hole interactions,[40,41] and p-hole interactions[42−44]) does not allow us to determine which specific element, and from which specific group of the Periodic Table, is involved in the formation of a specific type of noncovalent interaction. The subdivision of the noncovalent interactions based on the elements in a group acting as an electrophile, *e.g.*, phosphorus bond (group 15), allows one to unequivocally capture the noncovalent bond formation ability, as well as the chemical reaction profile, of that specific element (for example, "fluorine chemistry"[45] or "iodine chemistry"[46]).

Halogen bonds were often abbreviated as XBs,[2,3,14,47−49] although recently the abbreviation HaB has come into use.[50−54] Formal definitions became desirable with the increasing appreciation of the significance of noncovalent interactions in areas as diverse as crystal engineering, chemistry; physics; molecular biology; crystallography; and polymer, supramolecular, medicinal, and materials sciences, among others.

The definition of the hydrogen bond (HB) was revised in 2011, accompanied by a series of characteristics and features.[55] A similar definition was subsequently applied to elements of groups 14−17. For instance, when transferred to HaBs, PnBs, and ChBs, the definition proposed for HBs was virtually unchanged (except for obvious terms such as halogen/chalcogen atom or halogen/chalcogen bond), yet the number of characteristics were significantly reduced without any in-depth explanation, and the original literature featuring the characteristics of HaBs and ChBs was not referenced. Therefore, the semi-formal definitions and characteristics of HaB[34] and ChB[31] still require a revisit.

The concepts underlying the electrophilic nature of σ-[37,56,57] or π-holes[41,58,59] have greatly assisted as umbrella terms in recognizing the occurrence of noncovalent interactions in many chemical systems.[57,60−62] These holes generally appear on the electrostatic surfaces of molecular or arene moieties along or orthogonal to the outer extensions of covalently bonded atoms, respectively. This distinctive conceptual framework[39,56,63−67] surprisingly has been overlooked as a possible characteristic of HaBs[34] and ChBs,[31] although it has been widely applied for the rationalization of these noncovalent interactions. We briefly incorporated the underlying concept of σ- and π-holes in our recently proposed definitions of PnB[28] and TtB.[26] Subsequent to our proposals for PnB, the IUPAC working group proposed a definition of the PnB that incorporated these concepts.[24] Therefore, given the importances of these concepts in many studies focusing on noncovalent interactions, it is apparent that the previously proposed IUPAC definitions and characteristic features of the halogen and chalcogen bonds may be incomplete without the inclusion of the concept of an electrophilic σ-hole and an electrophilic π-/p-hole (or even π-/p-belt).

An electrophilic σ-hole appears in a region on the electrostatic surface of an atom A in a molecule R−A (where R is the remainder part of the molecular entity), which has been attributed to be the result of an anisotropy of the atom's charge density distribution.[39] It is not only electron-density-deficient (and associated with a positive electrostatic potential) but also appears on the side of A opposite to the outer extension of a covalent or coordinate bond, where A is, for example, a tetrel, pnictogen, chalcogen, or halogen derivative. A visual representation of the electron-density-deficient (electrophilic) and electron-density-rich (nucleophilic) regions (green/cyan/blue and red, respectively) on the electrostatic surface of covalently bonded halogen atoms in some simple molecules is presented in Figure 1. It is this electrophilic σ-hole on the halogen atom in molecules that has the capacity to act as a HaB donor (HaBD) in sustaining an attractive noncovalent engagement when in close proximity to the negative (nucleophilic) site on an interacting partner entity that acts as an HaB acceptor (HaBA).

Occasionally an electrophilic π-/p-hole (π-/p-belt) may be observed in halogen-containing molecules.[68,69] The halogen atom in molecules such as FCN and FCCCN is entirely electrophilic, *i.e.*, both the lateral and axial portions of the electrostatic surfaces of fluorine in these molecules are electrophilic.[68] The lateral portions of the electrostatic surface arise from the p-type orbitals; they are deficient in electron density. Past studies[68,70,71] have demonstrated that the axial regions generally have a larger electrophilicity than the lateral regions and are prone to the formation of halogen bonds with nucleophiles when in close proximity. This concept is also applicable, for instance, to oxygen-centered ChBs,[11,72] as well as triel and aerogen bonds.[176] For example, there are two positive regions on the outer surface of boron in BF_3 that appear orthogonal to the B−F bond, caused by its empty p-type orbital. One might refer to them either as π-holes or p-holes.[43,73] The π-/p-belt appears around covalent bonds, while the π-hole may appear on the surface of covalently bonded atoms or in the junction region of a pair, or array, of atoms in a molecular entity. Some have called the π-/p-belt around a covalent bond a "π-ringhole",[29,59] although what is present is not a "hole" but rather a "π-/p-belt". Interestingly, both σ- and π-holes in molecular entities have been experimentally observed using Kelvin probe force microscopy.[74,75]

The definition and features discussed in the IUPAC paper defining the HaB overlook the importance of the noncovalent bonding capacity of the heaviest halogen, astatine (At). When in molecules, At has the capacity to participate in simple and supervalent halogen bonding interactions with nucleophiles in

https://doi.org/10.1021/acs.cgd.4c00228
Cryst. Growth Des. 2024, 24, 5494−5525

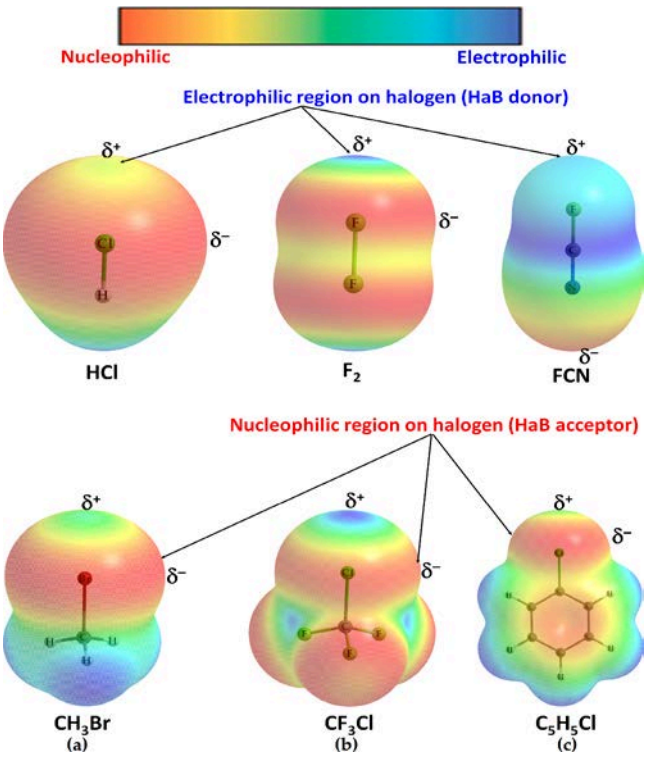

Figure 1. Visual representation of the electrophilic and nucleophilic regions (δ^+ and δ^-, respectively) on the electrostatic surface of a halogen atom in some simple molecules. Top, from left: HBr, F_2, and FCN. Bottom, from left: CH_3Br, CF_3Cl, and C_6H_5Cl. The electrophilic regions (δ^+) on the halogen atom on the side of X opposite to the extension of the R−X (X = halogen) covalent bonds are typically referred to as (positive) σ-holes, which may be involved in attractive engagements with the nucleophilic regions on the surface of the interacting partner molecules to form halogen bonds. R is the remaining part of the molecule. The most electrophilic and nucleophilic regions are colored blue and red, respectively. The molecular graph obtained from the application of the quantum theory of atoms in molecules (QTAIM[97,98]) is superimposed with the molecular electrostatic surface potential (MESP) in each case. The potential was mapped with the 0.001 au (electrons bohr^{-3}) isoelectronic density envelope of each system, and the [ωB97X-D/aug-cc-pVTZ] level of theory was used. Atom labeling is shown for each case.

neighboring molecules.[76,77] Astatine can behave as a halogen bond donor—possibly a stronger one than iodine—owing to its much more electrophilic (σ-hole) character.[78] Similarly, a number of studies[68,69,79−86] have been reported that demonstrate the ability of covalently bonded fluorine in molecules to form a halogen bond (or counterintuitive interactions) upon donating a σ-hole on the fluorine to the Lewis base of the interacting molecular entity. Nevertheless, the ten features listed in ref 34 alone may be insufficient for rationalizing HaBs, and citations to the original literature highlighting these features are missing.

The IUPAC recommendations[34] are merely a short overview of HaBs. No illustrative examples are given; thus, the recommendations may not be sufficient to identify chemical instances where halogen bonding occur. Furthermore, the recommendations[34] do not mention the possibility that halogen bonding can also be formed by hypervalent halogen derivatives and cations containing halogen atoms, as well as by electrophilic π-/p-holes (π-/p-belt) on halogen derivatives in molecular entities. Many crystal structures have been reported that provide evidence for this (see the illustrative examples below). Furthermore, the IUPAC recommendation[34] is also silent on the occurrence of antielectrostatic halogen bonds,[87−90] as well as those that have been reported as negative−negative and positive−positive halogen-centered noncovalent interactions involving halogen atoms in the same[91,92] or a neighboring[68,79,81,93−95] (interacting) molecular entity.[91,92,96]

This Article revisits and expands upon the IUPAC definition of the halogen bond.[34] We list a number of notes and characteristic features, keeping essentially the format of the original IUPAC recommendations (and transferable in principle to any noncovalent interaction), that are likely to assist when exploring halogen bonds in chemical systems. We also list a rich variety of halogen bond donors and halogen bond acceptors, as well as caveats that should be borne in mind when classifying an attractive interaction as a halogen bond. It is customary not to confuse the terms "donor" and "acceptor" in this context with those that have been widely used in chemistry as "electron donor" and "electron acceptor". In current scenario, a HaBD refers to the donor of a "halogen bond" that is an "electron density acceptor" or simply an "electron acceptor". Similarly, a HaBA should be understood as an acceptor of a "halogen bond", which is an "electron density donor" or simply an "electron donor". This view is applicable to all kinds of noncovalent interactions, regardless of whether it is a hydrogen bond, chalcogen bond, or tetrel bond, pnictogen bond, among others. Nevertheless, illustrative examples retrieved from crystal structures deposited in the Cambridge Structural Database (CSD)[100] are presented. A first-principles-based case study focusing on simple dimer systems is also presented to validate some of the recommended notes and characteristic features of the halogen bond and to further a basic understanding of this type of noncovalent interaction. The concept of a π-/p-hole (or π-/p-belt) halogen bond formed by halogen's π-/p-hole (or π-/p-belt) in molecules is introduced. Some of the annotations may seem repetitive, but this is to clarify the terminology. We interchangeably use terms such as "bond" or "interaction" to mean the same thing, even though some[99] have suggested that terms such as "σ-, π-, and p-hole bonds" should be read as "σ-, π-, and p-hole interactions". In our opinion, the terms "bond" and "interaction" have the same meaning; a "covalent bond", for example, is unequivocally a "covalent interaction" in a pair of two atoms in a molecular entity. π- or p-type interactions/bonds occur when electrophilic π- or p-type orbitals are involved. Based on the non-negligible covalent character of the p-hole bond, we made no attempt to distinguish it from the π-hole bond.

■ DEFINITION

The IUPAC definition[34] of the halogen bond is as follows: "A halogen bond occurs when there is evidence of a net attractive interaction between an electrophilic region associated with a halogen atom in a molecular entity and a nucleophilic region in another, or the same, molecular entity". We recommend that this is expanded to read as follows: *A halogen bond (HaB) develops in a chemical system when a net attractive engagement occurs between an electron-density-deficient (electrophilic) region on the electrostatic surface of a halogen atom in a molecular entity and a close-lying electron-density-rich (nucleophilic) region on the electrostatic surface of the same or another identical or different molecular entity.*

https://doi.org/10.1021/acs.cgd.4c00228
Cryst. Growth Des. 2024, 24, 5494−5525

RECOMMENDED NOTES FOR IDENTIFYING A HALOGEN BOND

Note 1. The definition is general and, in principle, is transferable to any noncovalent interaction, including HBs, TtBs, ChBs, PnBs, triel and aerogen bonds,[101] etc., obviously replacing the term "halogen atom" with the appropriate term for the attractive interaction being referred to.

Note 2: A HaB, like an HB, is a noncovalent interaction between interacting sites of opposite (local) polarity. It is not recognized as such when the HaBD site X is not apparently identifiable as having an electrophilic region but engages in an attractive interaction with a nucleophilic region in the HaB acceptor site Y, a view that is transferable to other attractive interactions such as the PnB (see *Note 4* of the definition of PnB).[102] The electrophilic region on the halogen atom in a halogen-containing molecule may be induced when placed in the vicinity of any strong electrostatic field of the interacting partner molecular entity.[95] The electrophilic and nucleophilic regions stand out on the outer electrostatic surfaces of a HaBD and HaBA, respectively.

Note 3. A HaB is represented by the structural motif R−X···Y, where X (X = F, Cl, Br, I, At) is the HaB donor, a halogen atom (which may or may not be hypervalent) that must feature an electrophilic region on its outer electrostatic surface, and R is the remainder part of the molecule containing the HaBD. The HaBD can be seen either in an electrically neutral molecule or in a fragment of a molecular cation, which may or may not be a π-system; Y is an HaB acceptor, which may be a lone-pair region in a molecule, a molecular anion, or an atomic anion and must possess a nucleophilic region.

Note 4. A HaB is either intermolecular[3] or intramolecular[103] and cannot simultaneously possess both characteristics: when it develops in the same molecular entity containing the electrophile X and nucleophile Y, it is intramolecular; when it occurs between two molecular entities (one with a HaB donor X and the other with a HaBA acceptor Y) that are either identical or different, it is intermolecular.

Note 5. A HaB can be very strong,[104,105] strong,[12] of medium strength,[12,106] weak,[107,108] or of the van der Waals type[108,109] depending on the binding (or interaction) energy of the interaction. The bond strength of the HaB, in many instances, is comparable to that of a HB, TtB, ChB, or PnB. It should not always be assumed to be a weak interaction,[24] since it appears in different flavors depending on the strength of the interaction.

Note 6. The combination of *Notes 2* and *3* may read "a HaB is an attractive interaction between HaB donor site X and HaB acceptor site Y of opposite charge capacity ($X^{\delta+}$ and $A^{\delta-}$)"; here, δ^+ and δ^- symbolically refer to the positive and negative local charge polarity on the interacting regions on the electrostatic surfaces of X and Y, respectively (see Figure 1). This also applies to HBs, TtBs, ChBs, PnBs, and any other noncovalent interaction as far as their definitions are concerned (*i.e.*, a positive site on the noncovalent donor atom A attracts a negative site on the noncovalent acceptor atom Y when in close proximity, where A refers to a triel, tetrel, pnictogen, chalcogen, halogen, or aerogen atom, among others).

Note 7. The definition of the HaB requires that an electrophile on a HaB donor X attracts a nucleophile on a HaB acceptor Y; however, it is not necessarily the case that regions of opposite charge polarity on the electrostatic surfaces of interacting molecules will always attract each other to form a HaB when in close proximity. The actual sites on X and Y that interact attractively are determined by the spatial rearrangement that corresponds to the maximization of the attractive (electrostatic) interaction between X and Y.

Note 8. The surface charge polarities of HaB donor site on X and HaB acceptor site on Y may be determined by examining the extrema (local maxima and minima) of the potential on the electrostatic surfaces of the interacting molecular entities. The HaBA Y is often (but not always!) characterized by a local minimum of (negative) potential, and the HaB donor site X is characterized by a local maximum of (positive) potential. This is also applicable to other noncovalent interactions, such as ChBs and PnBs; however, formation of a PnB with a PnB donor site Pn, characterized by a local minimum of (positive) potential,[110] and a PnB acceptor site Y, characterized by a local maximum of (negative) potential, is not unlikely (for example, the N≡P···F−H dimer).

Note 9. An intermolecular HaB is likely to follow a type II geometric topology of a noncovalent bonding interaction; a type II topology, which relates to ∠R−X···Y, is often linear or quasi-linear (but may be nonlinear) and satisfies the local differential charge polarity condition (see *Note 6*).[3,111,112] An intramolecular HaB does not generally follow the same geometric topology of bonding; it is often nonlinear, following a type I geometry (∠R−X···Y < 140°); if an electrophilic π-/p-hole (or π-/p-belt) on a halogen derivative in a molecule is involved in making up a HaB with a HaBA Y, R−X···Y is often an orthogonal HaB interaction and is nonlinear (there can be exceptions!).

Note 10. The formation of a HaB between interacting sites may result from an attractive engagement between an electrophilic σ-hole region characterized by a positive electrostatic potential on the side of HaB donor X opposite to the R−X bond extension and a nucleophilic site on Y. A HaB may also occur when an attractive interaction develops between the lateral electrophilic site(s) on X in R−X and the nucleophilic site on Y (see *Notes 7*−*8*).

Note 11. An electrophile on covalently bonded halogen atom X in HaBD need not always have the characteristic of a σ-hole but can have the characteristics of a π-/p-hole instead. An electrophilic σ-hole is a region of lower electronic density on X, not a region of electrostatic potential,[37,113,114] which may appear linearly along or off the outer extension of the R−X covalent bond axis;[115] its exact location depends on the nature of R (*e.g.*, its electronegativity and electron-withdrawing capacities). It is often observed that the stronger the electron-withdrawing capacity of R, the greater the electrophilicity on the side of X opposite to the outermost extension of the R−X covalent bond. An electrophilic π-/p-hole (or π-/p-belt) in a molecule containing the HaBD may appear on the outer surface of X, orthogonal to the R−X covalent bond, which may have the capacity to attract a nucleophile Y on the same or a different molecule to form an R−X···Y π-/p-hole (or even π-/p-belt) halogen bond (see examples in following sections).[110]

Note 12. It should not always be assumed that regions of higher electron density on HaBA Y will have negative electrostatic potentials and that regions of lower electron density on HaBD will have positive ones, given that the electrostatic potential reflects the effects of the nuclei as well as the electrons.[37] It is the local potentials—not the σ-holes(or π-/p-holes)—that are responsible for the development of halogen bonding.[56] A nucleophilic σ-hole (or simply a negative σ-hole, or a σ-hole accompanied by a negative electrostatic potential) may also appear on the outer electrostatic surface on the side of X in R−X (as on F in H−F), which is often weakly nucleophilic

https://doi.org/10.1021/acs.cgd.4c00228
Cryst. Growth Des. 2024, 24, 5494−5525

compared to the lateral sides of the same atom X. If the weakly nucleophilic σ-hole on X (frequently fluorine) forms an attractive noncovalent interaction with an electron density donor site on Y, this may not be recognized readily as a HaB, since the halogen atom in the HaBD moiety X in the isolated molecular entity acts as a nucleophile. However, a nucleophilic σ-hole (as a HaBA) on a covalently bonded halogen molecule may attract an electrophilic σ-hole on the halogen in another molecule to form a HaB. The electrophilic and nucleophilic natures of σ-holes on atom X in R−X are characterized by the positive and negative signs of the local most maximum of electrostatic potential, respectively.[81,82] The positive character of the σ-hole on X increases going from the lighter to the heavier (more polarizable) halogen atoms within the group 17 and as the remainder of the molecule becomes more electron-withdrawing[116] (*viz.* $F_2 > Cl_2 > Br_2 > I_2$ ($> At_2$)). Positive and negative π-/p-holes on X in a HaBD are characterized by the positive and negative signs of the potential, respectively; they represent a maximum or (even sometimes a minimum) of potential depending on the extent of the electron density delocalization on the surface of X.

Note 13. Halogens, and especially Br, I and At, may be hypervalent in molecules; they may concurrently form multiple HaBs with more than one HaBA site Y on the molecules with which they interact.[117,118] This is especially true when the HaB donor atom X is entirely electrophilic or part of a cation; the HaB donor atom X may also form multiple HaBs when it manifests both π-/p- and σ-holes and interacts simultaneously with more than one nucleophile, a hypothesis that may be transferrable to ChB/PnB donors in molecules (see *Note 5* of the definition paper of the PnB[34]).

Note 14. Two halogen sites on two different molecules in close proximity may involve in an attractive engagement to form a HaB; in this case, one of them would act as a HaB donor X and the other as a HaBA Y (*viz.* X−X···Y−Y′; X, Y, Y′ = halogen).

Note 15. A halogen bond may occur between the HaB donor X and the HaB acceptor Y within a neutral molecule, or between two neutral molecules in close proximity. It may also occur between a neutral molecule with a HaB donor X and an anion (or a negative π-/p-belt as in HC≡CH or a π-hole on an arene moiety (C_6H_6) with negative π-density) containing Y, or between the HaB donor X in a molecular cation and a nucleophile (lone-pair or negative π-density) on Y in a neutral molecule, or between two molecules of opposite charge polarity with a HaB donor X in the cation and a HaB acceptor Y in the anion (*i.e.*, an ion-pair).

Note 16. An electrophilic σ-hole (or π-/p-hole) on a HaB donor X in molecules need not always form a halogen bond when in close proximity to an HaBA Y. For example, the weak σ-hole on Cl in HCl does not form a HaB with the nucleophile on the lateral portion of F in HF when the latter faces the σ-hole on Cl. The placement of electron-withdrawing substituents on the Lewis base Y may reverse the sign of the electrostatic potential in its lone pair or π-bond region to positive, and this may enable it to engage in the formation of a HaB with the positive σ-hole of a Lewis acid. A reverse scenario may also be likely in certain circumstances, as a negative σ-hole is likely to form a HaB with the negative lone pair region of a HaBA Y.[95] The highly negative σ-hole may become less negative because of electron-withdrawing substituents at the peripheral sites of a halogenated molecule.[81] A positive σ-hole on covalently bonded halogen X may be introduced in an anion in the presence of cation that enables it to engage attractively with a HaBA site Y, developing a halogen bond between them, as observed in the case of a tetrel derivative in an anion.[119]

Note 17. An attractive noncovalent interaction between an electrophilic (or nucleophilic) region on a halogen atom in one molecular entity and an electrophilic (or nucleophilic) region in the same or a neighboring interacting molecular entity may not be considered to be a halogen bond if both carry the same charge polarity (see *Notes 2*, *6*, and *7* and the definition).[91,92] This could arise for several reasons, for example, as the forced consequence of primary interactions (HB, PnB, or HaB) and/or the dominant role of polarization/dispersive forces. It can also be caused by the heterogeneous distribution of charge density on the surfaces of interacting atomic basins or by charge transfer interactions between interacting sites. An attraction caused by the latter is referred to as "antielectrostatic" halogen bonding,[87−90] a term that should not be confused with the definition of halogen bonding. It should be borne in mind that polarization is a physical observable, while charge transfer between orbitals, in this context, arises from a mathematical model;[120,121] some have questioned the "false claims" regarding the observation of orbitals,[122−124] while others are of the view that charge transfer is indistinguishable from polarization[38,121,125] but occurs when a shift in electron density from a nucleophile to an electrophile passes through a (somewhat arbitrary) boundary between them.

Note 18. It is sometimes incorrectly assumed that "electron-rich" and "electron-poor" regions have negative and positive electrostatic potentials, respectively, and that the electrostatic potential follows the electronic density. This is often, but not always, the case. For example, the internuclear regions of covalent bonds usually have accumulated electron density, but the electrostatic potential in these regions is generally positive and is due to the proximity of the nuclei (also see *Note 12*).[126]

■ RECOMMENDED FEATURES FOR CHARACTERIZING A HALOGEN BOND

On the formation of a typical halogen bond R−X···Y between two interacting molecular entities R−X and Y:

(a) A Coulombic engagement (attraction) may occur locally between the interacting regions on HaB donor X and HaB acceptor Y.

(b) The sign of the binding energy (also the interaction energy, complexation energy, or stabilization energy) is likely to be negative to signify an energetically favorable interaction (also see *Note* 5); this energy refers to the difference of the sum of the total electronic energies of the isolated HaBD R−X and HaBA Y moieties from the total electronic energy of the halogen bonded system R−X···Y.

(c) An energy decomposition analysis, for instance, using symmetry adapted perturbation theory (SAPT),[127] may indicate the energetic contributions to the interaction energy of the HaB arise from electrostatics, exchange, induction (polarization and/or charge transfer), and long-range dispersion. The role of an individual energy component of the HaB may vary depending on the nature and the extent of the interaction between HaBD X and HaBA Y (in accord with the fifth feature in ref 34), although the interaction energy is not readily dissected into individual components. Dispersion is not a measurable quantity, even though its prevalence has been discussed and justified many times. Others[121,128−130] have demonstrated that dispersion and polarization are an integral part of an electrostatic

https://doi.org/10.1021/acs.cgd.4c00228
Cryst. Growth Des. 2024, 24, 5494−5525

interaction and that they emerge from the Hellmann–Feynmann theorem,[131,132] which asserts that forces acting on nuclei in a molecule or molecular complex are entirely Coulombic in nature.

(d) The distance between the HaBD site X and the HaBA site Y tends to be smaller than the sum of the van der Waals (vdW) radii of the respective interacting atomic basins but larger than the sum of their covalent bond radii; deviation from the former criterion is likely, since the known vdW radii of atoms are only accurate to within ±0.2 Å[37,133−135] (the first part of *d* accords with first feature in ref 34). This criterion may not apply to *π*-/p-hole (or *π*-/p-belt) HaB if multiple atoms describe the HaBD entity (viz. the bonding region of X_2).

(e) The HaBD site X tends to approach the HaBA Y along the outer extension of a *σ*-covalent bond, R−X. The angular deviation from the R−X bond extension is often less pronounced in HaBs than in HBs, ChBs, and PnBs; the directionality of these interactions is driven by electrostatics and the location of the *σ*-hole (along or off the R−X bond axis),[115] although charge transfer and lone-pair repulsion contribute non-negligibly to the linearity of HaBs.[136,137]

(f) The angle of interaction, ∠R−X···Y, tends to be linear or quasi-linear when the approach of the electrophilic site on X is along the R−X *σ*-covalent bond extension, but can be nonlinear or bent when the HaB occurs between the lateral portion of an entirely electrophilic HaBD site X (as in a molecular cation, for example) and the nucleophilic region on Y, as well as when the same HaBD X is simultaneously involved in secondary interactions with the same or a different HaBA Y. Part of *f* accords with the third feature proposed in ref 34; however, this feature fails to account for the directionality of the *π*-/p-hole (or *π*-/p-belt) halogen bonds formed by the electrophilic *π*-/p-hole (or *π*-/p-belt) hosted by a bonded halogen derivative in molecules and the nucleophile on HaB Y. Accordingly, the angle of interaction, ∠R−X···Y, tends to be nonlinear (60° < ∠R−Y···A < 135°) when the approach of the electrophilic site on X is orthogonal the R−X *σ*-covalent bond extension (as in Cl_3Br···CO and Cl_3Br···N_2).[110]

(g) When the nucleophilic region on the HaBA entity Y is a lone-pair orbital or a (negative) *π*-/p- region, the HaBD entity X tends to approach HaBA entity Y along the axis of the lone-pair or orthogonal to the *π*-/p-hole (or bond) plane regardless of the nature of the halogen bond (also see *e*).

(h) The length of the R−X covalent bond opposite to the HaB (called the halogen bond donor distance) is typically longer than that in the isolated (unbound) HaBD entity; this accords with the second feature proposed in ref 34. However, this may not always be the case (*e.g.*, shortening of the halogen donor bond R−X may be seen);[138−141] geometric deformation to other parts of the HaBD/HaBA entities may occur upon the formation of a linear (or an orthogonal) halogen bond.[110]

(i) The infrared absorption (IR) and Raman scattering observables of both R−X and Y are affected by HaB formation; compared to the harmonic frequency of the same bond in the isolated molecule, the vibrational frequency of the R−X bond may be red-[142−144] or blue-shifted[141,145,146] depending on the extent of the interactions involved.[15] New vibrational modes associated with the formation of the (R−)X···Y intermolecular halogen bond may also be observed, as for HBs, TtBs, ChBs, and PnBs, in accordance with the seventh feature in ref 34.

(j) The nuclear magnetic resonance (NMR) chemical shifts of nuclei in both R−X and Y are typically affected as found for R−Ch···Y ChBs; the isotropic coupling constant of the HaB donor in the complex system tends to decrease relative to that of the isolated HaB donor,[27,103,118,147−149] as observed for HBs, TtBs, ChBs, and PnBs. This accords with the second feature in ref 34.

(k) The UV−vis absorption bands of the HaBD chromophore may experience a shift to shorter wavelengths;[150−152] the binding energies of the peaks associated with X with the X-ray photoelectron spectrum (XPS) of the R−X···Y complex shift to lower energies relative to unbonded X, in accordance with the eighth and tenth features, respectively, in ref 34.

(l) A bond path and a bond critical point between HaBD X and HaBA Y may be found when an electron density topology analysis based on the quantum theory of atoms in molecules (QTAIM)[97,98] is carried out, together with the appearance of other charge density-based signatures such as those associated with the sign and magnitude of the Laplacian of the charge density and the total energy density at bond critical points.[15] This may be in accordance with the sixth feature in ref 34.

(m) Isosurface volumes (colored greenish, blue, or blue-green between HaBD X and HaBA Y, representative of attractive interactions[134,135,153,154]) may be seen if a noncovalent index analysis (NCI) based on reduced density gradients is performed;[155−157] similar isosurface features may also emerge when an independent gradient model (IGM),[156,157] an IGM based on Hirshfeld partition of molecular density (IGMH), or an interaction region indicator (IRI) analysis is performed.[158,159] Feature *l* may fail in some chemical systems, especially in the weak bonding regime,[68,119,160−163] but the isosurface analysis is expected to recover inter- and/or intramolecular interaction between interacting atomic basins.[13,161,164]

(n) At least some transfer of charge density from the frontier HaBA orbital to the frontier HaBD orbital may occur (viz. from a (filled) lone-pair type orbital (*n*) to an empty *σ**-/*π**-type anti-bonding orbital);[12] when the transfer of charge density between the orbitals is significant, the formation of a dative (covalent) interaction is likely.[9] The occurrence of the phenomenon IUPAC recommended for HBs is also applicable to TtBs, ChBs, and PnBs; the nature of charge transfer (hyperconjugation) may be assessable upon computing the second-order perturbation theory based stabilization energy using natural bond orbital (NBO)[15,140,165,166] and/or block-localized wave function (BLW) method approaches.[167,168]

(o) The halogen bond strength typically increases with a given HaBA Y, as the electronegativity of X decreases in the order F > Cl > Br > I (> At) and the electron-withdrawing ability of R increases; there may be an exception when the chemical environment alters the nature of the reactivity between the HaBD and HaBA moieties (in accord with the fourth feature in ref 34).

(p) The halogen bond strength may increase for a specific HaBA Y and R of the R−X entity as the polarizability of the X atom increases ((At >) I > Br > Cl > F). This is

https://doi.org/10.1021/acs.cgd.4c00228
Cryst. Growth Des. 2024, 24, 5494−5525

analogous to the effect observed in the case of TtB (Pb > Sn > Ge > Si > C), ChB (Te > Se > S > O),[169] and PnB (Bi > Sb > As > P > N); if a secondary interaction (*e.g.*, hydrogen bond, halogen bond, chalcogen bond, tetrel bond, pnictogen bond, etc.) is involved either with the HaB bond donor or the acceptor, the order of interaction strength may alter.

(q) The strength of a halogen bond[170] can be ultrastrong (*i.e.*, interaction/binding energy > −40 kcal mol^{-1}), very strong (−25 < energy ≤ −40 kcal mol^{-1}), strong (−25 < energy < −15 kcal mol^{-1}), moderately strong (−5 < energy < −15 kcal mol^{-1}), weak (−3 < energy < −5 kcal mol^{-1}), very weak (−1 < energy < −3 kcal mol^{-1}), or of the vdW type (−0.01 < energy ≤ −1.0 kcal mol^{-1}).[26,28,108] Chemical systems with the HaB energies falling into different categories depend largely on the reactivity of the HaBD X and HaBA Y sites in the interacting molecular entities. For example, if an anion Y attracts an electrophilic region on X in R−X, the interaction energy can be of the ultrastrong type (*e.g.*, bond energies for FI···F$^-$ and II···F$^-$ are −69.0 and −75.0 kcal mol^{-1}, respectively[12]); the interaction energy can be categorized as very strong and moderately strong when the identities of HaBD X and HaBA Y are changed (*e.g.*, bond energies of the ion−molecule interactions IF···I$^-$, II···I$^-$, and IF···Cl$^-$ are −37.4, −16.9 and −14.5 kcal mol^{-1}, respectively).[12] VdW interactions are expected between neutral molecules when X and Y have weakly electrophilic and nucleophilic regions on their electrostatic surfaces, respectively (*e.g.*, as in HCl···N_2 and HCl···O_2); when the interaction energy is appreciable (> −15 kcal mol^{-1}), a non-negligible degree of covalency in halogen bonds is likely.[15,49,171,172]

(r) The electrophilicity and nucleophilicity of specific regions on the halogen atom in molecular entities may be assigned using the sign of the local most maxima and minima of potential ($V_{S,max}$ and $V_{S,min}$, respectively).[13,66,68,173,174] Signatures such as the positive and negative signs of $V_{S,max}$ or $V_{S,min}$ ($V_{S,max} > 0$ or $V_{S,min} > 0$ and $V_{S,max} < 0$ or $V_{S,min} < 0$, respectively) may be used to determine the electrophilicity and nucleophilicity on the surface of the halogen atom X in R−X. The electrophilic and nucleophilic σ- and π-holes[126,175,176] (or even π-/p-type belts) on atom X (or around the bonding region in a pair of halogen atoms) may be characterized by $V_{S,max} > 0$ and $V_{S,max} < 0$, respectively. It is often observed that the σ-hole on the surface of halogen atom X in R−X covalent bond is characterized by $V_{S,max} > 0$; when $V_{S,max} < 0$, a negative σ-hole on X in R−X is inferred. This view is transferable to π-/p-holes (or π-/p-belts) as well.

(s) Similar insight as in *r* may be gained about the character of a σ-hole from an analysis of the extended transition-state method with natural orbitals for chemical valence (ETS-NOCV);[177−180] in addition, this approach may also be used to evaluate the charge transfer between the halogen bond donor and acceptor orbitals,[181,182] as well as to gain insight into the electrostatics, exchange-correlation, Pauli's exchange-repulsion, and orbital interaction energies of a halogen bond.

SOME EXPERIMENTALLY AND THEORETICALLY IDENTIFIED HALOGEN BOND DONORS AND ACCEPTORS

The list of HaB donors and acceptors is vast. Some of them are from theoretical studies reported by a number of research groups, while others are taken from structures deposited in the CCDC.[100] The list below is not comprehensive, but illustrative.

The HaB donor entity X in R−X may be

- the axial outer portion on the side of halogen atom X in hydrogen halides HX (X = Br, Cl, I, At) and haloalkanes (CH_3X, CH_2X_2,[183] CHX_3 (X = Cl, Br, I, At),[184] CX_4 (X = F, Cl, Br, I, At), and $C_nF_{2n+1}I$);
- the axial outer portion on the side of X in OX_2[185] and in dihalogen molecules X_2 and XX′ (X, X′ = F, Cl, Br, I, At);
- the axial outer portion on the side of X in NX_3,[186] as well as XCN and XCCCN (X = F, Cl, Br, I, At);[68]
- the axial outer portion on the side of halogen X in haloethene C_2X_4,[187] C_6H_5X, and C_6X_6 (X = Cl, Br, I);
- the axial outer portion of halogen X in $-NO_2$ substituted arene moieties (as in 1,3,5-triiodo-2,4,6-trinitrobenzene,[188] 2-chloro-1-iodo-4-nitronaphthalene,[189] and 1,3,5-trichloro-2,4,6-trinitrobenzene);[190]
- the axial outer portion of halogen in haloalkynes, such as the arene derivatives (C_2I_2,[191] haloprogin ($C_9H_4Cl_3IO$),[192] and 1-halo-2-phenylacetylene (C_8H_5X (X = Br, I)),[193] 1-fluoro-4-(iodobutadiynyl)benzene ($C_{10}H_4FI$),[194] 2,6-bis(iodoethynyl)pyridine ($C_9H_3I_2N$),[195] 3-iodo-2-propynyl-*N*-butylcarbamate,[196] 3-(iodoethynyl)-benzoic acid ($C_9H_5IO_2$),[197] 2-(bromoethynyl)-1,3-dichlorobenzene ($C_8H_3BrCl_2$),[198] 1,4-difluoro-2,5-bis-(iodoethynyl)benzene ($C_{10}H_2F_2I_2$),[199] 1,4-bis(iodoethynyl)benzene ($C_{10}H_4I_2$),[200] 2,3-bis(bromoethynyl)-1,4-dimethoxybenzene,[201] 2,2′,4,4′,6,6′-hexafluoro-3,3′,5,5′-tetrakis(iodoethynyl)biphenyl ($C_{20}F_6I_4$),[202] 1,3,5-tris(bromoethynyl)benzene ($C_{12}H_3Br_3$),[203] 1,1′,1″,1‴-methanetetrayltetrakis[4-(iodoethynyl)benzene] ($C_{33}H_{16}I_4$),[204] 1,3,5-trifluoro-2,4,6-tris(iodoethynyl)benzene ($C_{12}F_3I_3$),[205] 1,4-bis(5-chloro-pent-4-ynyloxy)benzene ($C_{16}H_{16}Cl_2O_2$),[206] 2,6-bis(iodoethynyl)-pyridine ($C_9H_3I_2$),[195] 2,3,5,6-tetrafluoro-1,4-bis(iodoethynyl)benzene ($C_{10}F_4I_2$),[207] and 3-(iodoethynyl)pyridine (C_7H_4IN));[197]
- hypervalent halogen derivative in molecules, as in (dichloro-trifluoromethyl)iodine (CCl_2F_3I),[208] dichloro-(phenyl)iodane ($C_6H_5Cl_2I$),[209] *o*-(dichloriodo)nitrobenzene ($C_6H_4Cl_2INO_2$),[210] *p*-(dichloriodo)nitrobenzene ($C_6H_4Cl_2INO_2$),[210] 2-(dichloroiodo)pyridine ($C_5H_4Cl_2IN$),[211] bis(pentafluorophenyl)iodonium trifluoroacetate ($C_{14}F_{13}IO_2$),[212] trifluoromethyl-tetrafluoro-iodine (CF_7I),[213] and pentafluorophenyl-tetrakis-(fluoro)iodine (C_6F_9I));[214]
- the halogen in imide and amide derivatives such as *N*,*N*′-dibromoethanedi-imidoyl-difluoride ($C_2Br_2F_2N_2$)[215] and 1-chloropyrrolidine-2,5-dione ($C_4H_4ClNO_2$);[216] 1,3-dibromo-5,5-dimethylimidazolidine-2,4-dione ($C_5H_6Br_2N_2O_2$),[217] *N*-bromosuccinimide ($C_4H_4BrNO_2$),[218] *N*-chloro-*N*-(2,6-dichlorophenyl)trichloroacetamide ($C_8H_3Cl_6NO$),[219] 1-iodopyrrolidin-2-one (C_4H_6INO),[220] 1-chloro-1*H*-1,2,3-benzotriazole ($C_6H_4ClN_3$),[221] *N*,*N*,*N*′-trichlorobenzamidine ($C_7H_5Cl_3N_2$),[222] *N*,*N*-dichloromethylsulfonamide ($CH_3Cl_2NO_2S$),[223] *N*-chloro-*N*-methoxyurea ($C_2H_5ClN_2O_2$),[224] 1,3-dichloro-5,5-di-

https://doi.org/10.1021/acs.cgd.4c00228
Cryst. Growth Des. 2024, 24, 5494−5525

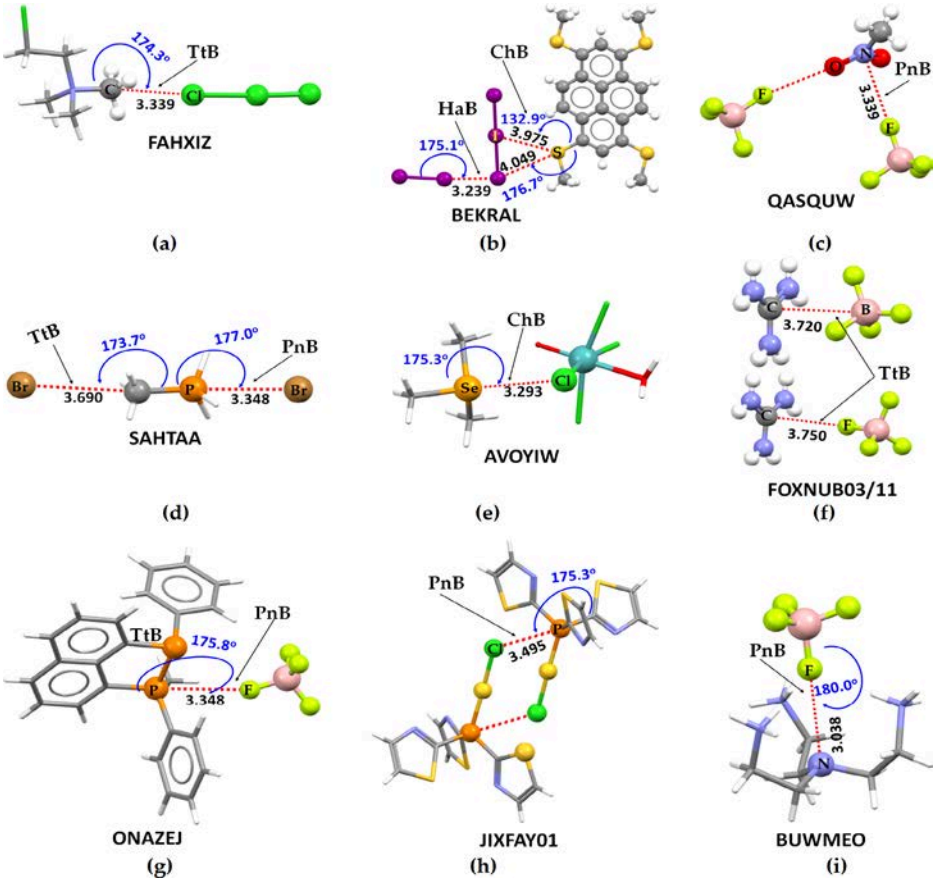

Figure 2. Ball-and-sick (and/or mixed capped stick) models of halogen-centered intermolecular close contacts observed between atomic basins of interacting molecules in some crystals. (a) *N*,*N*,*N*-trimethyl-*N*-(2-chloro-ethyl)ammonium trichloride,[239] (b) tris(1,3,6,8-tetrakis(methylthio)pyrenium) tris(triiodide) heptaiodine,[240] (c) bis(η^6-benzene)-ruthenium(II) bis(tetrafluoroborate)nitromethane solvate,[241] (d) methylphosphanium bromide,[242] (e) trimethylselonium aqua-tetrachloro-oxo-molybdenum,[243] (f) guanidinium tetrafluoroborate,[244] (g) *rac*-1-methyl-1,2-diphenyl-1,2-dihydronaphtho[1,8-*cd*][1,2]diphosphol-1-ium tetrafluoroborate,[245] (h) chloro-(tris(thiazol-2-yl)phosphine)gold(I),[246] and (i) 2,2′,2″-nitrilotris-(ethan-1-aminium) tris[tetrafluoroborate].[247] For clarity, some of the molecules in the crystal were deleted, such as bis(η^6-benzene)-ruthenium(II) in (c), for example. The CSD reference code in each case is shown in uppercase letters, and selected bond distances and angles are in Å and degrees, respectively. Labeling of selected atoms is shown in each case.

methylhydantoin ($C_5H_6Cl_2N_2O_2$),[225] 1,3-dichloro-2,4-imidazolidinedione ($C_3H_2Cl_2N_2O_2$),[225] *N*-chloro-*N*-phenyl-2-chloroacetamide ($C_8H_7Cl_2NO$),[219] and 1,3-dichloro-1,3-diazetidine-2,4-dione ($C_2Cl_2N_2O_2$);[226]

- the halogen derivative in systems containing boron such as hexachloroborazine ($B_3Cl_6N_3$),[227] (naphthalene-1,8-diyl)bis(dichloroborane) ($C_{10}H_6B_2Cl_4$),[228] 1-carba-2,-3,4,5,6,7,8,9,10,11,12-undecachlorododecaborate ($CHB_{11}Cl_{11}$),[229] and 2,3,4,5,6-pentachloro-7,8,9,-10,11,12-hexaiodoaza-closo-dodecaborane ($HB_{11}Cl_5I_6N$);[230]
- the halogen derivative in cations, *e.g.*, fluoroammonium (FNH_3^+),[231] 3-(iodoethynyl)pyridin-1-ium ($C_7H_5IN^+$),[232] 5-bromosulfenyl-1,3,2,4-dithiadiazolium ($CBrN_2S_3^+$),[233] 2-(iodoethynyl)pyridinium ($C_7H_5IN^+$),[232] 2-chlorodibenzo[*b*,*d*]bromol-5-ium ($C_{12}H_7BrCl^+$),[234] 1,2,3,4-tetrafluorodibenzo[*b*,*d*]iodol-5-ium ($C_{12}H_4F_4I^+$),[235] bis(pentafluorophenyl)iodonium ($C_{12}F_{10}I^+$),[236] [4-(ethoxycarbonyl)phenyl](phenyl)iodanium ($C_{15}H_{14}IO_2^+$),[237] and bis(4-chlorophenyl)iodanium ($C_{12}H_8Cl_2I^+$).[238]

The HaB acceptor entity Y may be

- a lone-pair on an atom in a molecular entity (a Lewis base), with many possibilities including the lateral portions of covalently bonded halides in HX, CH_3X, and CX_4 (X = F, Cl, Br, I); N in pyridines, amines, or even in N_2; O in H_2O, O_2, H_2CO, CO, CO_2, and an ether or carbonyl group; covalently bonded halogens in molecules; As in $AsMe_3$; a chalcogen in a heterocycle such as a thio-, seleno-, and tellurophene derivatives, as well as fused polycyclic derivatives thereof; furoxans, 2,5-thiadiazoles *N*-oxides, sulfoxide, aryl sulfoxides, and tellurazoles *N*-oxides; O, S, and/or N in derivatives of macrocyclic aza- and/or thia-crown-ethers such as 18-crown-6, 18-aza-crown-6, 15-crown-5, *N*-phenylaza-15-crown-5, and 21-crown-7, cyclam, [2.2.2]cryptand, 1,4,7-triazacyclononane, monothiadibenzo[24]crown-8-ethers, dithiadibenzo[24]crown-8-ethers, trithiadibenzo[24]-crown-8-ethers, tetrathiadibenzo[24]crown-8-ethers, etc.;
- an anion, such as the halide anions X^-, OH^-, NO_3^-, $CF_3SO_3^-$, tetraphenylborate $C_{24}H_{20}B^-$, CN^-, Cl_3^-, I_3^-, Br_3^-, Cl_2I^-, Br_2I^-, $Br_3I_2^-$, I_2Cl^-, I_4^{2-}, I_5^-, $Cl_3I_2^-$, I_8^-, $Br_3Cl_4^-$, NO_3^-, ClO_4^-, 5-oxotetrazole (CHN_4O^-), N_3^-, BF_4^-, $AuCl_4^-$, PF_6^-, AsF_6^-, pentazolide (N_5^-), 5,5′-bistetrazolates ($C_2N_8^{2-}$), *p*-tosylate ($C_7H_7SO_3^-$), hexa-

https://doi.org/10.1021/acs.cgd.4c00228
Cryst. Growth Des. 2024, 24, 5494−5525

bromo-pentamethyl-1-carbadodecaborane ($C_6H_{16}B_{11}Br_6^-$), *closo*-dodecaborate ($H_{12}B_{12}^{2-}$), and polyatomic oxyanions such as $C_2O_4^{2-}$, ReO_4^-, $AsCl_4^-$, SbF_6^-, $SbCl_4^-$, $BiCl_4^-$, $GaCl_4^-$, $ZnCl_4^{2-}$, SiX_6^{2-}, GeX_6^{2-}, SnX_6^{2-} and PbX_6^{2-} (X = F, Cl, Br), PbI_6^{4-}, $SnCl_3^-$, SnI_3^-, $GeCl_3^-$, $GeBr_3^-$, GeI_3^-, Br_4Sn^{2-}, I_4Sn^{2-}, Cl_4Pb^{2-}, I_5Pb^{3-}, $B_2Cl_6^{2-}$, $CHB_{11}Cl_{11}^-$, $B_{12}Br_{12}^{2-}$, $B_{12}I_{12}^{2-}$, $B_{12}Cl_{12}^{2-}$, $CH_6B_{11}Br_6^-$, etc.;

- a (negative) π-/p-belt containing system (species featuring a double or triple bond, for example, the midpoints of the C═C and C≡C bonds in $H_2C{=}CH_2$ and HC≡CH, respectively) and the negative π-hole regions of arene moieties of any kind, such as the centroid regions of arenes (for example, C_6H_6, C_6H_5OH, C_6H_5F, $C_6H_5NHCH_3$, C_6H_5NHOH, and $C_6(NH_2)_6$; the C═C bonding regions in fullerene C_{60} and C_{70}; N in NO_3^-, etc.).

What follows are illustrative crystal systems in which the packing between the molecular building blocks is solely or partly driven by halogen bonding of various types. They include intermolecular and intramolecular HaBs discussed in *Notes 4 and 15*. We begin by providing examples of chemical systems that may appear to have halogen bonds but actually do not. We applied some theoretical approaches in cases where conclusions were difficult to reach. Considering that different studies use different levels of theory and basis sets to study halogen bonds, we have chosen a similar strategy but opted for the most frequently used theoretical methods to explore the reactivity of molecular entities, subject to their sizes and available computational resources.

■ ILLUSTRATIVE CRYSTAL SYSTEMS *NOT* FEATURING HALOGEN BONDING

It is often found that the halogen derivative in molecules can be engaged attractively with a similar or different neighboring molecule, contributing to the solid-state structure of many crystals. However, the engagement is not always driven by halogen bonding. For example, the C···Cl close contact in the crystal of *N,N,N*-trimethyl-*N*-(2-chloro-ethyl)ammonium trichloride (Figure 2a) is not a halogen bond; it is a charge-assisted tetrel bond. The S···I close contacts in the crystal of $[3(C_{20}H_{18}S_4^+),3(I_3^-),7(I_2)]$ (Figure 2b) are not HaBs; they are charge-assisted ChBs. The N···F close contact in $[C_{12}H_{12}Ru^{2+},2(BF_4^-),CH_3NO_2]$ is not a HaB; it is a charge-assisted PnB, since N has an electrophillic π-/p-hole and the F in BF_4^- is a HaBA (Figure 2c). The C···Br and P···Br close contacts in the crystal of $[CH_6P^+,Br^-]$ (Figure 2d) are not HaBs; they are a charge-assisted tetrel bond and a pnictogen bond, respectively. The Se···Cl close contact in the crystal of $[C_3H_9Se^+,H_2Cl_4MoO_2^-]$ (Figure 2e) is not a HaB; it is a charge-assisted ChB.

The C···B and C···F close contacts in $[CH_6N_3^+,BF_4^-]$ (Figure 2f) are charge-assisted TtBs; they are not halogen bonds, since the boron/fluorine atom in the anion in BF_4^- is a HaBA. The P···F close contact in the crystal of $[C_{23}H_{19}P_2^+,BF_4^-]$ (Figure 2g) is not a halogen bond; it is a charge-assisted pnictogen bond. The P···Cl close contact between the building blocks responsible for the crystal of $[C_9H_6AuClN_3PS_3]$ (Figure 2h) is a pnictogen bond, not a halogen bond. Similarly, the N···F close contact in $[C_6H_{21}N_4^{3+},3(BF_4^-)]$ is not a halogen bond; it is a charge-assisted PnB because the N is electrophillic in the $C_6H_{21}N_4^{3+}$ cation so is a pnictogen bond donor (PnBD) (Figure 2i).

In the crystal of $[C_{11}H_{24}N^+,C_6H_5F_5I^-,C_2H_3N]$ (not shown; CSD ref NACSEQ[248]), the three interacting molecular building blocks are packed such that two I···F close contacts occur between a pair of close $C_6H_5F_5I^-$ ions. The I···F close contact distance, 3.392 Å, is significantly shorter than the vdW radii of I and F (2.04 Å (I) + 1.47 Å (F) = 3.51 Å);[249] the C−I···F angle is 149.2°, which suggests the presence of a directional interaction. An analysis of the geometric feature alone is insufficient to determine whether the I···F close contact is a HaB. However, as we will show below, and have demonstrated recently elsewhere,[119] the I···F close contact could be regarded as HaB given that the interaction between the anion and the cation in the crystal is likely to play an important role in polarizing the electrostatic field of the anion; the induction of a positive potential on the surface of the I in $C_6H_5F_5I^-$ along the C−I bond extension may occur, which shall interact attractively with the lateral portion of F in a neighboring $C_6H_5F_5I^-$. This speculative scenario for the occurrence of halogen bonding in the crystal is very different from that found in the crystals of trifluoromethyl-tetrafluoro-iodine (CF_7I)[213] and pentafluorophenyl-tetrakis-(fluoro)iodine (C_6F_9I)[214] (*vide infra*).

■ ILLUSTRATIVE CRYSTAL SYSTEMS FEATURING HALOGEN BONDING

Halogen Bonding in Anion-Molecule Systems in Crystal Adducts. Some examples of chemical systems where close contacts occur that might not be readily identified as halogen bonds are given in Figure 3.

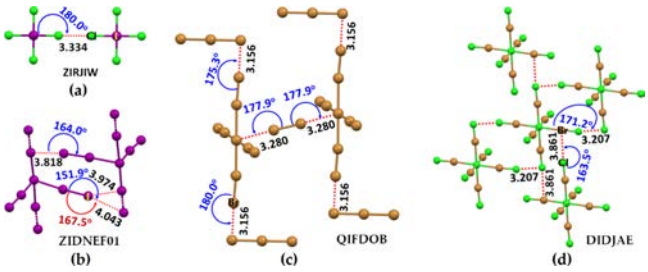

Figure 3. Illustration of X···X close contacts between inorganic halide frameworks in some organic−inorganic ion-pair adducts in the crystalline phase. The CSD reference in each case is shown in uppercase letters, and selected bond distances and angles are in Å and degrees, respectively. (a) Tetrachloroiodate $[Cl_4I^-,C_8H_{20}N^+]$,[250] (b) catena-(18-crown-6 oxonium clathrate heptaiodide) $[(C_{12}H_{24}O_6)_n,n(H_3O^+),n(I_7^-)]$,[251] (c) bis(bromotris(4-fluorophenyl)phosphonium) bromine nonabromide tribromide $[2(C_{18}H_{12}BrF_3P^+),Br_9^-,Br_3^-,Br_2]$,[252] and (d) bis(triphenylphosphine)iminium hexakis(chlorobromo)chloride $(C_{36}H_{30}NP_2^+,Br_6Cl_7^-)$.[253] For clarity, the organic cations, *viz.* $C_8H_{20}N^+$ in (a), $[(C_{12}H_{24}O_6)_n,n(H_3O^+)]$ in (b), $2(C_{18}H_{12}BrF_3P^+)$ in (c), and $C_{36}H_{30}NP_2^+$ in (d), have been omitted. Labeling of selected atoms is shown in each case.

The Cl···Cl close contact in the crystal of tetraethylammonium tetrachloroiodate $[Cl_4I^-,C_8H_{20}N^+]$[250] (Figure 3a) develops along the outer extensions of the I−Cl bond axes between two Cl atoms belonging to two neighboring $[Cl_4I^-]$ anions, and the angle of interaction, ∠I−Cl···Cl, is 180.0°. The inorganic framework ($\cdots ICl_4^-\cdots Cl_4I^-$) of the crystal features Cl···Cl close contacts (Figure 3a), which are stabilized by an extensive number of Cl···H hydrogen bonds (not shown) due to the presence of the organic counterpart. The latter contacts are likely to cause changes to the charge density distribution around the chlorine atoms in the anion, forcing the Cl in the anions to

https://doi.org/10.1021/acs.cgd.4c00228
Cryst. Growth Des. 2024, 24, 5494−5525

interact with each other constructively. The 1D chain-like inorganic framework [···ICl_4^-···Cl_4I^-] stabilized by Cl···Cl close contacts is probably the forced consequence of the primary hydrogen bonding interactions. At first glance, the Cl···Cl close contacts might not be regarded as HaBs, considering that they appear between two entirely negative sites. However, their engagements display linearity (type II, the angle of interaction), satisfying feature *f*, and the intermolecular distance between the two Cl atoms, 3.344 Å, is less than twice the vdW radius of Cl (3.64 Å),[249] satisfying feature *d* of a halogen bond. These two features are not sufficient to determine whether or not the halogen···halogen contacts in the crystal can be characterized as halogen bonds and whether they are the result of electrostatic polarization caused by hydrogen bonds (and the cation); this is surely a topic for a future investigation.

The I···I close contacts between the I_7^- anions in the crystal of catena-(18-crown-6 oxonium clathrate heptaiodide), $(C_{12}H_{24}O_6)_n$,n(H_3O^+),*n*(I_7^-)[251] (Figure 3b), may not merely be considered as attractive interactions between the entirely negative I_7^- sites that cause the development of the inorganic framework. From the geometry of the I_7^- anion alone, it may be inferred that the anion is an assembly between an I_3^- anion and two I_2 molecules, which is driven by a two σ-hole HaBs. The attractive interaction occurs between the electrophilic σ-hole on the surface of an I atom opposite to the I−I bond extension in the I_2 molecule and the nucleophile on the central I atom of the I_3^- anion. The I_7^- anions are also halogen bonded to each other via covalently bonded σ-holes (*r*(I···I) = 3.974 and 4.043 Å) of I_2 that are common to the [I_5^-] framework. As noted above, the formation of the I_7^- anion, and the interaction between these ions, contributes to the development of the inorganic framework; and the interactions occur in the presence of the polarizing field of the oxonium cation, which plays a critical role the assembly through hydrogen bonding.

The Br···Br close contacts between a pair of Br_9^- anions caused by a Br_2 molecule as a spacer in the crystal of [2($C_{18}H_{12}BrF_3P^+$),Br_9^-,Br_3^-,Br_2][252] (Figure 3c) are halogen bonds, with *r*(Br···Br) = 3.280 Å and ∠Br−Br···Br_9^- = 177.9°. Similarly, the Br···Br close contacts between the Br_3^- anion and the Br_2 molecule responsible for rigid framework of Br_9^- are also halogen bonds. This is not surprising, since each outer end of the Br_2 molecule that has an electrophilic σ-hole assists in the development of the Br_9^- anion framework via a (covalent) halogen bond and the other end of the same molecule halogen bonds with the Br_3^- cation [*r*(Br···Br) = 3.156 Å], contributing to the development of the inorganic framework. The latter are quasi-linear, and the Br···Br intermolecular distances are less than twice the vdW radius of Br (3.73 Å).[249]

The Cl···Cl and Cl···Br close contacts between $Br_6Cl_7^-$ anions in the bis(triphenylphosphine)iminium hexakis(chlorobromo)-chloride ($C_{36}H_{30}NP_2^+$,$Br_6Cl_7^-$) crystal[253] (Figure 3d) are halogen bonds. The inorganic anion, $Br_6Cl_7^-$, is an assembly between a Cl^- anion and six Cl−Br molecules; this is driven by the positive σ-holes on HaBD halogen, each on the side of the Br atom lying opposite to the Cl−Br bond extension in Cl−Br. In addition, the $Br_6Cl_7^-$ anions are linked to each other via Cl···Cl and Cl···Br halogen bonds, in which the electrophilic σ-hole on the side of the Cl atom opposite to the Br−Cl bond extension donates the halogen bond and the lateral portions of the Cl and Br atoms behave as acceptors (*r*(Cl···Cl) = 3.207 Å, ∠Br−Cl···Cl = 172.2°; *r*(Cl···Br) = 3.861 Å; ∠Br−Cl···Br = 163.5°).

The X_n^- (*n* = 3, 5, 7, 9) anions can be viewed as the result of an attractive engagement between an halide anion and two or more dihalogen (X_2) molecules, and are driven by HaBs. Accordingly, the Br_9^- anion (Figure 3c) is actually an assembly of a Br^- anion with four Br_2 molecules. That is, a single Br^- anion (HaBA) (covalent) halogen bonds with four neighboring electrophilic σ-holes; each resides on the side of a Br atom opposite to the Br−Br covalent bond extension in a Br_2 molecule (HaBD), resulting in the formation of the Br_9^- anion.

Since the formal charge of Br_9^- and Br_3^- is −1, their presence as counterions stabilizes the organic cation, (*viz.* $C_{18}H_{12}BrF_3P^+$ in Figure 3c), leading to the formation of an organic−inorganic hybrid crystalline material. The crystal, tripropylammonium nonabromide [$C_{12}H_{28}N^+$,Br_9^-] (CSD ref ODAQER[254]), is another example (not shown), where Br···Br HaB occurs between the Br atoms of close-lying Br_9^- inorganic anions, which is driven by the presence of the organic cation; in this case, *r*(Br···Br) = 3.395 Å and ∠Br−Br···Br = 173.3°. The chemical systems outlined above (*viz.* $Br_6Cl_7^-$ and X_n^-), and those illustrated in Figure 3, are stabilized by σ-hole centered halogen bonds,[68,255,256] validating the expanded definition, as well as *Notes 1−4*, *6−11*, and *15* and features *a* and *d−f*.

The 2D-like layers formed by Cl_{13}^- anions are separated by organic spacers in the crystal of bis(triphenylphosphine)-iminium tridecachloride [$C_{36}H_{30}NP_2^+$,Cl_{13}^-] (CSD ref PIGCIU[257]), producing an inorganic−organic hybrid material. The inorganic layers are linked through Cl···Cl HaBs, with *r*(Cl···Cl) = 3.964 Å and ∠Cl−Cl···Cl = 161.1°. These close contacts are longer than those observed in the crystal of bis(*N*,*N*,*N*-trimethylanilinium)dodecachloride [2($C_9H_{14}N^+$,Cl_{12}^{2-}] (CSD ref PIGDER[257]), where *r*(Cl···Cl) = 3.00−3.45 Å and ∠Cl−Cl···Cl = 168.1°−174.9°. Both the angular and bond distance features are in agreement with *Notes 1−4*, *6−11*, and *15*, features *a* and *d−f*, and the definition of a halogen bond, since Cl_{13}^- may be viewed as consisting of an anion attractively assembled with six Cl_2 molecules, [Cl^-···$(Cl_2)_6$].

The HaB interactions above may to some extent resemble those investigated theoretically for cesium tetrel halide perovskite oligomers [Cs^+·TtX_3^-]$_n$ (*n* = 2, 3, 4)[67] and [$CH_3NH_3^+$·TtX_3^-]$_2$ (Tt = Ge, Sn, Pb; X = Cl, Br, I) ion-pair dimers.[119] Upon the formation of the [Cs^+·TtX_3^-] ion-pairs, the cesium cation polarizes TtX_3^- through Coulombic and charge transfer interactions, creating electrophilic σ-holes on the surface of Tt. These σ-holes on an ion-pair then attract the negative halogen sites on another ion pair(s) in close proximity, leading to the formation of [Cs^+·TtX_3^-]$_n$ oligomers. This explains why, in the presence of Cs^+, the [TtX_3^-] anions attract each other, leading to the formation of inorganic cage-like 3D structures in the solid state. This result complements *Note 16* in the sense that an electrophilic σ-hole can be induced in an anion, which can then interact with a nucleophile.

Hypervalent Halogen as a Halogen Bond Donor for Halogen Bonding. The iodine atom is hypervalent in molecular CF_7I[213] and C_6F_9I[214]. These neutral molecules are the building blocks of their corresponding crystalline materials. The MESP plots of the two entities show that both the axial and lateral portions of covalently bonded I are electrophilic (see Figure 4a and b, respectively, top). The [ωB97X-D/def2-TZVPPD]-level analysis suggests that there is no σ-hole on the side of the covalently bonded I atom opposite to the C−I bond extension. Instead, a p-type hole is evident; it is, however, characterized not by a $V_{S,max}$ but by a positive $V_{S,min}$ of 37.9 kcal mol^{-1} in CF_7I (see feature *r*). Additionally, there are four maxima of potential (filled tiny red circles) on I that surround the p-hole, each described by a $V_{S,max}$ of 41.4 kcal mol^{-1}; they

https://doi.org/10.1021/acs.cgd.4c00228
Cryst. Growth Des. 2024, 24, 5494−5525

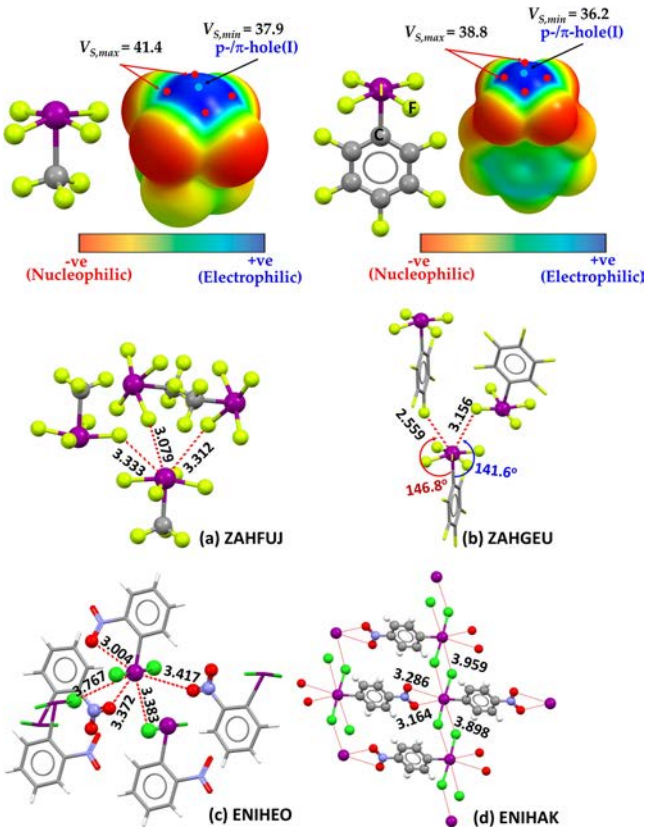

Figure 4. (Top) The molecular skeletal framework (left) and 0.001 au isoelectronic density-mapped molecular electrostatic surface potential graph (right) of (a) trifluoromethyl-tetrafluoro-iodine (CF_7I);[213] and (b) pentafluorophenyl-tetrakis(fluoro)iodine (C_6F_9I),[214] obtained with [ωB97X-D/def2-TZVPPD]. The blue region on the outer surface of covalently bonded I shows the dispersed nature of its electrophile, composed of I's π-/p-hole. Selected maxima and minima of potential ($V_{S,max}$ and $V_{S,min}$; in kcal mol^{-1}) on the surface of covalently bonded I are shown as filled tiny circles in blue and red, respectively. (a and b) Nonlinear I···F halogen bonding interactions in the crystals of these systems. (c and d) HaB environment in the crystals of *o*-(dichloriodo)-nitrobenzene ($C_6H_4Cl_2INO_2$)[210] and *p*-(dichloriodo)nitrobenzene ($C_6H_4Cl_2INO_2$),[210] respectively. The CSD reference in each case is depicted in uppercase letters, and selected bond distances and angles are in Å and degree, respectively. Hanging contacts in red are marked in (d).

each appear on the surface of I but in the junction (nonbonding) region between a pair of F atoms. The strengths of the corresponding extrema of potential in C_6F_9I are 36.2 and 38.8 kcal mol^{-1}, respectively. The chemical situation in CF_7I is very similar to that observed in the case of the P≡N molecule, in which a σ-hole was not found on the electrostatic surface of the molecule on the side of P opposite to the N≡P bond extension but instead a positive minimum of potential with its origin from a p-type orbital ($V_{S,\min} > 0$).[110]

The packing in the CF_7I[213] and C_6F_9I[214] crystals is driven by many C−I···F nonlinear halogen bonds that follow a type II topology of noncovalent bonding (see *Note 9*). They are the result of Coulombic attraction between HaB donor I in one molecule and the HaB acceptor F in the adjacent molecules with which the former interacts (in agreement with feature *a*). The hypervalent I atom is a multicentered HaB donor site (see *Note 13*), forming several I···Y (Y = Cl, O) noncovalent interactions between the building blocks in the crystals of *o*-(dichloriodo)-nitrobenzene (Figure 4c) and *p*-(dichloriodo)nitrobenzene (Figure 4d), respectively. Similarly, along with other attractive interactions, the crystal structure of tetrafluoro[4-(pentafluoro-l^6-sulfanyl)phenyl]-l^5-iodane ($C_6H_4F_9IS$) (CSD ref UNILIP[258]) shows reasonably strong I···F close contacts between the five-coordinate hypervalent I atom in one molecule and the lateral portion of a F atom in an interacting partner molecule (r(I···F) = 2.906 Å and ∠C−I···F = 144.5°), providing stability to the supramolecular assembly. That hypervalent halogen in molecular entities can halogen bond with nucleophiles in an interacting partner molecule has also been reported elsewhere.[259] These conclusions validate several *Notes* (for example, *Notes 3, 6, 9,* and *13−15*) and features *a* and *d−f*.

An interesting feature of chemical bonding that develops between the engaging molecules, for instance, in CF_7I, is the π-/p-hole halogen bond that emerges from the donation of the halogen's π-/p-hole to the interacting nucleophile (F); this is quasi-linear, following a type II geometric bonding topology. This may contrast with the conventional view that π-/p-hole bonds are orthogonal interactions and nonlinear, as discussed elsewhere[110] and observed in other instances, which are discussed below.

Intramolecular Halogen Bonding in Crystals. Shown in Figure 5 are a few instances in which intramolecular I···O halogen bonding interactions occur; they are not chalcogen bonds, since carbonyl oxygen serves as a HaB acceptor site Y and the covalently bonded I atom is the HaB donor site X. The HaBs are either nonlinear in $C_{10}H_9ClINO_3$[260] (see ∠C−I···O in Figure 5a) or quasi-linear in $C_9H_7F_3INO_3S$[261] and $C_{15}H_{14}INO_3$[262] (see ∠N−I···O in Figure 5b and c, respectively). The I···O close contact in *o*-nitrodiphenyliodonium iodide (CSD ref ENIGEN[210]) is not a chalcogen bond; it is an intramolecular halogen bond (r(I···O) = 2.735; ∠C−I···O = 157.5°). The hypervalent I(III) motif in bis(pentafluorophenyl)iodonium trifluoroacetate (CSD ref BIHFIK[212]) (Figure 5c) does not form a chalcogen bond with nearest-neighbor O and F atoms; it forms I···F and I···O intramolecular halogen bonds. The electrophilic σ-hole on the extension of the C−I and N−I covalent bonds in this molecule cannot be visualized since it is annihilated during the formation of noncovalent bonds. The F···O, Cl···N, and F···N close contacts in crystals $C_6H_4FN_5O_6$,[263] $C_{15}H_{13}ClN_2O$,[264] and $C_{16}H_3F_7N_2S$[265] shown in Figure 5d−f, respectively, are examples of intramolecular HaBs formed with HaB acceptors O, N, and N, respectively. The occurrence of one of the F···N halogen bonds in Figure 5f is a result of crystal packing, as our calculations suggested that the molecule is nonplanar in the gas phase. The illustrations validate several *Notes 4 and 13*, including *Note 3*.

Halogen Bonding in Charge-Assisted Systems (*viz.* Ion-Pairs) in Crystals. Further examples of the occurrence of halogen bonds in crystalline materials are shown in Figure 6. They occur between ions in adducts. The bond distance and bond angles for the I···F, Br···Cl, I···I, I···Cl, and Br···I close contacts in the ion-pairs shown, respectively, in Figure 6a−e are charge-assisted halogen bonds. They are quasi-linear, and the intermolecular X···Y contact distance in each case is less than the sum of the vdW radii of X and Y. The remaining I···F close contact in Figure 6a that occurs between two cationic species (phenyl-trifluoro-iodine), is probably a σ-hole centered lump−hole interaction.[266,267] Whether or not it can be referred to as a HaB requires a detailed theoretical investigation.

Examples of chemical systems containing various halogen bonds are shown in Figure 7. The Br···Br, I···I, and I···I close

https://doi.org/10.1021/acs.cgd.4c00228
Cryst. Growth Des. 2024, 24, 5494−5525

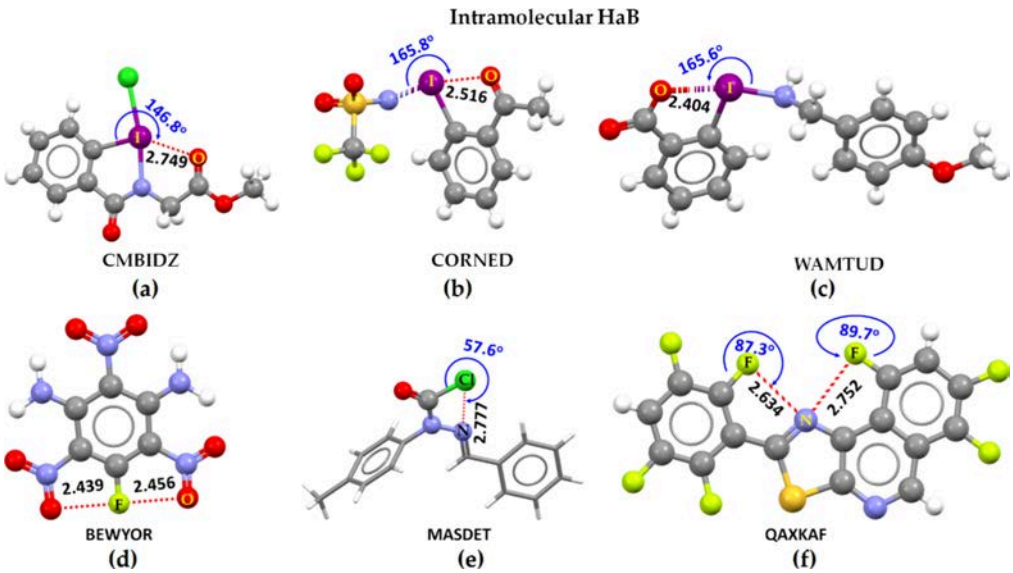

Figure 5. Illustration of intramolecular C−I···O and N−I···O halogen bonding interactions observed in crystals of (a) 1-chloro-2-carbomethoxymethyl-1,3-dihydro-3-oxo-1,2-benziodazole ($C_{10}H_9ClINO_3$),[260] (b) (*N*-(trifluoromethanesulfonyl)imino)(2-acetylphenyl)-λ^3-iodane ($C_9H_7F_3INO_3S$),[261] (c) 1-[[(4-methoxyphenyl)methyl]amino]-1λ^3,2-benziodoxol-3(1*H*)-one ($C_{15}H_{14}INO_3$),[262] (d) 5-fluoro-2,4,6-trinitro-1,3-benzenediamine ($C_6H_4FN_5O_6$),[263] (e) 2-benzylidene-1-(4-methylphenyl)hydrazine-1-carbonyl chloride ($C_{15}H_{13}ClN_2O$),[264] and (f) 6,7,9-trifluoro-2-(2,3,5,6-tetrafluorophenyl)[1,3]thiazolo[5,4-*c*]isoquinoline ($C_{16}H_3F_7N_2S$).[265] Selected intramolecular I···O bond distances and ∠C−I···O (or ∠N−I···O) bond angles are in Å and degrees, respectively. Halogen bonds are represented as dotted lines. The CSD reference in each case is shown in uppercase letters. Labeling of selected atoms is shown in each case.

contacts between the building blocks in the crystals shown in Figure 7a−c, respectively, are a result of halogen bonding formed when the HaB donor X in a neutral molecule is in close proximity to the HaB acceptor Y in an anionic entity. The I···Cl, I···Cl/I···F, and I···Cl close contacts shown in Figure 7d−f, respectively, are halogen bonds, but they are formed when the HaB donor X in a cationic molecule is in close proximity to the HaB acceptor Y in an anionic entity (*i.e.*, an ion-pair). Of the two halogen bonds marked in Figure 7e, the I···Cl HaB is intermolecular and the I···F HaB is intramolecular.

Halogen Bonding in Neutral Molecular Systems in Crystals. The Br···N, I···C$_\pi$, I···O, Br···N, I···O, and I···N close contacts shown in Figure 7g−k are HaBs formed between neutral molecules as building blocks in the crystals. They are the result of attraction between the electrophile on the HaB donor X in a neutral molecule and a lone-pair region on HaB acceptor Y in a neighboring neutral molecule. Of the two I···O halogen bonds shown in Figure 7i, one is quasi-linear and the other is bent because of the nature of the skeletal framework of the molecule containing the HaB acceptor. The I···O intramolecular HaB is shorter than that of the intermolecular HaB (r(I···O) = 2.356 vs 2.770 Å; Figure 7k). All the intermolecular HaBs in these systems are directional in a sense that a positive site on the covalently bonded halogen attacks a negative site during the process of HaB formation, obeying feature *a*, and the angle of approach of the electrophile is greater than 170°.

There are two exceptional cases to the angle of approach of the electrophile, notable of Figure 7e and i. The approach angle is nonlinear in both, with the approach being intramolecular in the former and intra/intermolecular in the latter. For the latter, the nonlinearity in the intermolecular HaB arises as a result of the two neighboring C═O groups of the $-C_6H_2O_3$ fragment in $C_{12}H_7IO_3$ being simultaneously engaged attractively with the hypervalent I atom in the making of the two I···O HaBs. Although the hypervalent I atom is capable of donating two σ-holes, one of them is involved in making two I···O HaBs, one linear (∠C−I···O = 170.6°/174.6°) and one nonlinear (∠C−I···O = 135.5°/130.6°) (one pair shown); this is similar to what was observed for the system in Figure 7f, where the iodine atom is hypervalent but carries a charge of +1. Moreover, the $C_{12}H_7IO_3$ molecule may also contain a pair of intramolecular I···O HaBs, which can be captured from the r(I···O) values of 3.187−3.189 and 3.192−3.205 Å (not shown) that are less than the sum of the vdW radii of I and O, *i.e.*, 3.59 Å (r_{vdw}(I) = 2.04 Å and r_{vdw}(O) = 1.55 Å). These intramolecular HaBs are nonlinear (*viz.* ∠C−I···O = 86.4−98.9° and 68.3−70.3°), as expected.

Halogen Bonding via Arene-Based Halogen Bond Acceptors in Crystals. Crystalline systems in which the packing is driven by cation−π and neutral−π HaBs, among other noncovalent interactions, are shown in Figure 8. Here, π means the delocalized charge density regions on electrostatic surface of an arene moiety that act as the nucleophilic site Y. In all four examples in Figure 8, the centroid region of the arene moiety (marked by a tiny sphere in red) in the interacting partner entity serves as the HaB acceptor Y for the HaB donor X in the entity with which it interacts. For example, the I···π(arene) close contact in $[C_{12}H_{10}I^+,C_{24}H_{20}B^-]$[284] (Figure 8a) is a charge-assisted HaB between the ions in an ion-pair; the iodine atom is hypervalent and positively charged and donates two σ-centered halogen bonds. The I···π(arene) and Br···π(arene) close contacts in crystals shown in Figure 8b−d occur between two identical neutral molecules. In these cases, it is very difficult to use feature *d* to validate the concept of "intermolecular distance is smaller than the sum of the vdW radii of respective atoms that are bonded with each other" because the HaB acceptor site is not just a single C atom as shown in the case of fullerene C_{70} and I_2 (Figure 7h) but the centroid of an array of C atoms. However, the HaBs in all these systems are directional, and obeying feature *a*.

https://doi.org/10.1021/acs.cgd.4c00228
Cryst. Growth Des. 2024, 24, 5494−5525

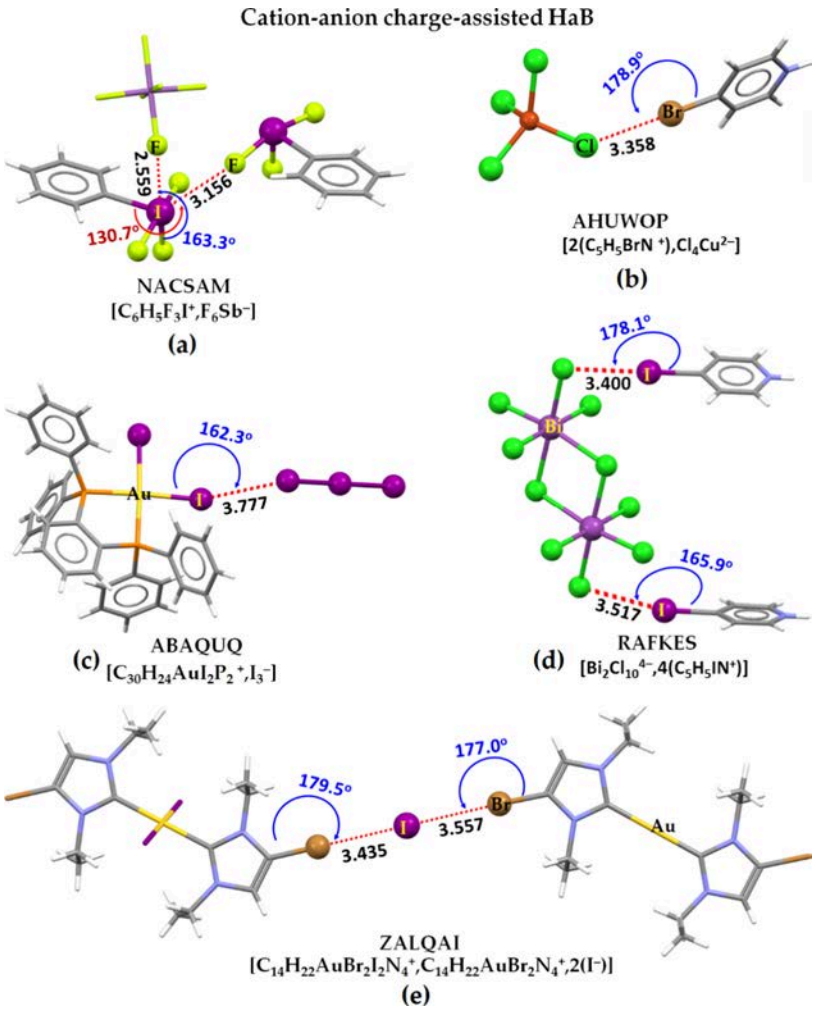

Figure 6. Charge-assisted halogen bonding in some ion-pair adducts. (a) Phenyl-trifluoro-iodine hexafluoroantimonate,[248] (b) bis(4-bromopyridinium) tetrachloro-copper(II),[268] (c) diiodo-(1,2-bis(diphenylphosphino)benzene)-gold(III) triiodide,[269] (d) tetrakis(4-iodopyridin-1-ium) bis(μ-chloro)-octachloro-dibismuth,[270] and (e) bis(4-bromo-1,3-diethylimidazol-2-ylidene)-bis(iodo)-gold bis(4-bromo-1,3-diethylimidazol-2-ylidene)-gold bis(iodide).[271] For clarity, selected ions $C_5H_5BrN^+$, $C_5H_5IN^+$, and I^- were deleted from (b−e), respectively. Halogen bonds are represented as dotted lines in red. The CSD reference in each case is shown in uppercase letters.

Figure 9 shows HaBs that develop when the nucleophilic region on the HaBA Y is a (negative) π-region and when the HaBD X approaches it orthogonally (or near orthogonally) to the C≡C π-bond plane. The X···π (acetylenic C≡C) HaBs between the interacting moieties are quasi-linear in all cases, as evidenced by the angles of interaction, *i.e.*, 175.0° < ∠C−X···π(C≡C) (X=Cl, Br, I) < 177.5°, and also obey feature *a*. The small deviation of the angle of approach indicates that the HaB donor atom I/Br is not not covalently bonded to the midpoint of the C≡C bond but rather to a region in the vicinity of a carbon atom that manifests relatively larger nucleophilicity.

■ A CASE STUDY USING FIRST-PRINCIPLES CALCULATIONS

Whether an electrophilic σ-hole region on a halogen atom in a molecule is able to form a halogen bond depends not only on the strength of its potential but also on the nature of the interacting nucleophile and the chemical environment developed between them. Consequently, calculating the electrostatic potential on the interacting monomer entities provides a good first approximation to an understanding of the possible development of an attractive noncovalent interaction before its full characterization (see feature *r*).[115] The same insight may be gained when the ETS-NOCV approach is employed.[177]

To exemplify this, we considered an H−Cl molecule. It has an electrophilic σ-hole on the surface of the Cl atom, which appears on the side of Cl opposite to the outermost extension of the H−Cl covalent bond and may serve as an HaBD site X. We considered the nucleophiles (lone-pair region) on the halogen in three other simple molecules, *i.e.*, HF, F_2, and Cl_2, which could serve as a HaBA site Y. The electrophilic and nucleophilic regions on the electrostatic surfaces of the four molecules can be inferred from the MESP plots shown in Figure 10a−d. AIMAll[292] and MultiWfn[293,294] were used, and the wave functions were generated using their respective optimized ground state geometries obtained with Gaussian 16.[295] Second-order Møller−Plesset perturbation theory (MP2),[296,297] together with Dunning's all-electron correlated basis set, aug-cc-pVTZ, was employed.

The charge density on the electrostatic surface of the halogen is anisotropic regardless of the molecular entities examined (HF, HCl, F_2, and Cl_2). For instance, the potential on the axial and lateral sites of F along and around the H−F covalent bond extension is negative but anisotropic ($V_{S,max}$ = −18.9 kcal mol^{-1};

https://doi.org/10.1021/acs.cgd.4c00228
Cryst. Growth Des. 2024, 24, 5494−5525

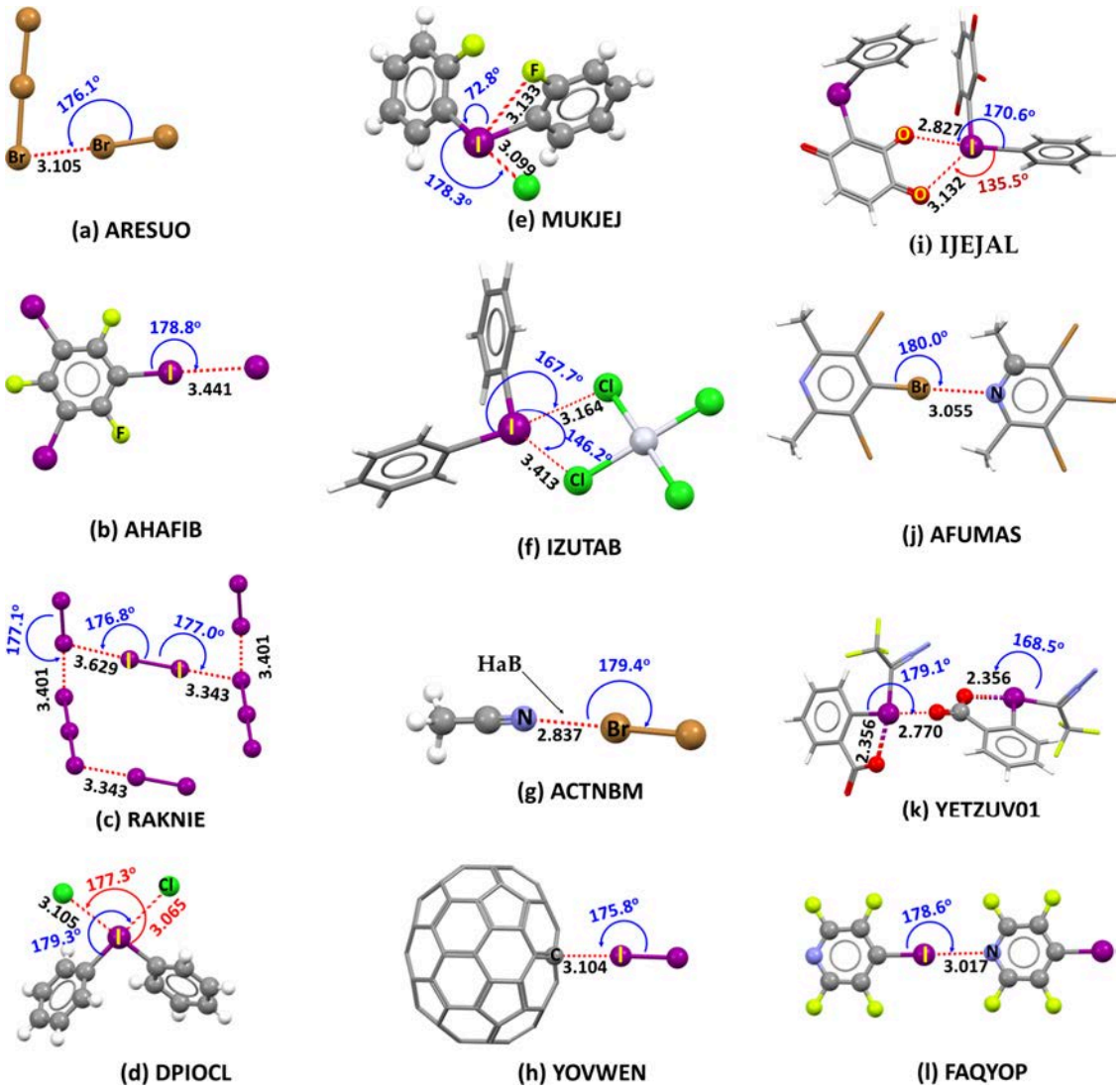

Figure 7. Illustration of the occurrence of halogen bonding between building blocks in some crystalline materials. (a) Tris(1,10-phenanthroline)-iron bis(tribromide) hemikis(dibromine) [$C_{36}H_{24}Fe\ N_6^{2+}$,2(Br_3^-),0.5(Br_2)],[272] (b) bis(2,2′:6′,2″-terpyridine)-cobalt bis(iodide) tetrakis(1,3,5-trifluoro-2,4,6-tris(iodo)benzene) methanol solvate [$C_{30}H_{22}CoN_6^{2+}$,4($C_6F_3I_3$),CH_4O,2(I^-)],[273] (c) di(isoquinolin-2-yl)iodanium tris(iodine) triiodide [$C_{18}H_{14}IN_2^+$,I_3^-,3(I_2)],[274] (d) diphenyliodonium chloride [$C_{12}H_{10}I^+$,Cl^-],[275] (e) bis(2-fluorophenyl)iodonium chloride [$C_{12}H_8F_2I^+$,Cl^-],[276] (f) bis(diphenyliodonium) tetrachloro-platinum [2($C_{12}H_{10}I^+$),Cl_4Pt^{2-}],[277] (g) bis(acetonitrile) bromine [2(C_2H_3N),Br_2];[278] (h) C_{70} fullerene di-iodine [I_2,C_{70}],[279] (i) 3,6-dioxo-2-(phenyliodaniumyl)cyclohexa-1,4-dien-1-olate [$C_{12}H_7IO_3$],[280] (j) 3,4,5-tribromo-2,6-dimethylpyridine [$C_7H_6Br_3N$],[281] (k) 1-(1-diazo-2,2,2-trifluoroethyl)-1,2-benziodoxol-3(1H)-one [$C_9H_4F_3IN_2O_2$],[282] and (l) 2,3,5,6-tetrafluoro-4-iodopyridine toluene solvate [C_7H_8,C_5F_4IN].[283] For clarity, some molecules in (a−d), (f) and (g) are omitted. Halogen bonds are represented as dotted lines in red. The CSD reference in each case is shown in uppercase letters, and selected halogen bond distances and bond angles are in Å and degrees, respectively. Labeling of selected atoms is shown in each case.

$V_{S,min}$ = −20.4 kcal mol^{-1}, Figure 10a). The F atom in H−F features a nucleophilic σ-hole ($V_{S,max}$ < 0) (see *Note 12*), and the $V_{S,\min}$ represents the lone-pair region on F that dominates. In the case of the other three molecules shown in Figure 10b−d, the strength of the electrophilic σ-hole (see Note 11) on the electrostatic surface of the halogen increases in the order: H−Cl (9.0 kcal mol^{-1}) < F−F (16.5 kcal mol^{-1}) < Cl−Cl (25.5 kcal mol^{-1}).

We then built four 1:1 dimer models (Figure 10e−h), that were fully relaxed at the [MP2/aug-cc-PVTZ] level of theory. The resulting optimized geometries of the corresponding binary systems are shown in Figure 10i−l, in which, the positive σ-hole (HaBD) in one molecule is engaged attractively with a nucleophile (HaBA) on the partner molecule (see *Notes 1−4* and *11*) and the nature of attraction between them is intermolecular (*Note 4*).

The final geometry of the dimers is very similar to the starting geometry for all cases, except for FH···ClH (*cf.* Figure 10e and Figure 10I represent initial and final (optimized) geometries, respectively). In Figure 10e, the electrophilic σ-hole on Cl in HCl was placed with its orientation toward the nucleophilic lone-pair density on F on HF. This arrangement between the two molecules did not cause any Coulombic engagement between them, despite the electrophilic σ-hole on Cl in HCl facing toward a nucleophile F on HF. The HF molecule had rather adjusted the positions of its atomic constituents during the energy-minimization process so as to maximize its Coulombic interaction with the nucleophile on the Cl atom in HCl. This led to the determination of the optimum geometry of

https://doi.org/10.1021/acs.cgd.4c00228
Cryst. Growth Des. 2024, 24, 5494−5525

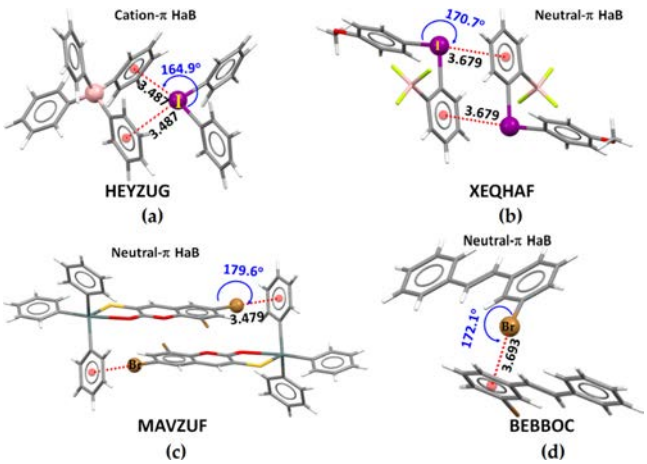

Figure 8. Illustration of mixed ball-and-stick and capped stick models of (a) diphenyliodonium tetraphenylborate [$C_{12}H_{10}I^+$,$C_{24}H_{20}B^-$],[284] (b) trifluoro[2-[(4-methoxyphenyl)iodaniumyl]phenyl]borate [$C_{13}H_{11}BF_3IO$],[285] (c) (6,8-dibromo-3-sulfanyl-2H-1-benzopyran-2-one-O,S)-triphenyl-tin [$C_{27}H_{18}Br_2O_2SSn$],[286] and (d) 1-bromo-3-(2-phenylethenyl)benzene [$C_{14}H_{11}Br$].[287] Halogen bonds are represented as dotted lines in red. The CSD reference in each case is shown in uppercase letters, and selected halogen bond distances and bond angles are in Å and degrees, respectively. The tiny sphere at the center of the arene moiety in molecules (a−d) represents the centroid. Labeling of selected atoms is shown in each case.

ClH···FH (Figure 10i), which is driven by a hydrogen bond. This validates *Note 7*, as well as *Notes 6* and *16*, rationalizing a pair of neutral molecules forming complexes, as well as features *a* and *g*, revealing the overriding importance of Coulombic forces and the nature of the approach of the electrophile toward the lone-pair region.

For chemical systems in Figure 10j−l, the σ-hole-centered lone-pair type interaction leading to the formation of the HaB may be seen: HCl···FH in Figure 10j, HCl···F_2 in Figure 10k, and HCl···Cl_2 in Figure 10l. The formation of a HaB in HCl···FH in Figure 10j accords with the hypothesis in *Note 12* that a nucleophilic σ-hole on F in HF attracts an electrophilic σ-hole on Cl in HCl. In all cases, the interaction energy, ΔE, is negative, in agreement with feature *b*. The quasi-linear nature of the directionality associated with the intermolecular interactions in the binary systems is consistent with *Note 9*; that two halogen atoms in two different molecules can be attractively engaged to form a halogen bond is in line with *Note 14*, including the validation of features *a*, *b*, and *d*−*g*.

Some previous studies have demonstrated that an electrophilic σ-hole in a molecule can attract an electrophilic σ-hole on another interacting molecule, thus forming a halogen···halogen interaction. An attractive interaction, albeit weak, develops between them as a result of a marginal difference in charge density between the interacting regions,[68,298] which may also involve some charge transfer between the HOMO and LUMO orbitals. These halogen···halogen interactions are not halogen bonds as far as the definition is concerned, and it is not easy to guess which atom is an electrophile and which one is a nucleophile. These have been referred to as "counterintuitive" interactions[79,84,95] or "unconventional bonds".[93] The stability of these complexes arises largely from the dispersion and polarization contributions to the interaction energy.[80,84] Similarly, the intramolecular halogen···halogen contacts observed in perhalogenated ethanes, X_3C-CY_3 (X, Y = F, Cl),[91] and hexahalogenated benzene derivatives (*viz.*, C_6X_6 (X = Cl, Br, I)), along with their seven fully mixed hexahalogenated benzene analogues,[92] should not be regarded as halogen bonds as per the definition and insofar as *Notes 2*, *6*, *7*, and *17* and feature *a* are concerned.

Nevertheless, in all four dimers of Figure 10, the intermolecular bond distance is smaller than the sum of the vdW radii of the noncovalently bonded atomic basins, and the intermolecular interactions are directional (cf. *Note 9* and feature *e*). The appearance of dotted bond paths and nonzero

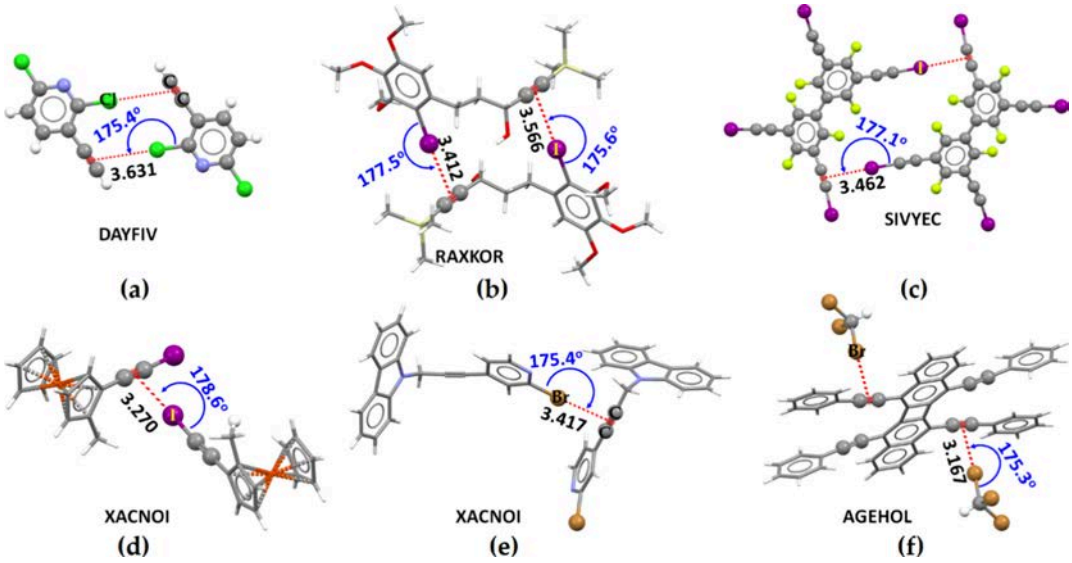

Figure 9. Illustration of the halogen bonding interaction between neutral molecules formed between HaBD X and the acetylenic (negative) π-density on HaBA Y in some crystals. (a) 2,6-Dichloro-3-ethynylpyridine ($C_7H_3Cl_2N$),[288] (b) (3*R*)-5-(2-iodo-3,4,5-trimethoxyphenyl)-1-(trimethylsilyl)pent-1-yn-3-ol ($C_{17}H_{25}IO_4Si$),[289] (c) 2,2′,4,4′,6,6′-hexafluoro-3,3′,5,5′-tetrakis(iodoethynyl)biphenyl ($C_{20}F_6I_4$),[202] (d) (*R*)-1-methyl-2-(iodoethynyl)-ferrocene ($C_{13}H_{11}FeI$),[290] (e) 9-[3-(2-bromopyridin-4-yl)prop-2-yn-1-yl]-9*H*-carbazole ($C_{20}H_{13}BrN_2$),[291] (f) 5,6,11,12-tetrakis(phenylethynyl)dibenzo[b,h]biphenylene bromoform solvate ($C_{52}H_{28}$,2($CHBr_3$)).[184] Selected atom types, bond distances (Å), and bond angles (degree) are shown; the CSD ref code for each case is depicted in uppercase letters.

https://doi.org/10.1021/acs.cgd.4c00228
Cryst. Growth Des. 2024, 24, 5494−5525

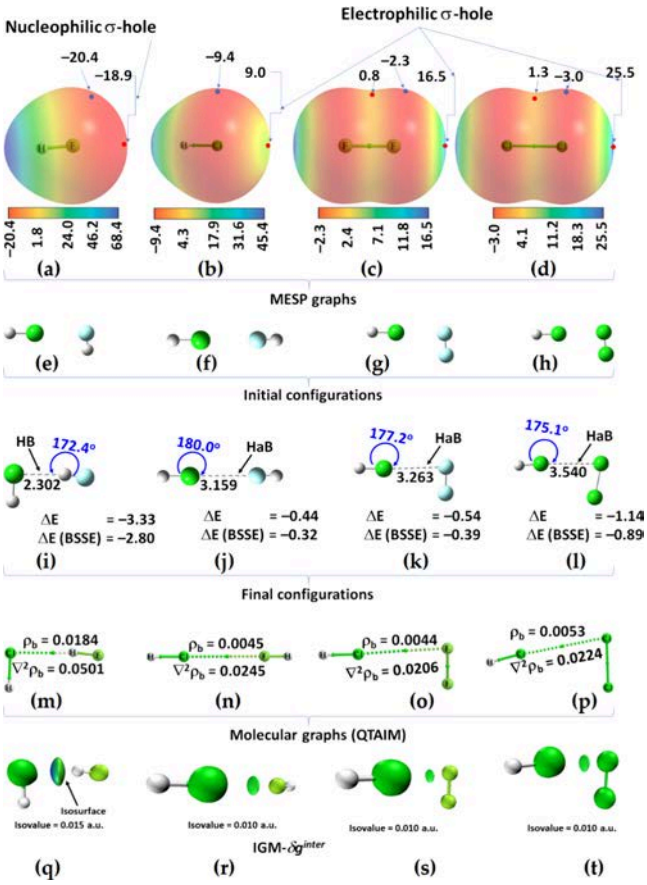

Figure 10. [MP2/aug-cc-pVTZ]-computed potential on the electrostatic surfaces of (a) HF, (b) HCl, (c) F_2, and (d) Cl_2, mapped on their respective 0.001 au (electrons bohr^{-3}) isoelectronic density envelopes. The tiny circles in red and blue represent $V_{S,max}$ and $V_{S,min}$, respectively, and values in the color bar are in kcal mol^{-1}. (e−h) Initial configurations of selected dimers of HCl with (e and f) HF, (g) with F_2, and (h) with Cl_2) used for energy-minimization. (i−l) Energy-minimized geometries of the corresponding dimers from (e−h), respectively; selected bond distances and bond angles are in Å and degrees, respectively, and the uncorrected and BSSE-corrected interaction energies (ΔE and ΔE(BSSE)) are in kcal mol^{-1}. (m−p) QTAIM-based molecular graphs of the corresponding dimers. Atoms are shown as large spheres; bond paths are shown as solid and dotted lines that represent covalent and noncovalent interactions, respectively; bond critical points are shown as tiny spheres between atomic basins; and the charge density (ρ_b) and the Laplacian of charge density ($\nabla^2\rho_b$) values at selected bcps are given in a.u. (q−t) IGM-δg^{inter} isosurfaces (colored blue or green) of the corresponding dimers.

charge density (ρ_b) values at the bond critical points (bcps) between the interacting molecules (cf. Figure 10m−p) provide evidence of the presence of noncovalent closed-shell interactions (feature *l*), and the positive signs of the Laplacian of the charge density ($\nabla^2\rho_b$) at these bcps confirm that they are closed-shell interactions.[299−305] These results are in agreement with the results of IGM-δg^{inter} that reveal (attractive) isosurfaces between atomic basins corresponding to the interacting monomers in each dimer configuration (feature *m*). The isosurfaces are colored bluish-green for the weak attractive interaction in FH···ClH (see Figure 10q) and green for the vdW-type interaction in HCl···FH, HCl···F_2, and HCl···Cl_2 in (cf. Figure 10r−t).

An evaluation of the dissected interaction energy of each dimer was performed at the [SAPT2 + 3(CCD)/aug-cc-pVTZ] level of theory; this was based on the wave function and density functional descriptions of the monomers and the dimers, and the interaction energy is the difference between the two. (CCD refers to the coupled-cluster double equations[306] that account for dispersion, and SAPT is symmetry-adapted perturbation theory.[307]) This approach has been successful in explaining intermolecular interactions in a variety of chemical systems.[308] SAPT, coded in PSI4,[309] decomposes the net interaction energy into four components: electrostatics, exchange, induction (polarization), and dispersion terms.

Our [SAPT2 + 3(CCD)/aug-cc-pVTZ]-based results are summarized in Table 1; they were computed using the [MP2/aug-cc-pVTZ] geometry of each dimer. From the results, it is apparent that the energy due to dispersion supersedes the individual component energy arising from electrostatics and induction for the three halogen bond systems (Figure 10j−l). All three attractive components complement the exchange (repulsion) energy without affecting the negative sign of the overall interaction energy (see features *b* and *c*).

In the case of the hydrogen bonded dimer FH···ClH (Figure 10i), the component energy due to electrostatics is larger than that arising due to induction or dispersion, revealing the greater importance of the former compared to the latter two. The nature of the total interaction energy, ΔE(SAPT2 + 3(CCD)), agrees well with the MP2-level BSSE-corrected interaction energy, ΔE[MP2/aug-cc-pVTZ], for each dimer (features *b* and *c*), where BSSE is the basis set superposition error accounted for by the counterpoise procedure of Boys and Bernardi.[310] Since the ΔE of each halogen bonded dimer is less than −1.0 kcal mol^{-1}, each can be classified as a vdW dimer. By contrast, FH···ClH can be classified as a weakly hydrogen bonded dimer since its interaction energy is greater than −1.0 kcal mol^{-1} (see feature *q*). We have not examined the NMR, UV−vis, and vibrational features of the intermolecular complexes investigated and are thus unable to comment on features *i*−*k*.

Our second-order perturbation theory analysis of the Fock matrix in NBO suggests that the second-order energy $E^{(2)}$ can explain the nature of the orbital interactions involved between

Table 1. SAPT2 + 3(CCD)-Level Decomposed Energy Components (in kcal mol^{-1}) Arising from Electrostatics, Exchange-Repulsion, Induction, and Dispersion Interactions Obtained on [MP2/aug-cc-pVTZ] Relaxed Geometries of Some Selected Dimers of HCl with HF, F_2 and Cl_2[a]

system	figure	electrostatics	exchange	induction	dispersion	ΔE(SAPT2 + 3(CCD))	ΔE[MP2/aug-cc-pVTZ]
FH···ClH	Figure 10(i)	−3.54	5.08	−2.42	−2.09	−2.97	−2.80
HCl···FH	Figure 10(j)	−0.21	0.73	−0.13	−0.74	−0.35	−0.32
HCl···F_2	Figure 10(k)	−0.23	0.73	−0.04	−0.85	−0.39	−0.39
HCl···Cl_2	Figure 10(l)	−0.55	1.74	−0.17	−1.76	−0.74	−0.89

[a]Included are the [MP2/aug-cc-pVTZ]-level basis set superposition error (BSSE) corrected interaction energies, ΔE[MP2/aug-cc-pVTZ], for the corresponding systems for comparison with ΔE(SAPT2 + 3(CCD)).

https://doi.org/10.1021/acs.cgd.4c00228
Cryst. Growth Des. 2024, 24, 5494−5525

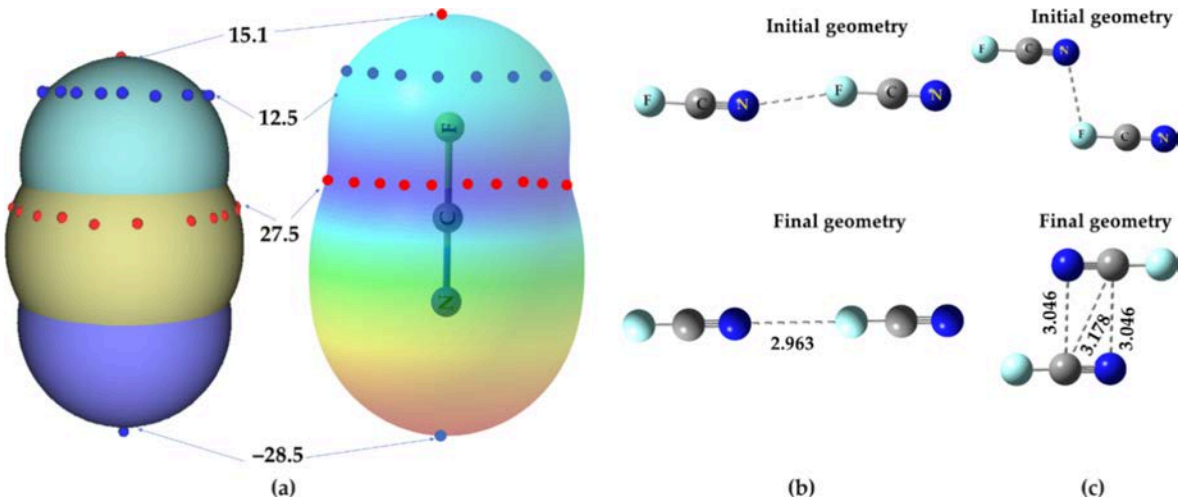

Figure 11. (a) [MP2/aug-cc-pVTZ]-level (left) van der Waals surface and (right) the 0.001 au mapped potential on the electrostatic surface the FCN molecule. (b) The initial and final geometries of two conformations of the $(FCN)_2$ dimer, with intermolecular bond distances in Å. Selected local maxima and minima of potential ($V_{S,max}$ and $V_{S,min}$, respectively), with values in kcal mol^{-1}, are shown as tiny circles in red and blue, respectively.

the "filled" (donor) Lewis-type NBOs and "empty" (acceptor) non-Lewis NBOs, shedding some light on the formation of the dimers in Figure 10i−l. $E^{(2)}$ values for the dominant charge transfer delocalizations, *viz.*, $n(3)Cl \rightarrow \sigma^*(H-F)$, $n(1)F \rightarrow \sigma^*(Cl-H)$, $n(3)F \rightarrow \sigma^*(Cl-H)$, and $n(3)Cl \rightarrow \sigma^*(Cl-H)$ explaining the dimers FH···ClH, HCl···FH, HCl···F_2, and HCl···Cl_2, are 6.39, 0.32, 0.37, and 0.59 kcal mol^{-1}, respectively, where n and σ^* represent the lone-pair and antibonding orbitals, respectively. The trend in the nature of energy of the charge transfer interaction accords with the ΔE[MP2/aug-cc-pVTZ] values for the same dimers (cf. Table 1). The orbital-based hyperconjugative interactions reflect that the σ-type antibonding orbital associated with the σ-hole portion of the molecule (HaBD) is the acceptor of charge density from lone-pair donors (HaBA), validating feature *n*.

A further example is illustrated in Figure 11 to validate *Note 16*. As far as the definition is concerned,[34] the fluorine in FCN should not form a halogen bond with the lone-pair on nitrogen on another identical molecule. This is based on the (somewhat dated) presumption that the lone-pairs on fluorine are electron-density-rich and that when both the negative sites on N and F on the two interacting molecules come in close proximity, they repel each other.

That fluorine in molecular entities can behave as an electrophile becomes apparent after applying the MESP model (as Murray et al.[115,311,312] and Scheiner[313] have noted previously). Its application enables us to demonstrate that fluorine in FCN is entirely positive, and the net electron density is concentrated on the electrostatic surface of the bonded nitrogen atom (Figure 11a). The surface of covalently bonded fluorine features a maximum and a belt of minima of potential. The axial portion on the side of F opposite to the C−F covalent bond extension has an electrophilic σ-hole, characterized by a positive $V_{S,max}$ ($V_{S,max}$ = 15.1 kcal mol^{-1}), and the lateral portion features a belt of positive $V_{S,min}$ ($V_{S,min}$ = 12.5 kcal mol^{-1}). The surface of the carbon atom has a positive π-/p-belt characteristic of the positive signs of several near-equivalent $V_{S,max}$ values ($V_{S,max}$ = 27.5 kcal mol^{-1}), and the nucleophilic region located on the surface of the bonded nitrogen atom is characterized by $V_{S,min}$ = −28.5 kcal mol^{-1}.

A question that arises is whether the axial and equatorial sites of F in FCN are both appropriately activated for halogen bond formation when in close proximity to another FCN molecule, especially when they are placed in orientations shown as the initial geometries in Figure 11b and c (top). *Notes 12* and 16 suggest that they may or they may not; according to the definition in ref 34, they may do so, based on the assumption that fluorine is sufficiently electrophilic revealed using the MESP model. However, our [MP2/aug-cc-pVTZ] calculations suggest that the linear configuration is stable (see Figure 11b (top and bottom)), while the slipped-parallel configuration (see Figure 11c (top and bottom)) is not. The interacting molecules in the latter have markedly adjusted their positions during the course of geometry optimization, producing the dimeric structure shown in Figure 11c (bottom). The uncorrected and BSSE-corrected interaction energies of the corresponding complexes are −1.53 (−1.18) and −3.81 (−3.36) kcal mol^{-1}, respectively, demonstrating the presence of noncovalent interactions that are very weak and weak, respectively. The slipped-parallel configuration is −2.26 kcal mol^{-1} more stable than quasi-linear one at the applied level of theory.

Both the dimeric structures in Figure 11b and c are local energy minima, but a halogen bond is not present in the optimized geometry of the dimer in Figure 11c (bottom). This result shows that definition alone in ref 34 in insufficient to rationalize the bonding scenario revealed for the slipped-parallel configuration, given that the formation of a halogen bond did not occur even when there was sufficient evidence of an electrophilic region on F in FCN and when it was placed in the close vicinity of the nucleophilic region in a similar neighboring molecule. However, the hypothesis developed in *Note 16* explains the failure: an electrophilic region on HaB donor X in molecules need not *always* form a halogen bond when in close proximity to an HaB acceptor Y. The slipped-parallel configuration is primarily a result of tetrel bonds driven primarily by carbon's electrophilic π-/p-belt.

■ HALOGEN'S π-/p-HOLE ON COVALENTLY BONDED HALOGEN IN MOLECULES

The similarities and differences between σ- and π-holes in molecules have been discussed.[314] Instances where a distinct π-/

https://doi.org/10.1021/acs.cgd.4c00228
Cryst. Growth Des. 2024, 24, 5494−5525

p-hole occurs on the outer surface of a covalently bonded halogen are not particularly rare,[110,176] and our investigation of the CSD came up with several examples. In the crystal of 1-(trifluorobromanyl)pyridine (CSD ref MIJQII[315]), the non-covalently bonded Br atom features a pair of negative holes on its electrostatic surface (one above and one below the plane of the molecule surrounding Br). The [ωB97X-D/aug-cc-pVTZ]-level MESP plot of the molecule, highlighting the locations of hole on Br, is shown in Figure 12a. The strength of each hole on Br is weak, each characterized by $V_{S,\min}$ of −1.2 kcal mol^{-1}; we call each a negative π-/p-hole despite the fact that such a hole on atoms in molecules is characterized by the positive or negative sign of the $V_{S,max}$ (see feature *r*). Additionally, four maxima of potential ($V_{S,max} < 0$) (two of them, marked as filled tiny red circles, face the viewer, and the remaining two are on the opposite side to the viewer) also appear in the junction region between a pair of F atoms of noncovalently bonded BrF_3, which may be also regarded as halogen's negative π-/p-hole.

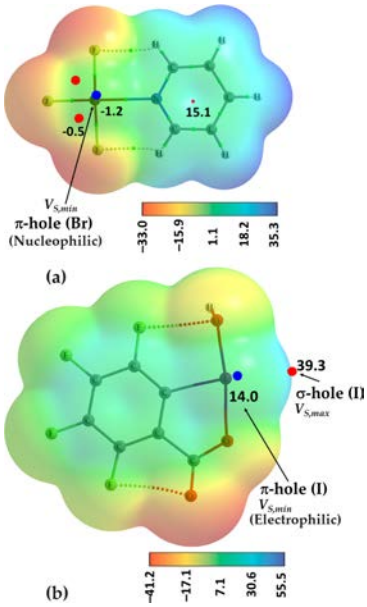

Figure 12. [ωB97X-D/aug-cc-pVTTZ]-computed potential on the electrostatic surfaces of (a) 1-(trifluorobromanyl)pyridine[315] and (b) 4,5,6,7-tetrafluoro-1-hydroxy-1λ^3,2-benziodoxol-3(1H)-one.[316] The 0.001 au isoelectronic density envelope was used to map the potential. Values are shown in kcal mol^{-1}. Selected local maxima and minima of potential ($V_{S,max}$ and $V_{S,min}$, respectively) are shown as tiny circles in red and blue, respectively. The QTAIM-based molecular graph of each molecule is superimposed; bond critical points are shown as tiny spheres in green, and bond paths that connect bonded atomic basins (large spheres) are represented by solid and dotted lines for covalent and noncovalent interactions, respectively.

The shape of the crystal structure of 1-(trifluorobromanyl)-pyridine[315] (Figure 12a) is predominantly driven by various noncovalent interactions between the building blocks, including C−H···F and $\pi\cdots\pi$ noncovalent interactions. The occurrence of (Br(π/p)···F) contacts between the interacting molecules in the crystal is likely given that *r*(Br(π/p)···F) is 3.463 Å. In addition, the rigid framework of the molecule is stabilized by two nonlinear C−H···F hydrogen-bonded intramolecular interactions (see *Note 4*), each evidenced by a dotted bond path and a (3, −1) bond critical point of charge density (Figure 12a). This is supported by feature *l* above, recommended for a HB.[55] It is worth emphasizing that halogen in many molecular entities reported in the solid state carries a negative π-/p-belt on its electrostatic surface of X ($V_{S,\min} < 0$), lying orthogonal to the bond axis (as in X_2 (X = F, Cl, Br) and dominated by its lone-pair region,[68,255,256,317] and a π-/p-belt of positive potential around the central portion of the bonding region ($V_{S,max} > 0$) (Figures 10c and d confirm this for F_2 and Cl_2, respectively.)

Planar molecules like XCl_4^- (X = Br,[318] I[319]) have a negative π-/p-hole on the surface of the halogen atom X, which is orthogonal to the molecular plane. These molecular entities may offer themselves as HaBAs for interacting HaBDs in many crystals.

Crystals featuring electrophilic π-/p-holes on covalently bonded halogen atoms are not very uncommon, and this particular feature has yet to be fully explored both experimentally and computationally. The entity 4,5,6,7-tetra-fluoro-1-hydroxy-1λ^3,2-benziodoxol-3(1*H*)-one ($C_7HF_4IO_3$), Figure 12b,[316] is one such example. In this entity, covalently bonded iodine has both a π-/p-hole and a σ-hole on its electrostatic surface orthogonal to and along the outer extension of the C−I covalent bond, respectively, characterized by the

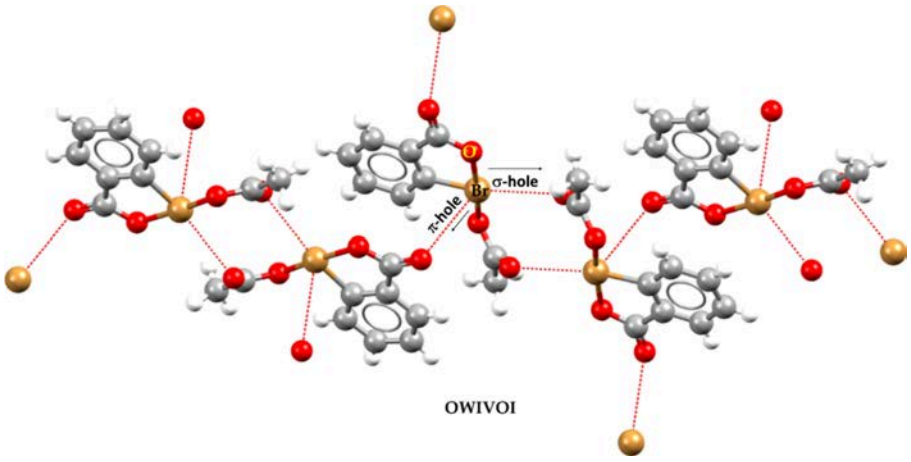

Figure 13. Anticipated networks of σ- and π-/p-hole halogen bonds formed by a covalently bonded Br atom in 1-acetoxy-1,2-bromobenzol-3(1*H*)-one ($C_9H_7BrO_4$),[320] appearing along and orthogonal to the C−Br covalent bond extensions, respectively. The CSD code is depicted in uppercase letters, and arrows indicate the respective directions of σ- and π-/p-holes. Intermolecular HaBs, including the hanging contacts, are shown as dotted lines, and the Br and O atoms are labeled.

https://doi.org/10.1021/acs.cgd.4c00228
Cryst. Growth Des. 2024, 24, 5494−5525

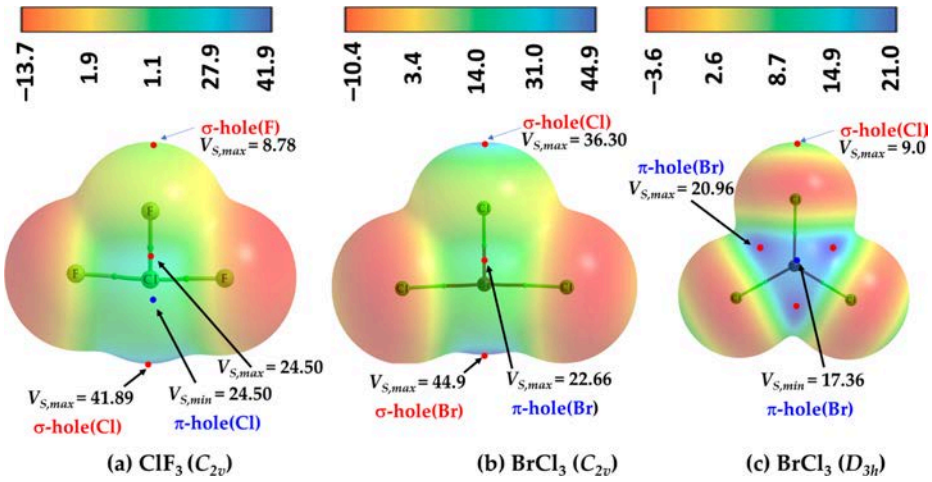

Figure 14. [ωB97X-D/aug-cc-pVTZ]-computed potential on the electrostatic surfaces of (a) ClF_3, (b) $BrCl_3$, and (c) $BrCl_3$. The 0.001 au isoelectronic density envelope was used to map the potential. Values are shown in kcal mol^{-1}. Selected local maxima and minima of potential ($V_{S,max}$ and $V_{S,min}$, respectively) are shown as tiny circles in red and blue, respectively. The point-group symmetry is depicted for each case. The QTAIM-based molecular graph of each molecule is superimposed; bond critical points are shown as tiny spheres in green, and bond paths that connect bonded atomic basins (large spheres) are represented by solid lines.

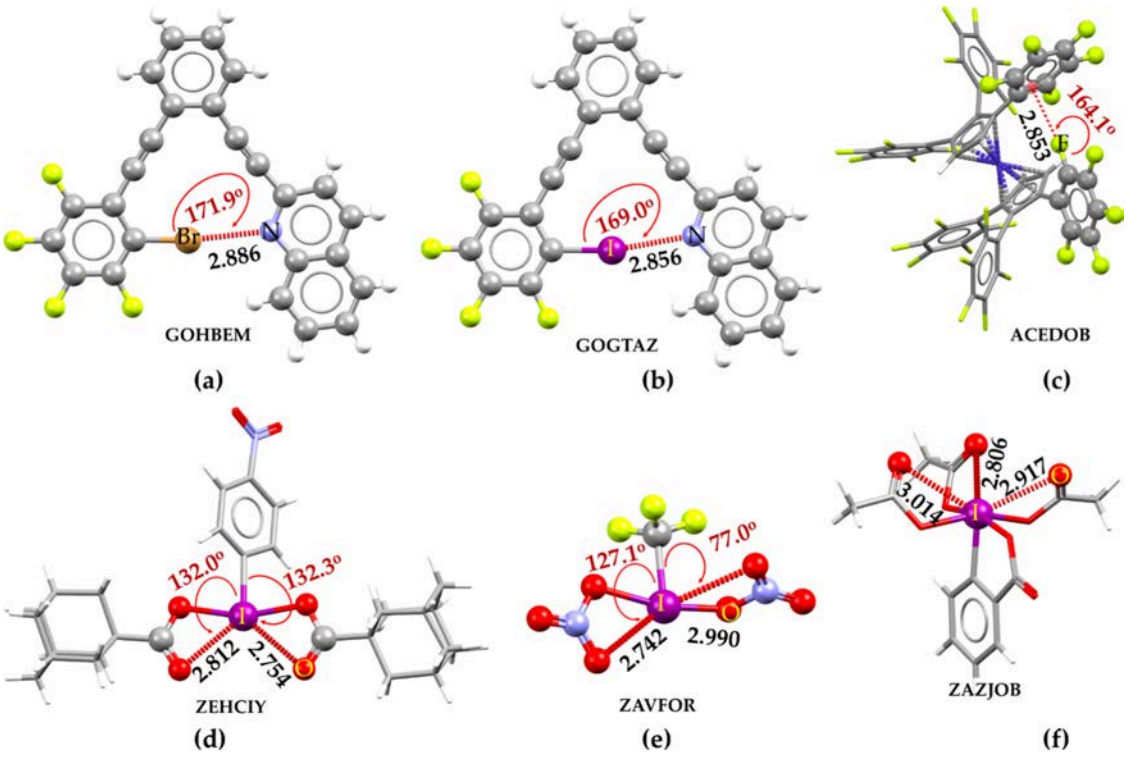

Figure 15. Selected crystal structures featuring quasi-linear and nonlinear intramolecular HaBs: (a) 2-((2-((2-bromo-3,4,5,6-tetrafluorophenyl)-ethynyl)phenyl)ethynyl)quinoline ($C_{25}H_{10}BrF_4N$),[324] (b) 2-((2-((2,3,4,5-tetrafluoro-6-iodophenyl)ethynyl)phenyl)ethynyl)quinoline ($C_{25}H_{10}F_4IN$),[324] (c) bis(η^5-1,2,3-tris(pentafluorophenyl)cyclopentadienyl)-cobalt(II) ($C_{46}H_4CoF_{30}$),[323] (d) 1-(bis(1-adamantylcarbonyloxy)-iodo)-4-nitrobenzene ($C_{28}H_{34}INO_6$),[325] (e) trifluoromethyliodine-dinitrate ($CF_3IN_2O_6$),[321] and (f) 1,1,1-triacetoxy-1λ^5,2-benziodoxol-3(1H)-one ($C_{13}H_{13}IO_8$).[326] Selected atom types, bond distances (Å), and bond angles (degree) are shown; the CSD ref code for each case is given in uppercase letters. The covalent and noncovalent (as well as halogen) bonds are shown as solid and dotted lines in atom color and red, respectively.

positive signs of $V_{S,min}$ and $V_{S,max}$ (values 14.0 and 39.3 kcal mol^{-1}). The development of a π-/p-hole on I is induced by its bonding with two neighboring O atoms.

The crystal of 1-acetoxy-1,2-bromobenzol-3(1*H*)-one ($C_9H_7BrO_4$)[320] (Figure 13) is unusual in that there is the possibility of both σ- and π-/p-hole halogen bonds, emanating from electrophilic σ- and π-/p-holes on the electrostatic surface of the covalently bonded Br. They are orthogonal to each other, and the π-/p-hole halogen bonds are shorter than the σ-hole halogen bonds. The Br(π-/p-hole)···O and Br(σ-hole)···O bond distances for HaBs are 3.498 and 3.029 Å, respectively. They are nonlinear (∠C−Br···O = 110.9°) and quasi-linear (∠C−Br···O = 161.5°), respectively, featuring opposite directional features (the latter quasi-linear and the former nonlinear) (see *Note 9*). The building blocks responsible for the extended crystal are

https://doi.org/10.1021/acs.cgd.4c00228
Cryst. Growth Des. 2024, 24, 5494−5525

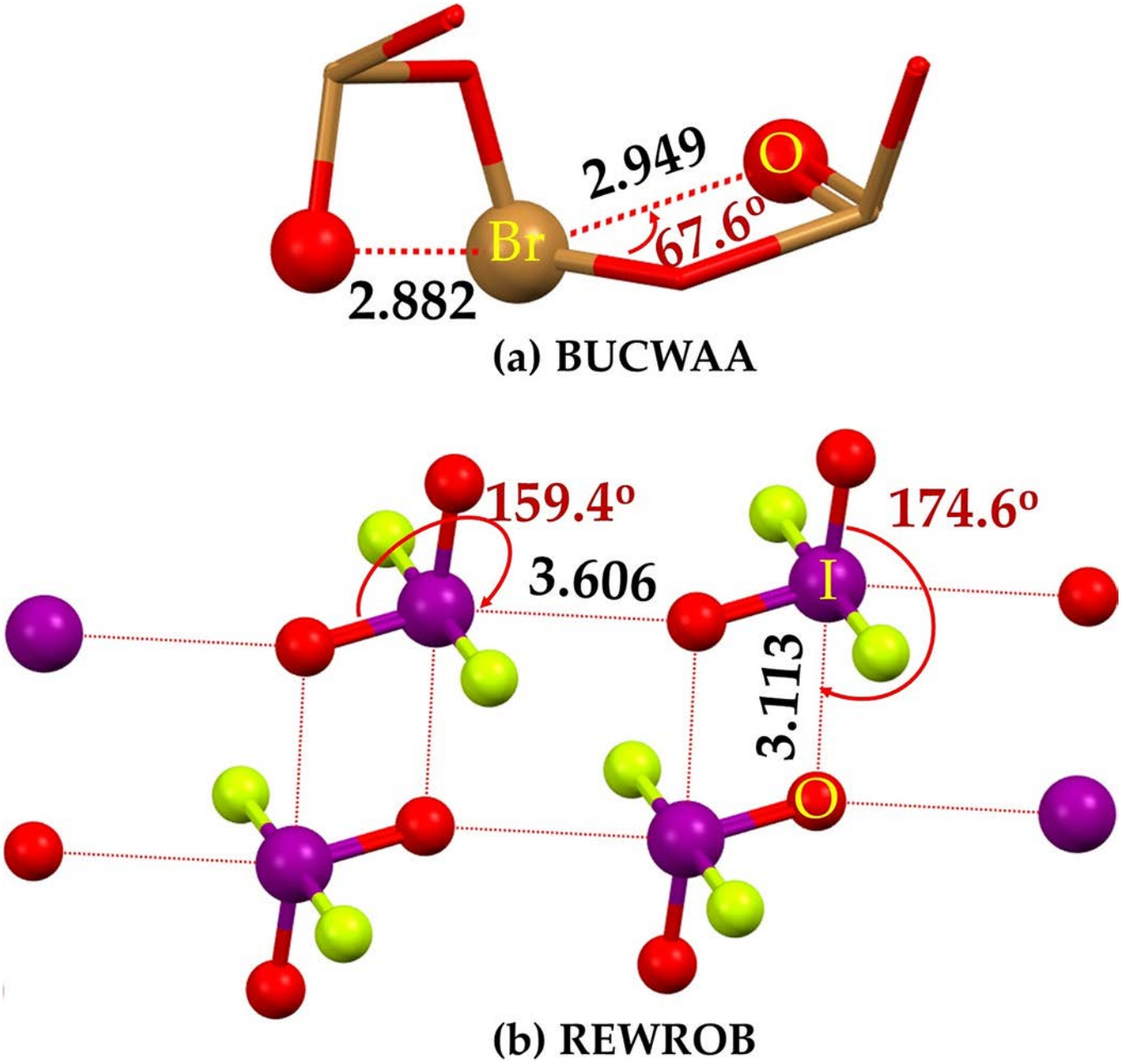

Figure 16. Ball-and-stick (or mixed with capped stick) models of (a) bis(bromyloxy)bromanium trifluoromethanesulfonate [$Br_3O_6^+$,$CF_3O_3S^-$][328] and (b) tetramethylammonium (difluoro(oxido)-λ^3-iodanyl)oxidanide [$C_4H_{12}N^+$,$F_2IO_2^-$].[329] For clarity, the anion and cation, respectively, in (a) and (b) are not shown. Selected bond distances (angles) are in Å (degrees). The CSD code is depicted in uppercase letters, and hanging/HaB contacts are present as dotted lines in red. Labeling of selected atoms in shown in each case.

linked to each other, among other interactions, through these halogen bonds.

Trifluoromethyliodine-dinitrate ($CF_3IN_2O_6$) (CSD ref ZAVFOR)[321] is another crystal system that features an extensive network of I(π-/p-hole)···O and I(σ-hole)···O halogen bonds between the building blocks, with close contact distances ranging between 3.1 and 3.6 Å (not shown). The geometry of the pentafluorophenyliodinedifluoride molecule in the crystal (CSD ref MEKGIS)[322] (not shown) is stabilized by I(π-/p-hole)···F intramolecular halogen bonds; there are two such close contacts with r(I···F) = 3.175 Å and ∠C−I···F = 48.1°.

Three simple halogenated molecules, which were geometry-minimized with [ωB97X-D/aug-cc-pVTZ], are shown in Figure 14a−c. They are stationary points with different point-group symmetries. Each of these displays a pair of electrophilic π-/p-holes on the surface of the central halogen atom that connects to three nearest neighbors; these pairs occur on both sides of, and orthogonal to, the molecular plane. The π-/p-holes are described by the positive sign of $V_{S,max}$ or $V_{S,min}$ (marked by arrows), in which the hypervalent halogen features both σ- and π-/p-holes on its electrostatic surface. For instance, $V_{S,min}$ is 17.70 and 20.96 kcal mol^{-1} on Cl in ClF_3 (Figure 14a) and $BrCl_3$ (Figure 14c), respectively, whereas $V_{S,max}$ is 22.66 kcal mol^{-1} on Br in $BrCl_3$ (Figure 14b). Because of their electrophilic nature, the π-/p-holes on these molecules may be able to engage with nucleophiles on molecules to form π-/p-hole-centered HaB interactions.

https://doi.org/10.1021/acs.cgd.4c00228
Cryst. Growth Des. 2024, 24, 5494−5525

To substantiate this view, one of us recently examined the electrophilic π-/p-hole on Br in $BrCl_3$ (HaBD) halogen bonded to the nitrogen/oxygen/carbon ends of N_2, CO, and CS molecules (HaBAs). The [MP2/aug-cc-PVTZ]-level basis set superposition-corrected interaction energies for Br(π-/p-hole)···N, Br(π-/p-hole)···O, and Br(π-/p-hole)···C halogen bonds in the corresponding complexes are ca. − 1.77, − 1.31, and −3.90 kcal mol^{-1}, respectively. The study provides a detail of the noncovalent bonding modes of halogen's π-/p-hole in some of these hypervalent molecules, along with their bond strengths and charge density topologies.[110] Some argue that $V_{S,max}$, but not $V_{S,min}$, on the surface of a molecular entity is the only descriptor to characterize the presence or absence of a π-/p-hole. The current chemical instances (Figures 12 and 14) clarify this, showing that the positive and negative signs of the $V_{S,min}$ may also be used as a descriptor to characterize a positive and negative π-/p-hole on molecular surfaces, respectively.

■ INTRAMOLECULAR HALOGEN BONDING AND OTHER COUNTERINTUITIVE HALOGEN-ASSISTED HALOGEN BONDED INTERACTIONS

While many crystal structures featuring intermolecular HaBs have been deposited in the CSD, there are a handful displaying intramolecular HaBs in which covalently bonded I and Br atoms act as HaBs. Shown in Figure 15 are six crystal systems that feature intramolecular HaB interactions within the building block, with four different types of nucleophiles (N, F, O, and $(C{=}C)_\pi$). In Figure 15a and b, the nucleophile is a covalently bonded nitrogen atom, whereas in Figure 15c and d−f, respectively, the π-density of the C═C double bond and lone-pair density on covalently bonded O serve as nucleophiles for the HaBDs. As can be seen, the Br···N and I···N halogen bonds are quasi-linear and shorter than sum of the vdW radii of X and N (X = Br, I).[249] This validates *Note 9*; intramolecular halogen bonds do not always follow a type I topology of noncovalent bonding interactions, and they can have a type II bonding topology depending on the spatial arrangement of the interacting basins giving rise to the halogen bond. The same argument is transferable to the quasi-linear F···$(C{=}C)_\pi$ halogen bond observed in the crystal of the transition metal complex bis(h^5-1,2,3-tris(pentafluorophenyl)cyclopentadienyl)-cobalt-(II) (Figure 15c).[323]

Nonlinear intramolecular halogen bonds are found in the crystals shown in Figure 15d−f, evidenced by ∠C−I···O/∠O−I···O < 150.0° (see *Note 9*). The presence of I···O close contacts in these molecules may not be appreciated based on the definition of a halogen bond proposed in ref 34 or the one developed in this study. The directional aspects (*Note 9* and feature *f*) and intramolecular distances less than the sum of the vdW radii (feature *d*) are the key geometric aspects required to recognize the halogen bonds in these molecular entities. Because electron-withdrawing fragments are covalently bonded with the hypervalent iodine atom in Figure 15d−f, it is expected they are capable of inducing electrophilic regions on the electrostatic surface of covalently bonded I along the C−I (and O−I) bond extensions, thereby developing an ability to halogen bond with the nearest nucleophiles on covalently bonded O. The crystal of 1,1,1-triacetoxy-1λ^5,2-benziodoxol-3(1*H*)-one ($C_{13}H_{13}IO_8$)[326] (Figure 15f), shows that the covalently bonded I atom can simultaneously form three I···O intramolecular HaBs with bond distances (∠C−I···O/∠O−I···O bond angles of interactions) of 3.104 (119.8 °), 2.806 (∠O−I···O = 141.2°), and 2.917 Å (148.3°). Potential nonlinearity in two of these HaBs indicates the involvement of a π-/p-type orbital in forming HaBs and the remaining one that develops along the extension of the C−I bond is a σ-hole HaB.

Two more crystal systems that contain halogen bonds that may not be obvious are shown in Figure 16. The geometry of the cation $[Br_3O_6]^+$, accompanied by two intramolecular nonlinear Br···O close contacts (r(Br···O) = 2.882 and 2.949 Å), is shown in Figure 16a. The $[Br_3O_6]^+$ units, in the presence of the anion (not shown), are bonded to each other via quasi-linear Br···O close contacts (∠O−Br···O = 160.0° and r(Br···O) = 2.916 Å). The bond distances associated with these contacts are appreciably smaller than the vdW radii of Br (r_{vdW}(Br) = 1.86 Å) and O (r_{vdW}(O) = 1.50 Å). The geometric stability of the crystal arises from the attraction between ions of opposite charge, which introduces nucleophiles on the O atoms in an ion-pair, and then engage attractively with another ion-pair via σ-hole driven Br···O halogen bonds. Similarly, Figure 16b shows the geometry of an inorganic layer-like structure formed by $[F_2IO_2]^-$ anions, which is a result of an extensive network of directional I···O noncovalent bonding interactions. They are I(σ-hole)-driven halogen bonds; the stability of the entire ion-pair adduct emerges due to the presence of the tetramethylammonium cation $[C_4H_{12}N]^+$, which induces electrophilic σ-holes on I that engage with a nucleophilic region on O.

To confirm the view developed above, we performed DFT calculations for the ammonium dioxo(difluoro)iodane, $[F_2IO_2]^-][NH_4]^+$, ion-pair, the crystal structure of which has been reported (CSD ref JELFOZ).[327] Our calculations suggest that the electrophilic σ-hole develops ($V_{S,max}$ = 28.1 kcal mol^{-1} with ωB97X-D/aug-cc-pVTZ (for all atoms) and aug-cc-pVTZ-PP (for I)) along the outer extensions of the two O−I covalent bonds in $[F_2IO_2]^-$, and the nucleophilic region ($V_{S,min}$ = −35.3 kcal mol^{-1}) is mainly concentrated around the O atom upon the formation of the $[F_2IO_2]^-][NH_4]^+$ ion-pair. These sites of opposite polarity on the O and I atoms on neighboring ion pairs attract each other, thus forming halogen bonds that are responsible for the stability of the inorganic layer in the crystal. This is consistent with what was demonstrated for organic−inorganic halide perovskites.[54,93] Clearly, the IUPAC-recommended definition and features[33] fail to identify and characterize HaB in these crystal systems. However, the definition provided in this study, accompanied by *Notes 11*, *12*, and *16*, enables one to characterize the close contacts as halogen bonds.

■ FURTHER EXAMPLES OF CATION-ASSISTED HALOGEN BONDS AND p-BELT HALOGEN BONDS

Further examples of chemical systems in which a cation that contains covalently bonded iodine (HaBD) can be attractively engaged with different anions (HaBA) to form halogen bonds are shown in Figure 17. Many such crystal systems where the solid-state structure is stabilized by charge-assisted halogen bonds can be found in the CSD. Shown in Figure 17a and b are illustrative cases where the development of I(σ-hole)···Cl and I(σ-hole)···O halogen bonds between interacting ion-pairs occur along the outer extension of the C−I covalent bonds, respectively, whereas that shown in Figure 17c consists of both I(σ-hole)···O and I(π-/p-hole)···O halogen bonds. Each of the I(σ-hole)···Cl, I(σ-hole)···O and I(π-/p-hole)···O intermolecular distances in these three ion-pairs is less than the sum of the vdW radii of respective bonded atomic basins. The first two are quasi-linear, and the third is an orthogonal nonlinear interaction. The crystal system shown in Figure 17c demonstrates the hypervalent character of covalently bonded iodine that is

https://doi.org/10.1021/acs.cgd.4c00228
Cryst. Growth Des. 2024, 24, 5494−5525

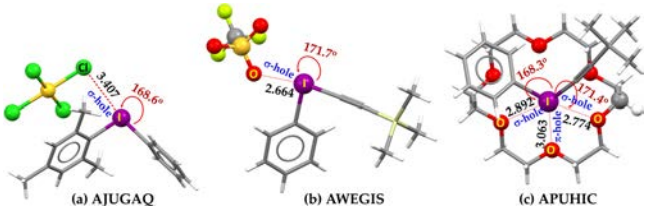

Figure 17. Mixed ball-and-stick and capped stick models of some selected ion-pairs from the CSD, showing (a and b) σ-hole and (c) σ and π-/p-hole halogen bonds: (a) phenyl(2,4,6-trimethylphenyl)-iodonium tetrachloro-gold(iii) [$C_{15}H_{16}I^+$,$AuCl_4^-$],[330] (b) (2-(trimethylsilyl)ethynyl)phenyliodonium trifluoromethanesulfonate [$C_{11}H_{14}ISi^+$,$CF_3O_3S^-$],[331] and (c) (*tert*-butylethynyl)(phenyl)(tetrafluoroborato)-λ^3-iodane 12-crown-6 clathrate [$C_{12}H_{14}I^+$,BF_4^-,0.5($C_{12}H_{24}O_6$)].[332] For clarity, tetrafluoroborato in (c) is omitted. Selected bond distances (Å) and bond angles (degrees) associated with the halogen bond are depicted. The CSD ref code is depicted in uppercase letters. Labeling of selected atoms in shown in each case.

capable of forming more than two halogen bonds with the nucleophilic O in 12-crown-6. The assigned halogen bonds in the crystals accord with *Note 15*: cations containing halogen derivatives can act as HaBDs and thus can be prone to form halogen bonds with close-lying nucleophiles on a neighboring molecule.

Figure 18a and b shows further examples of chemical systems in which each is stabilized by a "p-belt halogen bond", driven by

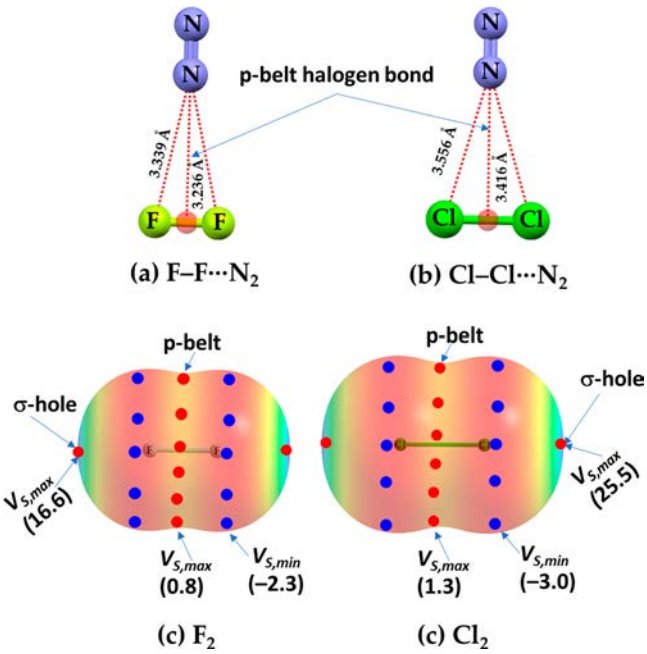

Figure 18. Ball-and-stick model of the [MP2/aug-cc-pVTZ]-optimized geometries of (a) F−F···N_2 and (b) Cl−Cl···N_2 dimers, illustrating the "p-belt halogen bond" between interacting monomer molecules. (c and d) Nature of extrema on the electrostatic surface of the F_2 and Cl_2 molecules, respectively; the filled tiny circles colored blue and red represent the minima and maxima of potential, respectively, with values of potential (kcal mol^{-1}) in parentheses. The potential associated with each tiny circle in a given ring is near-equivalent to the other. The σ-hole and p-belt regions are marked. The 0.001 au isoelectronic density was used to compute the potential. The dotted lines in a and b represent intermolecular contacts and the tiny sphere represents the mid-point of the X_2 bond (X = F, Cl).

an electron-density deficient p-type belt appearing around the bonding region in X_2. They are not examples of a "π-/p-hole halogen bond" considering that there is no real "hole" on the pseudo-ring/belt-like surface (see Figure 18c and d for the MESP plots of F_2 and Cl_2, respectively). Each dimer is a saddle-point structure at the applied level of theory.

The [MP2/aug-cc-pVTZ]-level uncorrected (and BSSE corrected) interaction energies were found to be −0.37 (−0.19) and −0.85 (−0.54) kal mol^{-1} for F−F···N_2 and Cl−Cl···N_2, respectively. The formation of F−F···N_2 and Cl−Cl···N_2 dimers was accompanied by the contraction of the F−F and Cl−Cl bonds, respectively. The corresponding bond distances of the isolated F_2 and Cl_2 molecules were 1.4014 and 1.9987 Å, respectively, decreasing by 0.0003 and 0.0012 Å, respectively, in F−F···N_2 and Cl−Cl···N_2 (feature *h*). The IR vibrational modes were blue-shifted by 0.3 and 0.7 cm^{-1} relative to the harmonic frequencies of 1003.3 and 573.6 cm^{-1} for isolated F_2 and Cl_2, respectively (feature *i*). The formation of a p-type halogen bond in each dimer is evidenced by the intermolecular Coulombic engagement (feature *a*) between the bonding region in X_2 (characterized by a p-type belt with $V_{S,max} > 0$; see Figure 18c and d) and the lone-pair electron-density-rich region localized on the side of N atom opposite to N_2's covalent bond[186] characterized by $V_{S,\min} < 0$ (*Note 15* and feature *r*). The intermolecular distances between the midpoint of the X_2 bond and N-end of N_2 are 3.236 and 3.416 Å for F−F···N_2 and Cl−Cl···N_2, respectively; the vdW criterion (feature *d*) may not be applicable to these systems.

■ CONCLUDING REMARKS

Halogen bonds are a special subset of noncovalent interactions that are central to the synthesis of a large body of crystalline materials. They are the inter- and/or intramolecular key forces for the design of such crystals and their growth, shape, and functionalities, and they are observed in areas as diverse as chemistry, biology, materials science, and crystal engineering. They were regarded as a charge transfer interaction (intermolecular hyperconjugation) in the days of Odd Hassel.[333] Although it took decades for researchers to recognize halogen bonds in crystals and develop a basic understanding of their nature and characteristics,[57] the conceptual framework of σ-[37,56,57] and π-hole theory[41,58,59] has brought them to light, revealing the nature of electron-density-deficient and electron-density-rich regions on halogens in molecules and the directional features that explain the character of halogen bonds in chemical systems. Without the concept of umbrella terms, such as σ- and π-/p-holes (or π-/p-belt), an understanding of halogen bonding is far from complete. Moreover, halogen bonding is not always determined by the positive σ-hole of the halogen in molecules.[334]

While the IUPAC working group has so far proposed a quasi-formal definition of halogen bonding and presented its (limited) features and characteristics,[34] the present study has extended the concept by adding annotations and illustrative crystal systems to clarify the essence of chemical instances in which halogen bonds occur and thus illustrate their versatility. It also discussed the concept of the electrophilic σ-and π-holes on halogens as HaB donors in molecules that cause the development of attractive interactions with nucleophiles in close proximity, an important aspect of noncovalent interaction that is missing in the proposed IUPAC definition of a halogen bond.[34] Despite the presence of many records in the CCDC highlighted in this revisit, theoretical studies centering on the halogen-bond-forming ability of

https://doi.org/10.1021/acs.cgd.4c00228
Cryst. Growth Des. 2024, 24, 5494−5525

halogen's electrophilic π-/p-holes (or π-/p-belts) in molecular entities with nucleophiles are rare and surely an important area worthy of further investigation. The development of a hole/belt may be realized as a result of "bond polarization" within the domain of the molecule, a view consonant with that of others.[335]

We believe that invoking the concept of the σ- and π-/p-holes and orbital-based charge transfer characteristics, among others, assists in the recognition and basic understanding of the halogen bond and other noncovalent interactions. The formation of halogen bonds between sites of opposite charge capacity fits within the theoretical framework of a Coulombic attraction, but it should be appreciated that the overall stability of the complex chemical system is the result of a delicate balance between different types of attraction (*i.e.*, electrostatics, dispersion and induction/polarization) and repulsion (*e.g.*, exchange repulsion), in which the net interaction/binding energy is difficult to dissect.

IUPAC's feature "the angle R−X···Y tends to be close to 180°, *i.e.*, the halogen bond acceptor Y approaches X along the extension of the R−X bond" is applicable only to "σ-hole halogen bonds" but fails to identify "π-/p-hole halogen bonds" (or "π-/p-belt halogen bonds") formed by halogen's π-/p-hole (or π-/p-belt) in molecules, especially when it engages attractively with negative sites on a neighboring interacting molecular entity.

The definition that the IUPAC working group previously proposed[34] and that was advanced in this work may not be applicable to antielectrostatic halogen bonds, a concept that has been developed elsewhere.[90] This is because the molecular/crystal adducts formed between anionic moieties as halogen bond donors and acceptors (as Lewis acids and Lewis bases) seem counterintuitive. By placing an electron-withdrawing substituent on the Lewis base, the sign of the potential in its lone pair or π-bond region can be altered to positive, and this base can then engage in making a halogen-centered noncovalent interaction with the positive σ-hole of the Lewis acid.[95] Since two positive sites are involved in making the intermolecular interaction, should we call this a HaB? Both the previous[34] and current definitions, along with various annotations and features presented in this study, do not recognize this as a HaB. The definitions are applicable to neither intramolecular halogen···halogen close contacts in halogenated molecules nor positive−positive and negative−negative intermolecular interactions formed by participating halogen derivatives as seen in some molecular complexes. It is not always straightforward to visualize/rationalize whether the occurrence of the latter type interaction is the result of an electrophilic σ-hole induced in the covalently bound halogen by the electric field generated by the interacting partner molecules. However, chemical instances are presented featuring counterintuitive or unconventional noncovalent interactions in which the close contacts between halogen and nucleophiles are perhaps not readily recognized as halogen bonds. They are indeed halogen bonds (see Figure 16b, for example), based on the fact that electrophilic regions on halogen can be induced on anions or the charge density profile on bonded halogen atoms in cations can be altered when they form ion-pair adducts. The newly developed electrophiles on the halogen derivative in these ion-pairs are capable of forming halogen bonds with nucleophiles on a neighboring molecular entity to form extended crystals. We believe that the hypotheses listed in this study as *Notes* are an important aspect of this revisit, not only clarifying the delicate aspects of the current definition, but also serving as a prerequisite for a better understanding and characterization of HaBs in chemical systems.

■ ASSOCIATED CONTENT

Data Availability Statement

All data used are readily accessible using the references in the paper.

■ AUTHOR INFORMATION

Corresponding Author

Pradeep R. Varadwaj − *Department of Chemical System Engineering, School of Engineering, The University of Tokyo 7-3-1, Tokyo 113-8656, Japan; Molecular Sciences Institute, School of Chemistry, University of the Witwatersrand, Johannesburg 2050, South Africa;* orcid.org/0000-0002-7102-3133; Email: pradeep@t.okayama-u.ac.jp, prv.aist@gmail.com

Authors

Arpita Varadwaj − *Department of Chemical System Engineering, School of Engineering, The University of Tokyo 7-3-1, Tokyo 113-8656, Japan;* orcid.org/0000-0001-8779-789X

Helder M. Marques − *Molecular Sciences Institute, School of Chemistry, University of the Witwatersrand, Johannesburg 2050, South Africa;* orcid.org/0000-0003-1675-3835

Koichi Yamashita − *Department of Chemical System Engineering, School of Engineering, The University of Tokyo 7-3-1, Tokyo 113-8656, Japan;* orcid.org/0000-0002-6226-3194

Complete contact information is available at: https://pubs.acs.org/10.1021/acs.cgd.4c00228

Author Contributions

Conceptualization, project design, and project administration, P.R.V.; formal analysis and investigation, P.R.V. and A.V.; software, P.R.V., H.M.M., and Y.M.; supervision, P.R.V.; writing−original draft, P.R.V.; writing−review, editing, discussion, and validation, P.R.V., A.V., H.M.M., and K.Y. All authors have read and agreed to the published version of the manuscript.

Funding

This research received no external funding.

Notes

The authors declare no competing financial interest.

■ ACKNOWLEDGMENTS

This work was entirely conducted using various laboratory facilities provided by the University of Tokyo (TU) and the University of the Witwatersrand. P.R.V. is currently affiliated with the University of the Witwatersrand (SA) and Nagoya University (Japan). A.V. is currently affiliated with Tokyo University of Science (Japan). K.Y. is currently affiliated with Yokohama City University (Japan). H.M.M. thanks the University of the Witwatersrand for funding. We are grateful to Prof. Jane Murray and the three reviewers for their excellent criticisms, which improved the scientific and technical quality of this manuscript.

■ REFERENCES

(1) Brammer, L.; Peuronen, A.; Roseveare, T. M. Halogen bonds, chalcogen bonds, pnictogen bonds, tetrel bonds and other [sigma]-hole

interactions: a snapshot of current progress. *Acta Crystal. C* **2023**, *79* (6), 204−216.
(2) Cavallo, G.; Metrangolo, P.; Milani, R.; Pilati, T.; Priimagi, A.; Resnati, G.; Terraneo, G. The Halogen Bond. *Chem. Rev.* **2016**, *116* (4), 2478−2601.
(3) Varadwaj, P. R.; Varadwaj, A.; Marques, H. M. Halogen Bonding: A Halogen-Centered Noncovalent Interaction Yet to Be Understood. *Inorganics* **2019**, *7* (3), 40.
(4) Nunes, R. S.; Vila-Viçosa, D.; Costa, P. J. Halogen Bonding: An Underestimated Player in Membrane−Ligand Interactions. *J. Am. Chem. Soc.* **2021**, *143* (11), 4253−4267.
(5) Lin, F.-Y.; MacKerell, A. D., Jr. Do Halogen−Hydrogen Bond Donor Interactions Dominate the Favorable Contribution of Halogens to Ligand−Protein Binding? *J. Phys. Chem. B* **2017**, *121* (28), 6813−6821.
(6) Metrangolo, P.; Neukirch, H.; Pilati, T.; Resnati, G. Halogen Bonding Based Recognition Processes: A World Parallel to Hydrogen Bonding. *Acc. Chem. Res.* **2005**, *38* (5), 386−395.
(7) Kolář, M. H.; Hobza, P. Computer Modeling of Halogen Bonds and Other σ-Hole Interactions. *Chem. Rev.* **2016**, *116*, 5155−5187.
(8) Bulfield, D.; Engelage, E.; Mancheski, L.; Stoesser, J.; Huber, S. M. Crystal Engineering with Multipoint Halogen Bonding: Double Two-Point Donors and Acceptors at Work. *Chem.-Eur. J.* **2020**, *26* (7), 1567−1575.
(9) de Azevedo Santos, L.; Hamlin, T. A.; Ramalho, T. C.; Bickelhaupt, F. M. The pnictogen bond: a quantitative molecular orbital picture. *Phys. Chem. Chem. Phys.* **2021**, *23* (25), 13842−13852.
(10) Esrafili, M. D.; Mousavian, P. Strong Tetrel Bonds: Theoretical Aspects and Experimental Evidence. *Molecules* **2018**, *23* (10), 2642.
(11) Varadwaj, P. R.; Varadwaj, A.; Marques, H. M. Very strong chalcogen bonding: Is oxygen in molecules capable of forming it? A First Principles Perspective. *arXiv* **2024**, 2210.11919.
(12) Wolters, L. P.; Bickelhaupt, F. M. Halogen bonding versus hydrogen bonding: A molecular orbital perspective. *ChemistryOpen* **2012**, *1*, 96−105.
(13) Varadwaj, P. R. Tetrel Bonding in Anion Recognition: A First Principles Investigation. *Molecules* **2022**, *27* (23), 8449.
(14) Kellett, C. W.; Kennepohl, P.; Berlinguette, C. P. π covalency in the halogen bond. *Nat. Commun.* **2020**, *11*, 3310.
(15) Oliveira, V.; Kraka, E.; Cremer, D. The intrinsic strength of the halogen bond: electrostatic and covalent contributions described by coupled cluster theory. *Phys. Chem. Chem. Phys.* **2016**, *18* (48), 33031−33046.
(16) Legon, A. The Hydrogen Bond, the Halogen Bond and Rotational Spectroscopy: A Personal Retrospective. *J. Indian Inst. Sci.* **2020**, *100* (1), 191−202.
(17) Legon, A. C. The halogen bond: an interim perspective. *Phys. Chem. Chem. Phys.* **2010**, *12* (28), 7736−7747.
(18) Banerjee, P.; Bhattacharya, I. Direct matrix isolation IR spectroscopic evidence of halogen bonding from a comparative study of complexes of CBr4 and CCl4with acetone and formic acid. *Spectrochim. Acta A: Mol. Biomol. Spectros.* **2021**, *250*, No. 119355.
(19) Pal, D.; Chakraborty, A.; Chakraborty, S. Investigation of [$CHCl_3$-CH_3OH] complex using matrix-isolation IR spectroscopy and quantum chemical calculation: Evidence of hydrogen- and halogen-bonding interaction. *Chem. Phys.* **2022**, *555*, No. 111451.
(20) Robinson, H. T.; Haakansson, C. T.; Corkish, T. R.; Watson, P. D.; McKinley, A. J.; Wild, D. A. Hydrogen Bonding versus Halogen Bonding: Spectroscopic Investigation of Gas-Phase Complexes Involving Bromide and Chloromethanes. *ChemPhysChem* **2023**, *24* (7), No. e202200733.
(21) Ganske, J. A.; Wingen, L. M.; Perraud, V.; Finlayson-Pitts, B. J. Role of Gas-Phase Halogen Bonding in Ambient Chemical Ionization Mass Spectrometry Utilizing Iodine. *ACS Earth Space Chem.* **2019**, *3* (7), 1315−1328.
(22) Karshikoff, A. *Non-Covalent Interactions in Proteins*, 2nd ed.; World Scientific: Singapore, 2021.
(23) Otero, R.; Gallego, J. M.; de Parga, A. L. V.; Martín, N.; Miranda, R. Molecular Self-Assembly at Solid Surfaces. *Adv, Mater.* **2011**, *23* (44), 5148−5176.
(24) Resnati, G.; Bryce, D. L.; Desiraju, G. R.; Frontera, A.; Krossing, I.; Legon, A. C.; Metrangolo, P.; Nicotra, F.; Rissanen, K.; Scheiner, S.; Terraneo, G. Definition of the pnictogen bond (IUPAC Recommendations 2023). *Pure Appl. Chem.* **2024**, *96* (1), 135.
(25) Muller, P. Glossary of terms used in physical organic chemistry (IUPAC Recommendations 1994). *Pure Appl. Chem.* **1994**, *66*, 1077−1184.
(26) Varadwaj, P. R.; Varadwaj, A.; Marques, H. M.; Yamashita, K. Definition of the tetrel bond. *CrystEngComm* **2023**, *25*, 1411−1423.
(27) Scheiner, S. Origins and properties of the tetrel bond. *Phys. Chem. Chem. Phys.* **2021**, *23* (10), 5702−5717.
(28) Varadwaj, A.; Varadwaj, P. R.; Marques, H. M.; Yamashita, K. Definition of the Pnictogen Bond: A Perspective. *Inorganics* **2022**, *10* (10), 149.
(29) de Azevedo Santos, L.; van der Lubbe, S. C. C.; Hamlin, T. A.; Ramalho, T. C.; Matthias Bickelhaupt, F. A Quantitative Molecular Orbital Perspective of the Chalcogen Bond. *ChemistryOpen* **2021**, *10* (4), 391−401.
(30) Mahmudov, K. T.; Gurbanov, A. V.; Aliyeva, V. A.; Resnati, G.; Pombeiro, A. J. L. Pnictogen bonding in coordination chemistry. *Coord. Chem. Rev.* **2020**, *418*, No. 213381.
(31) Aakeroy, C. B.; Bryce, D. L.; Desiraju, R. G.; Frontera, A.; Legon, A. C.; Nicotra, F.; Rissanen, K.; Scheiner, S.; Terraneo, G.; Metrangolo, P.; Resnati, G. Definition of the chalcogen bond (IUPAC Recommendations 2019). *Pure Appl. Chem.* **2019**, *91* (11), 1889−1892.
(32) Pascoe, D. J.; Ling, K. B.; Cockroft, S. L. The Origin of Chalcogen-Bonding Interactions. *J. Am. Chem. Soc.* **2017**, *139* (42), 15160−15167.
(33) Mahmudov, K. T.; Gurbanov, A. V.; Aliyeva, V. A.; Guedes da Silva, M. F. C.; Resnati, G.; Pombeiro, A. J. L. Chalcogen bonding in coordination chemistry. *Coord. Chem. Rev.* **2022**, *464*, No. 214556.
(34) Desiraju, G. R.; Ho, P. S.; Kloo, L.; Legon, A. C.; Marquardt, R.; Metrangolo, P.; Politzer, P.; Resnati, G.; Rissanen, K. Definition of the halogen bond (IUPAC Recommendations 2013). *Pure Appl. Chem.* **2013**, *85* (8), 1711−1713.
(35) Costa, P. J. The halogen bond: Nature and applications. *Phys. Sci. Rev.* **2017**, *2* (11), 20170136.
(36) Cavallo, G.; Metrangolo, P.; Pilati, T.; Resnati, G.; Terraneo, G. Naming Interactions from the Electrophilic Site. *Cryst. Growth Des.* **2014**, *14* (6), 2697−2702.
(37) Politzer, P.; Murray, J. S. σ-Hole Interactions: Perspectives and Misconceptions. *Crystals* **2017**, *7* (7), 212.
(38) Clark, T. Halogen bonds and σ-holes. *Faraday Discuss.* **2017**, *203* (0), 9−27.
(39) Politzer, P.; Murray, J. S.; Clark, T. Halogen bonding and other σ-hole interactions: a perspective. *Phys. Chem. Chem. Phys.* **2013**, *15* (27), 11178−11189.
(40) Politzer, P.; Murray, J. S.; Clark, T. The π-hole revisited. *Phys. Chem. Chem. Phys.* **2021**, *23* (31), 16458−16468.
(41) Murray, J. S.; Lane, P.; Clark, T.; Riley, K. E.; Politzer, P. σ-Holes, π-holes and electrostatically-driven interactions. *J. Mol. Model.* **2012**, *18* (2), 541−548.
(42) Grabowski, S. J. Magnesium Bonds: From Divalent Mg Centres to Trigonal and Tetrahedral Coordination. *ChemistrySelect* **2018**, *3* (11), 3147−3154.
(43) Tarannam, N.; Shukla, R.; Kozuch, S. Yet another perspective on hole interactions. *Phys. Chem. Chem. Phys.* **2021**, *23* (36), 19948−19963.
(44) Scheiner, S. Anatomy of π-hole bonds: Linear systems. *J. Chem. Phys.* **2021**, *155* (17), No. 174302.
(45) Gouverneur, V.; Seppelt, K. Introduction: Fluorine chemistry. *Chem. Rev.* **2015**, *115*, 563−565.
(46) *Iodine Chemistry and Applications*; Kaiho, T., Ed.; John Wiley & Sons: Hoboken, NJ, 2014.

https://doi.org/10.1021/acs.cgd.4c00228
Cryst. Growth Des. 2024, 24, 5494−5525

(47) Riel, A. M. S.; Decato, D. A.; Sun, J.; Massena, C. J.; Jessop, M. J.; Berryman, O. B. The intramolecular hydrogen bonded−halogen bond: a new strategy for preorganization and enhanced binding. *Chem. Sci.* **2018**, *9* (26), 5828−5836.
(48) Wang, Y.; Miao, X.; Deng, W. Halogen Bonds Fabricate 2D Molecular Self-Assembled Nanostructures by Scanning Tunneling Microscopy. *Crystals* **2020**, *10* (11), 1057.
(49) Robinson, S. W.; Mustoe, C. L.; White, N. G.; Brown, A.; Thompson, A. L.; Kennepohl, P.; Beer, P. D. Evidence for Halogen Bond Covalency in Acyclic and Interlocked Halogen-Bonding Receptor Anion Recognition. *J. Am. Chem. Soc.* **2015**, *137* (1), 499−507.
(50) Dortéz, S.; Fernández-Palacio, F.; Damián, J.; Gaiteiro, C.; Ramos, J.; Gómez-Sal, P.; Mosquera, M. E. G. Halogen bonding (HaB) in E−I···X−M systems: influence of the halogen donor on the HaB nature. *CrystEngComm* **2020**, *22* (5), 870−877.
(51) Mosquera, M. E. G.; Dortez, S.; Fernandez-Palacio, F.; Gomez-Sal, P. Pyridine-4-thiol as halogen-bond (HaB) acceptor: influence of the noncovalent interaction in its reactivity. *Acta Cryst. C* **2023**, *79* (4), 112.
(52) Wang, C.; Danovich, D.; Mo, Y.; Shaik, S. On The Nature of the Halogen Bond. *J. Chem. Theory Comput.* **2014**, *10* (9), 3726−3737.
(53) Ivanov, D. M.; Bokach, N. A.; Yu. Kukushkin, V.; Frontera, A. Metal Centers as Nucleophiles: Oxymoron of Halogen Bond-Involving Crystal Engineering. *Chem.-Eur. J.* **2022**, *28* (2), No. e202103173.
(54) Ishigaki, Y.; Shimomura, K.; Asai, K.; Shimajiri, T.; Akutagawa, T.; Fukushima, T.; Suzuki, T. Chalcogen Bond versus Halogen Bond: Changing Contributions in Determining the Crystal Packing of Dihalobenzochalcogenadiazoles. *Bull. Chem. Soc. Jpn.* **2022**, *95* (3), 522−531.
(55) Arunan, E.; Desiraju, G. R.; Klein, R. A.; Sadlej, J.; Scheiner, S.; Alkorta, I.; Clary, D. C.; Crabtree, R. H.; Dannenberg, J. J.; Hobza, P.; Kjaergaard, H. G.; Legon, A. C.; Mennucci, B.; Nesbitt, D. J. Definition of the hydrogen bond (IUPAC Recommendations 2011). *Pure Appl. Chem.* **2011**, *83* (8), 1637−1641.
(56) Politzer, P.; Murray, J. S.; Clark, T.; Resnati, G. The σ-hole revisited. *Phys. Chem. Chem. Phys.* **2017**, *19* (48), 32166−32178.
(57) Clark, T.; Hennemann, M.; Murray, J. S.; Politzer, P. Halogen bonding: the σ-hole. *J. Mol. Model.* **2007**, *13* (2), 291−296.
(58) Politzer, P.; Murray, J. S. Electrostatics and Polarization in σ- and π-Hole Noncovalent Interactions: An Overview. *ChemPhysChem* **2020**, *21* (7), 579−588.
(59) Politzer, P.; Murray, J. S. An Overview of Strengths and Directionalities of Noncovalent Interactions: σ-Holes and π-Holes. *Crystals* **2019**, *9* (3), 165.
(60) Politzer, P.; Laurence, P. R.; Jayasuriya, K. Molecular electrostatic potentials: an effective tool for the elucidation of biochemical phenomena. *Environ. Health Perspect.* **1985**, *61*, 191−202.
(61) *Molecular Electrostatic Potentials: Concepts and Applications*, 1st ed.; Murray, J. S., Sen, K., Eds.; Elsevier Science & Technology: Oxford, UK, 1996.
(62) Murray, J. S.; Politzer, P. The Molecular Electrostatic Potential: A Tool for Understanding and Predicting Molecular Interactions. In *Molecular Orbital Calculations for Biological Systems*, Sapse, A.-M.,, Ed.; Oxford University Press: Oxford, UK, 1998; pp 49−84.
(63) Bauzá, A.; Frontera, A. Competition between Halogen Bonding and π-Hole Interactions Involving Various Donors: The Role of Dispersion Effects. *ChemPhysChem* **2015**, *16* (14), 3108−3113.
(64) Bauzá, A.; Mooibroek, T. J.; Frontera, A. The Bright Future of Unconventional σ/π-Hole Interactions. *ChemPhysChem* **2015**, *16*, 2496−2517.
(65) Báuza, A.; Frontera, A.; Mooibroek, T. J. π-Hole Interactions Involving Nitro Compounds: Directionality of Nitrate Esters. *Cryst. Growth Des.* **2016**, *16* (9), 5520−5524.
(66) Varadwaj, A.; Varadwaj, P. R.; Marques, H. M.; Yamashita, K. The Pnictogen Bond, Together with Other Non-Covalent Interactions, in the Rational Design of One-, Two- and Three-Dimensional Organic-Inorganic Hybrid Metal Halide Perovskite Semiconducting Materials, and Beyond. *Int. J. Mol. Sci.* **2022**, *23* (15), 8816.
(67) Varadwaj, P. R.; Varadwaj, A.; Marques, H. M.; Yamashita, K. The Tetrel Bond and Tetrel Halide Perovskite Semiconductors. *Int. J. Mol. Sci.* **2023**, *24* (7), 6659.
(68) Varadwaj, A.; Marques, H. M.; Varadwaj, P. R. Is the Fluorine in Molecules Dispersive? Is Molecular Electrostatic Potential a Valid Property to Explore Fluorine-Centered Non-Covalent Interactions? *Molecules* **2019**, *24* (3), 379.
(69) Varadwaj, A.; Varadwaj, P. R.; Marques, H. M.; Yamashita, K. Comment on "Extended Halogen Bonding between Fully Fluorinated Aromatic Molecules: Kawai et al. *arXiv* **2018**, 1802.09995.
(70) Varadwaj, P. R.; Varadwaj, A.; Marques, H. M. Does Chlorine in CH_3Cl Behave as a Genuine Halogen Bond Donor? *Crystals* **2020**, *10* (3), 146.
(71) Varadwaj, P. R.; Varadwaj, A.; Jin, B.-Y. Halogen bonding interaction of chloromethane with several nitrogen donating molecules: addressing the nature of the chlorine surface σ-hole. *Phys. Chem. Chem. Phys.* **2014**, *16* (36), 19573−19589.
(72) Varadwaj, P. R. Does Oxygen Feature Chalcogen Bonding? *Molecules* **2019**, *24* (17), 3166.
(73) Grabowski, S. J. Boron and other Triel Lewis Acid Centers: From Hypovalency to Hypervalency. *ChemPhysChem* **2014**, *15* (14), 2985−2993.
(74) Mallada, B.; Gallardo, A.; Lamanec, M.; de la Torre, B.; Špirko, V.; Hobza, P.; Jelinek, P. Real-space imaging of anisotropic charge of s-hole by means of Kelvin probe force microscopy. *Science* **2021**, *374* (6569), 863−867.
(75) Mallada, B.; Ondráček, M.; Lamanec, M.; Gallardo, A.; Jiménez-Martín, A.; de la Torre, B.; Hobza, P.; Jelínek, P. Visualization of π-hole in molecules by means of Kelvin probe force microscopy. *Nat. Commun.* **2023**, *14*, 4954.
(76) Zhou, F.; Liu, Y.; Wang, Z.; Lu, T.; Yang, Q.; Liu, Y.; Zheng, B. A new type of halogen bond involving multivalent astatine: an ab initio study. *Phys. Chem. Chem. Phys.* **2019**, *21* (28), 15310−15318.
(77) Liu, L.; Rahali, S.; Maurice, R.; Gomez Pech, C.; Montavon, G.; Le Questel, J.-Y.; Graton, J.; Champion, J.; Galland, N. An expanded halogen bonding scale using astatine. *Chem. Sci.* **2021**, *12* (32), 10855−10861.
(78) Guo, N.; Maurice, R.; Teze, D.; Graton, J.; Champion, J.; Montavon, G.; Galland, N. Experimental and computational evidence of halogen bonds involving astatine. *Nat. Chem.* **2018**, *10* (4), 428−434.
(79) Varadwaj, A.; Varadwaj, P. R.; Marques, H. M.; Yamashita, K. Revealing Factors Influencing the Fluorine-Centered Non-Covalent Interactions in Some Fluorine-Substituted Molecular Complexes: Insights from First-Principles Studies. *ChemPhysChem* **2018**, *19* (12), 1486−1499.
(80) Bauzá, A.; Frontera, A. Electrostatically enhanced F···F interactions through hydrogen bonding, halogen bonding and metal coordination: an ab initio study. *Phys. Chem. Chem. Phys.* **2016**, *18* (30), 20381−20388.
(81) Varadwaj, P. R.; Varadwaj, A.; Marques, H. M.; Yamashita, K. Can Combined Electrostatic and Polarization Effects Alone Explain the F···F Negative-Negative Bonding in Simple Fluoro-Substituted Benzene Derivatives? A First-Principles Perspective. *Computation* **2018**, *6* (4), 51.
(82) Varadwaj, P. R.; Varadwaj, A.; Jin, B.-Y. Unusual bonding modes of perfluorobenzene in its polymeric (dimeric, trimeric and tetrameric) forms: entirely negative fluorine interacting cooperatively with entirely negative fluorine. *Phys. Chem. Chem. Phys.* **2015**, *17* (47), 31624−31645.
(83) Varadwaj, A.; Varadwaj, P. R.; Jin, B.-Y. Fluorines in tetrafluoromethane as halogen bond donors: Revisiting address the nature of the fluorine's σ-hole. *Int. J. Quantum Chem.* **2015**, *115*, 453−470.
(84) Varadwaj, A.; Varadwaj, P. R.; Jin, B.-Y. Can an entirely negative fluorine in a molecule, viz. perfluorobenzene, interact attractively with the entirely negative site(s) on another molecule(s)? Like liking like! *RSC Adv.* **2016**, *6* (23), 19098−19110.
(85) Chopra, D. Is organic fluorine really "not" polarizable? *Cryst. Growth Des.* **2012**, *12*, 541−546.

(86) Cole, J. C.; Taylor, R. Intermolecular Interactions of Organic Fluorine Seen in Perspective. *Cryst. Growth Des.* **2022**, *22* (2), 1352−1364.
(87) Wang, C.; Fu, Y.; Zhang, L.; Danovich, D.; Shaik, S.; Mo, Y. Hydrogen- and Halogen-Bonds between Ions of like Charges: Are They Anti-Electrostatic in Nature? *J. Comput. Chem.* **2018**, *39* (9), 481−487.
(88) Zhu, Z.; Wang, G.; Xu, Z.; Chen, Z.; Wang, J.; Shi, J.; Zhu, W. Halogen bonding in differently charged complexes: basic profile, essential interaction terms and intrinsic σ-hole. *Phys. Chem. Chem. Phys.* **2019**, *21* (27), 15106−15119.
(89) Loy, C.; Holthoff, J. M.; Weiss, R.; Huber, S. M.; Rosokha, S. V. Anti-electrostatic" halogen bonding in solution. *Chem. Sci.* **2021**, *12*, 8246−8251.
(90) Holthoff, J. M.; Engelage, E.; Weiss, R.; Huber, S. M. Anti-Electrostatic" Halogen Bonding. *Angew. Chem., Int. Ed.* **2020**, *59* (27), 11150−11157.
(91) Johansson, M. P.; Swart, M. Intramolecular halogen−halogen bonds? *Phys. Chem. Chem. Phys.* **2013**, *15* (27), 11543−11553.
(92) Varadwaj, P. R.; Varadwaj, A.; Jin, B.-Y. Hexahalogenated and their mixed benzene derivatives as prototypes for the understanding of halogen···halogen intramolecular interactions: New insights from combined DFT, QTAIM-, and RDG-based NCI analyses. *J. Comput. Chem.* **2015**, *36* (31), 2328−2343.
(93) Ibrahim, M. A. A.; Moussa, N. A. M. Unconventional Type III Halogen···Halogen Interactions: A Quantum Mechanical Elucidation of σ-Hole···σ-Hole and Di-σ-Hole Interactions. *ACS Omega* **2020**, *5* (34), 21824−21835.
(94) Wang, C.; Danovich, D.; Shaik, S.; Wu, W.; Mo, Y. Attraction between electrophilic caps: A counterintuitive case of noncovalent interactions. *J. Comput. Chem.* **2019**, *40* (9), 1015−1022.
(95) Scheiner, S. Does a halogen bond require positive potential on the acid and negative potential on the base? *Phys. Chem. Chem. Phys.* **2023**, *25* (10), 7184−7194.
(96) McDowell, S. A. C.; Joseph, J. A. Communication: An unusual halogen-bonding motif: The LiBr···BrF dimer as a model system. *J. Chem. Phys.* **2012**, *137* (17), No. 171103.
(97) Bader, R. F. W. Atoms in molecules. *Acc. Chem. Res.* **1985**, *18*, 9−15.
(98) Bader, R. F. *Atoms in Molecules: A Quantum Theory*; Oxford University Press: Oxford, UK, 1990.
(99) Taylor, R. Aerogen Bond, Halogen Bond, Chalcogen Bond, Pnictogen Bond,Tetrel Bond, Triel Bond ... Why So Many Names? *Cryst. Growth Des.* **2024**, *24*, 4003−4012.
(100) Groom, C. R.; Bruno, I. J.; Lightfoot, M. P.; Ward, S. C. The Cambridge Structural Database. *Acta Cryst. B* **2016**, *72* (2), 171−179.
(101) Bauzá, A.; Frontera, A. Aerogen Bonding Interaction: A New Supramolecular Force? *Angew. Chem., Int. Ed.* **2015**, *54*, 7340−7343.
(102) Resnati, G.; Bryce, D. L.; Desiraju, G. R.; Frontera, A.; Krossing, I.; Legon, A. C.; Metrangolo, P.; Nicotra, F.; Rissanen, K.; Scheiner, S.; Terraneo, G. Definition of the pnictogen bond (IUPAC Recommendations 2023). *Pure Appl. Chem.* **2024**, *96* (1), 135−145.
(103) Thorson, R. A.; Woller, G. R.; Driscoll, Z. L.; Geiger, B. E.; Moss, C. A.; Schlapper, A. L.; Speetzen, E. D.; Bosch, E.; Erdélyi, M.; Bowling, N. P. Intramolecular Halogen Bonding in Solution: ^{15}N, ^{13}C, and ^{19}F NMR Studies of Temperature and Solvent Effects. *Eur. J. Org. Chem.* **2015**, *2015* (8), 1685−1695.
(104) Puttreddy, R.; Jurček, O.; Bhowmik, S.; Mäkelä, T.; Rissanen, K. Very strong − N−X$^+$···−O−N$^+$ halogen bonds. *Chem. Commun.* **2016**, *52* (11), 2338−2341.
(105) Yu, S.; Ward, J. S.; Truong, K.-N.; Rissanen, K. Carbonyl Hypoiodites as Extremely Strong Halogen Bond Donors. *Angew. Chem. Int. Edn.* **2021**, *60* (38), 20739−20743.
(106) Luo, J.; Dai, H.; Zeng, C.; Wu, D.; Cao, M. A Theoretical Study of the Halogen Bond between Heteronuclear Halogen and Benzene. *Molecules* **2022**, *27* (22), 8078.
(107) Otte, F.; Kleinheider, J.; Hiller, W.; Wang, R.; Englert, U.; Strohmann, C. Weak yet Decisive: Molecular Halogen Bond and Competing Weak Interactions of Iodobenzene and Quinuclidine. *J. Am. Chem. Soc.* **2021**, *143* (11), 4133−4137.
(108) Peintner, S.; Erdélyi, M. Pushing the Limits of Characterising a Weak Halogen Bond in Solution. *Chem.-Eur. J.* **2022**, *28* (5), No. e202103559.
(109) Cunha, A. V.; Havenith, R. W. A.; van Gog, J.; De Vleeschouwer, F.; De Proft, F.; Herrebout, W. The Halogen Bond in Weakly Bonded Complexes and the Consequences for Aromaticity and Spin-Orbit Coupling. *Molecules* **2023**, *28* (2), 772.
(110) Varadwaj, P. R. Halogen Bond via an Electrophilic π-Hole on Halogen in Molecules: Does It Exist? *Int. J. Mol. Sci.* **2024**, *25* (9), 4587.
(111) Scheiner, S. Characterization of Type I and II Interactions between Halogen Atoms. *Cryst. Growth Des.* **2022**, *22* (4), 2692−2702.
(112) Metrangolo, P.; Resnati, G. (2014). 1, Type II halogen··· halogen contacts are halogen bonds. *IUCrJ.* **2014**, *1*, 5−7.
(113) Politzer, P.; Murray, J. S.; Lane, P. σ-Hole bonding and hydrogen bonding: Competitive interactions. *Int. J. Quantum Chem.* **2007**, *107*, 3046−3052.
(114) Murray, J. S.; Politzer, P. The electrostatic potential: an overview. *WIREs Comput. Mol. Sci.* **2011**, *1*, 153−163.
(115) Murray, J. S.; Macaveiu, L.; Politzer, P. Factors affecting the strengths of σ-hole electrostatic potentials. *J. Comput. Sci.* **2014**, *5* (4), 590−596.
(116) Murray, J. S.; Lane, P.; Politzer, P. Expansion of the σ-hole concept. *J. Mol. Model.* **2009**, *15*, 723−729.
(117) Heinen, F.; Engelage, E.; Cramer, C. J.; Huber, S. M. Hypervalent Iodine(III) Compounds as Biaxial Halogen Bond Donors. *J. Am. Chem. Soc.* **2020**, *142* (19), 8633−8640.
(118) Yoshida, Y.; Mino, T.; Sakamoto, M. Chiral Hypervalent Bromine(III) (Bromonium Salt): Hydrogen- and Halogen-Bonding Bifunctional Asymmetric Catalysis by Diaryl-λ3-bromanes. *ACS Catal.* **2021**, *11* (21), 13028−13033.
(119) Varadwaj, P. R.; Varadwaj, A.; Marques, H. M.; Yamashita, K. Methylammonium Tetrel Halide Perovskite Ion Pairs and Their Dimers: The Interplay between the Hydrogen-, Pnictogen- and Tetrel-Bonding Interactions. *Int. J. Mol. Sci.* **2023**, *24* (13), 10554.
(120) Clark, T.; Politzer, P.; Murray, J. S. Correct electrostatic treatment of noncovalent interactions: the importance of polarization. *WIREs Comput. Mol. Sci.* **2015**, *5* (2), 169−177.
(121) Politzer, P.; Murray, J. S.; Clark, T. Mathematical modeling and physical reality in noncovalent interactions. *J. Mol. Model.* **2015**, *21*, 52.
(122) Krylov, A. I. From orbitals to observables and back. *J. Chem. Phys.* **2020**, *153* (8), 080901.
(123) Pham, B. Q.; Gordon, M. S. Can Orbitals Really Be Observed in Scanning Tunneling Microscopy Experiments? *J. Phys. Chem. A* **2017**, *121* (26), 4851−4852.
(124) Scerri, E. R. Have Orbitals Really Been Observed? *J. Chem. Educ.* **2002**, *79* (3), 310.
(125) Clark, T.; Heßelmann, A. The coulombic σ-hole model describes bonding in CX3I···Y$^-$ complexes completely. *Phys. Chem. Chem. Phys.* **2018**, *20* (35), 22849−22855.
(126) Murray, J. S.; Politzer, P. Interaction and Polarization Energy Relationships in σ-Hole and π-Hole Bonding. *Crystals* **2020**, *10* (2), 76.
(127) Jeziorski, B.; Moszynski, R.; Szalewicz, K. Perturbation Theory Approach to Intermolecular Potential Energy Surfaces of van der Waals Complexes. *Chem. Rev.* **1994**, *94* (7), 1887−1930.
(128) Politzer, P.; Murray, J. S. The Hellmann-Feynman theorem: a perspective. *J. Mol. Model.* **2018**, *24*, 266.
(129) Politzer, P.; Murray, J. S. The conceptual power of the Hellmann−Feynman theorem. *Struct. Chem.* **2023**, *34* (1), 17−21.
(130) Clark, T.; Murray, J. S.; Politzer, P. A perspective on quantum mechanics and chemical concepts in describing noncovalent interactions. *Phys. Chem. Chem. Phys.* **2018**, *20* (48), 30076−30082.
(131) Hunt, K. L. C. Dispersion dipoles and dispersion forces: Proof of Feynman's "conjecture" and generalization to interacting molecules of arbitrary symmetry. *J. Chem. Phys.* **1990**, *92* (2), 1180−1187.
(132) Feynman, R. P. Forces in Molecules. *Phys. Rev.* **1939**, *56* (4), 340−343.
(133) Politzer, P.; Murray, J. S. The use and misuse of van der Waals radii. *Struct. Chem.* **2021**, *32* (2), 623−629.

https://doi.org/10.1021/acs.cgd.4c00228
Cryst. Growth Des. 2024, 24, 5494−5525

(134) Varadwaj, A.; Varadwaj, P. R.; Marques, H. M.; Yamashita, K. The Stibium Bond or the Antimony-Centered Pnictogen Bond: The Covalently Bound Antimony Atom in Molecular Entities in Crystal Lattices as a Pnictogen Bond Donor. *Int. J. Mol. Sci.* **2022**, *23* (9), 4674.
(135) Varadwaj, A.; Varadwaj, P. R.; Marques, H. M.; Yamashita, K. The Pnictogen Bond: The Covalently Bound Arsenic Atom in Molecular Entities in Crystals as a Pnictogen Bond Donor. *Molecules* **2022**, *27* (11), 3421.
(136) Huber, S. M.; Scanlon, J. D.; Jimenez-Izal, E.; Ugalde, J. M.; Infante, I. On the directionality of halogen bonding. *Phys. Chem. Chem. Phys.* **2013**, *15*, 10350−10357.
(137) Jentzsch, A. V. Applications of halogen bonding in solution. *Pure Appl. Chem.* **2015**, *87* (1), 15−41.
(138) Zhao, Q.; Feng, D.; Hao, J.; Cai, Z. Chemical origin of contracted C−Cl bonds in the halogen-bonded complexes. *J. Mol. Struct. THEOCHEM* **2010**, *958* (1), 71−75.
(139) Wang, W.; Wong, N.-B.; Zheng, W.; Tian, A. Theoretical Study on the Blueshifting Halogen Bond. *J. Phys. Chem. A* **2004**, *108* (10), 1799−1805.
(140) Zierkiewicz, W.; Bieńko, D. C.; Michalska, D.; Zeegers-Huyskens, T. On the nature of halogen bonded complexes between carbonyl bases and chlorotrifluoromethane. *Theor. Chem. Acc.* **2015**, *134*, 103.
(141) Amonov, A.; Scheiner, S. Relation between Halogen Bond Strength and IR and NMR Spectroscopic Markers. *Molecules* **2023**, *28* (22), 7520.
(142) Vasylyeva, V.; Catalano, L.; Nervi, C.; Gobetto, R.; Metrangolo, P.; Resnati, G. Characteristic redshift and intensity enhancement as far-IR fingerprints of the halogen bond involving aromatic donors. *CrystEngComm* **2016**, *18* (13), 2247−2250.
(143) Nagels, N.; Hauchecorne, D.; Herrebout, W. A. Exploring the C-X···π Halogen Bonding Motif: An Infrared and Raman Study of the Complexes of CF3X (X = Cl, Br and I) with the Aromatic Model Compounds Benzene and Toluene. *Molecules* **2013**, *18* (6), 6829−6851.
(144) Kalout, H.; Boubegtiten-Fezoua, Z.; Maurel, F.; Hellwig, P.; Ferlay, S. An accurate vibrational signature in halogen bonded molecular crystals. *Phys. Chem. Chem. Phys.* **2022**, *24* (24), 15103−15109.
(145) Wang, C.; Mo, Y. Classical Electrostatic Interaction Is the Origin for Blue-Shifting Halogen Bonds. *Inorg. Chem.* **2019**, *58* (13), 8577−8586.
(146) Wang, W.; Zhang, Y.; Ji, B. On the Difference of the Properties between the Blue-Shifting Halogen Bond and the Blue-Shifting Hydrogen Bond. *J. Phys. Chem. A* **2010**, *114* (26), 7257−7260.
(147) Southern, S. A.; Bryce, D. L. NMR Investigations of Noncovalent Carbon Tetrel Bonds. Computational Assessment and Initial Experimental Observation. *J. Phys. Chem. A* **2015**, *119* (49), 11891−11899.
(148) Cerreia Vioglio, P.; Catalano, L.; Vasylyeva, V.; Nervi, C.; Chierotti, M. R.; Resnati, G.; Gobetto, R.; Metrangolo, P. Natural Abundance ^{15}N and ^{13}C Solid-State NMR Chemical Shifts: High Sensitivity Probes of the Halogen Bond Geometry. *Chem.-Eur. J.* **2016**, *22* (47), 16694.
(149) Ellington, T. L.; Reves, P. L.; Simms, B. L.; Wilson, J. L.; Watkins, D. L.; Tschumper, G. S.; Hammer, N. I. Quantifying the Effects of Halogen Bonding by Haloaromatic Donors on the Acceptor Pyrimidine. *ChemPhysChem* **2017**, *18* (10), 1267−1273.
(150) Widner, D. L.; Robinson, E. R.; Perez, A. B.; Vang, H. G.; Thorson, R. A.; Driscoll, Z. L.; Giebel, S. M.; Berndt, C. W.; Bosch, E.; Speetzen, E. D.; Bowling, N. P. Comparing Strong and Weak Halogen Bonding in Solution: ^{13}C NMR, UV/Vis, Crystallographic, and Computational Studies of an Intramolecular Model. *Eur. J. Org. Chem.* **2017**, *2017* (38), 5739−5749.
(151) Adeniyi, E.; Grounds, O.; Stephens, Z.; Zeller, M.; Rosokha, S. V. Thermodynamics and Spectroscopy of Halogen- and Hydrogen-Bonded Complexes of Haloforms with Aromatic and Aliphatic Amines. *Molecules* **2022**, *27* (18), 6124.
(152) Grondin, J.; Aupetit, C.; Vincent, J.-M.; Méreau, R.; Tassaing, T. Visible-light induced photochemistry of Electron Donor-Acceptor Complexes in Perfluoroalkylation Reactions: Investigation of halogen bonding interactions through UV−Visible absorption and Raman spectroscopies combined with DFT calculations. *J. Mol. Liq.* **2021**, *333*, No. 115993.
(153) Varadwaj, P. R.; Varadwaj, A.; Marques, H. M.; Yamashita, K. The Phosphorous Bond, or the Phosphorous-Centered Pnictogen Bond: The Covalently Bound Phosphorous Atom in Molecular Entities and Crystals as a Pnictogen Bond Donor. *Molecules* **2022**, *27*, 1487.
(154) Narth, C.; Maroun, Z.; Boto, R. A.; Chaudret, R.; Bonnet, M.-L.; Piquemal, J.-P.; Contreras-García, J. A complete NCI perspective: From new bonds to reactivity. In *Applications of Topological Methods in Molecular Chemistry*, Esmail, A., Remi, C., Christine, L., Bernard, S.,, Eds.; Springer, 2016; Vol. *22*, pp 491−527.
(155) Johnson, E. R.; Keinan, S.; Mori-Sánchez, P.; Contreras-García, J.; Cohen, A. J.; Yang, W. Revealing Noncovalent Interactions. *J. Am. Chem. Soc.* **2010**, *132*, 6498−6506.
(156) Lefebvre, C.; Rubez, G.; Khartabil, H.; Boisson, J.-C.; Contreras-García, J.; Hénon, E. Accurately extracting the signature of intermolecular interactions present in the NCI plot of the reduced density gradient versus electron density. *Phys. Chem. Chem. Phys.* **2017**, *19* (27), 17928−17936.
(157) Lefebvre, C.; Khartabil, H.; Boisson, J.-C.; Contreras-García, J.; Piquemal, J.-P.; Hénon, E. The Independent Gradient Model: A New Approach for Probing Strong and Weak Interactions in Molecules from Wave Function Calculations. *ChemPhysChem* **2018**, *19* (6), 724−735.
(158) Lu, T.; Chen, Q. Independent gradient model based on Hirshfeld partition: A new method for visual study of interactions in chemical systems. *J. Comput. Chem.* **2022**, *43* (8), 539−555.
(159) Lu, T.; Chen, Q. Interaction Region Indicator: A Simple Real Space Function Clearly Revealing Both Chemical Bonds and Weak Interactions. *Chemistry Methods* **2021**, *1* (5), 231−239.
(160) Clark, T. How deeply should we analyze non-covalent interactions? *J. Mol. Model.* **2023**, *29*, 66.
(161) Lane, J. R.; Contreras-García, J.; Piquemal, J.-P.; Miller, B. J.; Kjaergaard, H. G. Are Bond Critical Points Really Critical for Hydrogen Bonding? *J. Chem. Theory Comput.* **2013**, *9* (8), 3263−3266.
(162) Shahbazian, S. Why Bond Critical Points Are Not "Bond" Critical Points. *Chem.-Eur. J.* **2018**, *24* (21), 5401−5405.
(163) Varadwaj, P. R.; Varadwaj, A.; Marques, H. M.; Yamashita, K. Halogen in materials design: Chloroammonium lead triiodide perovskite (ClNH3PbI3) a dynamical bandgap semiconductor in 3D for photovoltaics. *J. Comput. Chem.* **2018**, *39* (23), 1902−1912.
(164) Grabowski, S. J. Lewis Acid Properties of Tetrel Tetrafluorides—The Coincidence of the σ-Hole Concept with the QTAIM Approach. *Crystals* **2017**, *7* (2), 43.
(165) Weinhold, F. Natural bond orbital analysis: A critical overview of relationships to alternative bonding perspectives. *J. Comput. Chem.* **2012**, *33* (30), 2363−2379.
(166) Řezáč, J.; de la Lande, A. On the role of charge transfer in halogen bonding. *Phys. Chem. Chem. Phys.* **2017**, *19* (1), 791−803.
(167) Mo, Y.; Song, L.; Lin, Y.; Liu, M.; Cao, Z.; Wu, W. Block-Localized Wavefunction (BLW) Based Two-State Approach for Charge Transfers between Phenyl Rings. *J. Chem. Theory Comput.* **2012**, *8* (3), 800−805.
(168) Inscoe, B.; Rathnayake, H.; Mo, Y. Role of Charge Transfer in Halogen Bonding. *J. Phys. Chem. A* **2021**, *125* (14), 2944−2953.
(169) Scheiner, S. Participation of S and Se in hydrogen and chalcogen bonds. *CrystEngComm* **2021**, *23* (39), 6821−6837.
(170) Duarte, D. J. R.; Angelina, E. L.; Peruchena, N. M. On the strength of the halogen bonds: Mutual penetration, atomic quadrupolemoment and Laplacian distribution of the charge density analyses. *Comput. Theor. Chem.* **2012**, *998*, 164−172.
(171) Wolters, L. P.; Smits, N. W. G.; Guerra, C. F. Covalency in resonance-assisted halogen bonds demonstrated with cooperativity in N-halo-guanine quartets. *Phys. Chem. Chem. Phys.* **2015**, *17* (3), 1585−1592.

(172) Li, D.; Xia, T.; Feng, W.; Cheng, L. Revisiting the covalent nature of halogen bonding: a polarized three-center four-electron bond. *RSC Adv.* **2021**, *11* (52), 32852−32860.
(173) Varadwaj, P. R.; Varadwaj, A.; Marques, H. M.; Yamashita, K. The pnictogen bond forming ability of bonded bismuth atoms in molecular entities in the crystalline phase: a perspective. *CrystEngComm* **2023**, *25* (7), 1038−1052.
(174) Riley, K. E.; Tran, K.-A.; Lane, P.; Murray, J. S.; Politzer, P. Comparative analysis of electrostatic potential maxima and minima on molecular surfaces, as determined by three methods and a variety of basis sets. *J. Comp. Science* **2016**, *17*, 273−284.
(175) Scheiner, S. Dissection of the Origin of π-Holes and the Noncovalent Bonds in Which They Engage. *J. Phys. Chem. A* **2021**, *125* (30), 6514−6528.
(176) Zierkiewicz, W.; Michalczyk, M.; Scheiner, S. Noncovalent Bonds through Sigma and Pi-Hole Located on the Same Molecule. Guiding Principles and Comparisons. *Molecules* **2021**, *26* (6), 1740.
(177) Dyduch, K.; Mitoraj, M. P.; Michalak, A. ETS-NOCV description of σ-hole bonding. *J. Mol. Model.* **2013**, *19*, 2747−2758.
(178) Ziegler, T.; Rauk, A. On the calculation of bonding energies by the Hartree Fock Slater method. *Theor. Chim. Acta* **1977**, *46* (1), 1−10.
(179) Michalak, A.; Mitoraj, M.; Ziegler, T. Bond Orbitals from Chemical Valence Theory. *J. Phys. Chem. A* **2008**, *112* (9), 1933−1939.
(180) Mitoraj, M. P.; Michalak, A.; Ziegler, T. A Combined Charge and Energy Decomposition Scheme for Bond Analysis. *J. Chem. Theory Comput.* **2009**, *5* (4), 962−975.
(181) Kozyra, P.; Świetek, M.; Datka, J.; BrocŁawik, E. Ag+ and Cu+ Cations Ligated by Zeolite Environment Enhancing Hydrogen Activation − ETS-NOCV Charge-Transfer Analysis. *J. Comput. Chem. Japan* **2013**, *12* (1), 30−37.
(182) Mitoraj, M. P.; Parafiniuk, M.; Srebro, M.; Handzlik, M.; Buczek, A.; Michalak, A. Applications of the ETS-NOCV method in descriptions of chemical reactions. *J. Mol. Model.* **2011**, *17* (9), 2337−2352.
(183) Heinemann, F. W.; Blum, N.; Sellmann, D. CCDC 149105: Experimental Crystal Structure Determination. *Cambridge Crystallographic Data Centre*. 2021. DOI: 10.5517/ccdc.csd.cc504v4.
(184) Kumar, B.; King, B. T. Synthesis of 1,8,9,16-Tetrakis-(trimethylsilyl)tetra-cata-tetrabenzoquadrannulene. *J. Org. Chem.* **2012**, *77* (23), 10617−10622.
(185) Varadwaj, P. R.; Varadwaj, A.; Marques, H. M.; MacDougall, P. J. The chalcogen bond: can it be formed by oxygen? *Phys. Chem. Chem. Phys.* **2019**, *21* (36), 19969−19986.
(186) Varadwaj, P. R.; Varadwaj, A.; Marques, H. M.; Yamashita, K. The Nitrogen Bond, or the Nitrogen-Centered Pnictogen Bond: The Covalently Bound Nitrogen Atom in Molecular Entities and Crystals as a Pnictogen Bond Donor. *Compounds* **2022**, *2* (1), 80−110.
(187) Yamamoto, H. M.; Cui, H.; Kato, R. CCDC 910057: Experimental Crystal Structure Determination. *Cambridge Crystallographic Data Centre*. 2017. DOI: 10.5517/ccdc.csd.cczjzp4.
(188) Goud, N. R.; Bolton, O.; Burgess, E. C.; Matzger, A. J. Unprecedented Size of the σ-Holes on 1,3,5-Triiodo-2,4,6-trinitrobenzene Begets Unprecedented Intermolecular Interactions. *Cryst. Growth Des.* **2016**, *16* (3), 1765−1771.
(189) Kim, J.; Umerani, M. J.; Kurakake, R.; Qin, H.; Ziller, J. W.; Gorodetsky, A. A.; Park, Y. S. An aza-Diels−Alder approach to chlorinated quinolines, benzoquinolines, and polybenzoquinolines. *RSC Adv.* **2021**, *11* (23), 13722−13730.
(190) Gerard, F.; Hardy, A.; Becuwe, A. Structure of 1,3,5-trichloro-2,4,6-trinitrobenzene. *Acta Cryst. C* **1993**, *49* (6), 1215−1218.
(191) Ghassemzadeh, M.; Harms, K.; Dehnicke, K. Komplexe von Halogenid-Ionen mit Diiodacetylen. Die Kristallstrukturen von PPh4-[X(I-C≡C-I)2] mit X = Cl, Br, I. *Chem. Ber.* **1996**, *129* (2), 259−262.
(192) Baldrighi, M.; Bartesaghi, D.; Cavallo, G.; Chierotti, M. R.; Gobetto, R.; Metrangolo, P.; Pilati, T.; Resnati, G.; Terraneo, G. Polymorphs and co-crystals of haloprogin: an antifungal agent. *CrystEngComm* **2014**, *16* (26), 5897−5904.
(193) Ghassemzadeh, M.; Harms, K.; Dehnicke, K. Komplexe von Halogenid-Ionen mit 1-Halogen-2-phenylacetylenen. Kristallstrukturen von $PPh_4[X(I—C≡C—Ph)_4]$ mit X = Cl, Br, I, von $PPh_4[Br(Br—C≡C—Ph)_4]$ und von $NMe_4[F(I—C≡C—Ph)_2]$. *Chem. Ber.* **1996**, *129* (1), 115−120.
(194) Pigulski, B.; Gulia, N.; Męcik, P.; Wieczorek, R.; Arendt, A.; Szafert, S. Crystal Engineering of 1-Halopolyynes by End-Group Manipulation. *Cryst. Growth Des.* **2019**, *19* (11), 6542−6551.
(195) Barry, D. E.; Hawes, C. S.; Blasco, S.; Gunnlaugsson, T. Structure Direction, Solvent Effects, and Anion Influences in Halogen-Bonded Adducts of 2,6-Bis(iodoethynyl)pyridine. *Cryst. Growth Des.* **2016**, *16* (9), 5194−5205.
(196) Baldrighi, M.; Cavallo, G.; Chierotti, M. R.; Gobetto, R.; Metrangolo, P.; Pilati, T.; Resnati, G.; Terraneo, G. Halogen Bonding and Pharmaceutical Cocrystals: The Case of a Widely Used Preservative. *Mol. Pharmaceutics* **2013**, *10* (5), 1760−1772.
(197) Morin, V. M.; Szell, P. M. J.; Caron-Poulin, E.; Gabidullin, B.; Bryce, D. L. Mechanochemical Preparations of Anion Coordinated Architectures Based on 3-Iodoethynylpyridine and 3-Iodoethynylbenzoic Acid. *ChemistryOpen* **2019**, *8* (11), 1328−1336.
(198) Schreib, B. S.; Fadel, M.; Carreira, E. M. Palladium-Catalyzed C−H Alkynylation of Unactivated Alkenes. *Angew. Chem. Int. Edn.* **2020**, *59* (20), 7818−7822.
(199) Kosaka, Y.; Yamamoto, H. M.; Nakao, A.; Kato, R. Multicomponent Molecular Conductors with Supramolecular Assemblies Prepared from Neutral Iodine-Bearing pBIB (p-Bis(iodoethynyl)-benzene) and Derivatives. *Bull. Chem. Soc. Jpn.* **2006**, *79* (7), 1148−1154.
(200) González, L.; Graus, S.; Gaspar, B.; Espasa, S.; Velázquez-Campoy, A.; Munarriz, J.; Serrano, J. L.; Tejedor, R. M.; Uriel, S. Interplay between non-covalent interactions in 1D supramolecular polymers based on 1,4-bis(iodoethynyl)benzene. *Phys. Chem. Chem. Phys.* **2021**, *23* (5), 3531−3542.
(201) Hammershøj, P.; Reenberg, T. K.; Pittelkow, M.; Nielsen, C. B.; Hammerich, O.; Christensen, J. B. Synthesis and Properties of 2,3-Dialkynyl-1,4-benzoquinones. *Eur. J. Org. Chem.* **2006**, *2006* (12), 2786−2794.
(202) Yamamoto, H. M.; Kosaka, Y.; Maeda, R.; Yamaura, J.-i.; Nakao, A.; Nakamura, T.; Kato, R. Supramolecular Insulating Networks Sheathing Conducting Nanowires Based on Organic Radical Cations. *ACS Nano* **2008**, *2* (1), 143−155.
(203) Guo, W.; Galoppini, E.; Gilardi, R.; Rydja, G. I.; Chen, Y.-H. Weak Intermolecular Interactions in the Crystal Structures of Molecules with Tetrahedral Symmetry: Diamondoid Nets and Other Motifs. *Cryst. Growth Des.* **2001**, *1* (3), 231−237.
(204) Gunawardana, C. A.; Đaković, M.; Aakeröy, C. B. Diamondoid architectures from halogen-bonded halides. *Chem. Commun.* **2018**, *54* (6), 607−610.
(205) Lieffrig, J.; Jeannin, O.; Fourmigué, M. Expanded Halogen-Bonded Anion Organic Networks with Star-Shaped Iodoethynyl-Substituted Molecules: From Corrugated 2D Hexagonal Lattices to Pyrite-Type 2-Fold Interpenetrated Cubic Lattices. *J. Am. Chem. Soc.* **2013**, *135* (16), 6200−6210.
(206) Bart, J. C. J.; Bassi, I. W.; Calcaterra, M.; Piccardi, P. The structure of the new insect-growth regulator 1,4-bis(5-chloropent-4-ynyloxy)benzene. *Acta Cryst. B* **1980**, *36* (7), 1561−1564.
(207) Yamamoto, H. M.; Maeda, R.; Yamaura, J.-I.; Kato, R. Structural and physical properties of conducting cation radical salts containing supramolecular assemblies based on -bis(iodoethynyl)benzene derivatives. *J. Mater. Chem.* **2001**, *11* (4), 1034−1041.
(208) Minkwitz, R.; Berkei, M. A New Method for Preparation and Crystal Structure of (Trifluoromethyl)iodine Dichloride. *Inorg. Chem.* **1999**, *38* (22), 5041−5044.
(209) Poynder, T. B.; Chamorro Orué, A. I.; Tania; Sharp-Bucknall, L.; Flynn, M. T.; Wilson, D. J. D.; Athukorala Arachchige, K. S.; Clegg, J. K.; Dutton, J. L. On the activation of $PhICl_2$ with pyridine. *Chem. Commun.* **2021**, *57* (40), 4970−4973.
(210) Nikiforov, V. A.; Karavan, V. S.; Miltsov, S. A.; Selivanov, S. I.; Kolehmainen, E.; Wegelius, E.; Nissinen, M. *ARKIVOC* **2003**, *2003*, 191−196.

(211) Yoshimura, A.; Nguyen, K. C.; Nemykin, V. N.; Zhdankin, V. V. Preparation, structure, and oxidative reactivity of (dichloroiodo)-pyridines: recyclable hypervalent iodine reagents. *ARKIVOC* **2018**, *2018* (2), 40−49.
(212) Hokamp, T.; Mollari, L.; Wilkins, L. C.; Melen, R. L.; Wirth, T. Alternative Strategies with Iodine: Fast Access to Previously Inaccessible Iodine(III) Compounds. *Angew. Chem. Int. Edn.* **2018**, *57* (27), 8306−8309.
(213) Minkwitz, R.; Bröchler, R.; Preut, H. Fluorieren mit Trifluormethylhypochlorit CF3OCl. Darstellung und Kristallstrukturanalyse von Trifluormethyliodtetrafluorid CF3IF4. *Zeit. Anorg. Allg. Chem.* **1995**, *621* (7), 1247−1250.
(214) Frohn, H. J.; Görg, S.; Henkel, G.; Läge, M. Pentafluorphenyliod(V)-Verbindungen. 2. Pentafluorphenyliodtetrafluorid $C_6F_5IF_4$: Synthese durch Fluor-Aryl-Substitution an IF_5 — Eigenschaften und Struktur. Strukturanalyse der monovalenten Iodstammverbindung C_6F_5I. *Zeit. Anorg. Allg. Chem.* **1995**, *621* (7), 1251−1256.
(215) Waterfeld, A.; Isenberg, W.; Mews, R.; Clegg, W.; Sheldrick, G. M. N,N′-Dihalogenethandiimidoyldifluoride. *Chem. Ber.* **1983**, *116* (2), 724−731.
(216) Lynch, V.; Thompson, J. CCDC 1445805: Experimental Crystal Structure Determination. *Cambridge Crystallographic Data Centre*. 2016. DOI: 10.5517/cc1kjgwf.
(217) Nicolas, I.; Jeannin, O.; Pichon, D.; Fourmigué, M. Dibromohydantoins as halogen bond (XB) donors: a route toward the introduction of chirality in halogen bonded systems. *CrystEngComm* **2016**, *18* (48), 9325−9333.
(218) Svensson, C.; Albertsson, J.; Eberson, L. Caesium tris(*N*-bromosuccinimide)bromate(1-). *Acta Cryst. C* **1986**, *42* (11), 1500−1502.
(219) Dou, S.-q.; Gowda, B. T.; Paulus, H.; Weiss, A. The Bond N-Cl. Crystal Structures and ^{35}Cl NQR of *N*-Chloro-*N*-Phenyl-2-chloroacetamide, *N*-Chloro-*N*-phenyl-2,2-dichloroacetamide, *N*-Chloro-*N*-phenyl-2,2,2-trichloroacetamide, and *N*-Phenyl-2,2,2-trichloroacetamide. *Zeit. Naturforsch. A* **1994**, *49* (12), 1136−1144.
(220) Hennecke, U.; Müller, C. H.; Daniliuc, C. G. Synthesis of Chiral Heterocyclic *N*-Haloamides and -imides and Their Applications as Halogenating Agents and Mechanistic Probes. *Eur. J. Org. Chem.* **2017**, *2017* (3), 484−490.
(221) Yuan, M.-Y.; Zhao, X.; Zheng, L.-L. 1-Chloro-1*H*-1,2,3-benzotriazole. *Acta Cryst. E* **2012**, *68* (12), o3432.
(222) Martinu, T.; Dailey, W. P. Reactivity of 1-Chloro-3-phenyldiazirines. *J. Org. Chem.* **2006**, *71* (13), 5012−5015.
(223) Minkwitz, R.; Garzarek, P.; Neikes, F.; Kornath, A.; Preut, H. Neue N,N-Dichlormethylsulfonammoniumsalze $CH_3S(O)_2NCl_2X^+MF_6^-$ (X = CH_3, Cl, F; M = As, Sb) und Kristallstruktur von $CH_3S(O)_2NCl_2$. *Zeitschrift für anorganische und allgemeine Chemie* **1997**, *623* (1−6), 333−339.
(224) Shtamburg, V. G.; Shishkin, O. V.; Zubatyuk, R. I.; Kravchenko, S. V.; Tsygankov, A. V.; Mazepa, A. V.; Klots, E. A.; Kostyanovsky, R. G. *N*-Chloro-*N*-alkoxyureas: synthesis, structure and properties. *Mendeleev Commun.* **2006**, *16* (6), 323−325.
(225) Whitehead, D. C.; Staples, R. J.; Borhan, B. A simple and expedient method for the preparation of *N*-chlorohydantoins. *Tetrahedron Lett.* **2009**, *50* (6), 656−658.
(226) Belaj, F.; Nachbaur, E.; Faleschini, G.; Janoschek, R. Crystal structure and theoretical investigation of the configurations of 1,3-dichloro-1,3-diazetidine-2,4-dione and 1,3-bis(trimethylsilyl)-1,3-diazetidine-2,4-dione. *Heteroatom Chem.* **1991**, *2* (4), 487−494.
(227) Haasnoot, J. G.; Verschoor, G. C.; Romers, C.; Groeneveld, W. L. On the crystal and molecular structure of hexachloroborazine. *Acta Cryst. B* **1972**, *28* (7), 2070−2073.
(228) Becker, C.; Trapp, P. C.; Neumann, B.; Stammler, H.-G.; Mitzel, N. W. para-Chlorotetrafluorophenyl-boranes − syntheses and structures of a series of mono- and bidentate Lewis acids. *Dalton Trans.* **2022**, *51* (17), 6565−6575.
(229) Davidson, J. J.; DeMott, J. C.; Douvris, C.; Fafard, C. M.; Bhuvanesh, N.; Chen, C.-H.; Herbert, D. E.; Lee, C.-I.; McCulloch, B. J.; Foxman, B. M.; Ozerov, O. V. Comparison of the Electronic Properties of Diarylamido-Based PNZ Pincer Ligands: Redox Activity at the Ligand and Donor Ability Toward the Metal. *Inorg. Chem.* **2015**, *54* (6), 2916−2935.
(230) Yao, H.; Lomme, P.; Hu, C.; Paetzold, P. Haloaza-*closo*-dodecaboranes. *Zeit. Anorg. Allg. Chem.* **2001**, *627* (11), 2477−2480.
(231) Vij, A.; Wilson, W. W.; Haiges, R.; Edwards, K. C.; Dixon, D. A.; Christe, K. O. Fluoro-nitrogen Cations. *Angew. Chem. Int. Edn.* **2022**, *61* (8), No. e202116565.
(232) Szell, P. M. J.; Cavallo, G.; Terraneo, G.; Metrangolo, P.; Gabidullin, B.; Bryce, D. L. Comparing the Halogen Bond to the Hydrogen Bond by Solid-State NMR Spectroscopy: Anion Coordinated Dimers from 2- and 3-Iodoethynylpyridine Salts. *Chem.-Eur. J.* **2018**, *24* (44), 11364−11376.
(233) Wolmershäuser, G.; Krüger, C.; Tsay, Y.-H. $[CS_3N_2Br]^+Br^-$ ein Produkt der Bromierung von S_4N_4 in Schwefelkohlenstoff. *Chem. Ber.* **1982**, *115* (3), 1126−1131.
(234) Lanzi, M.; Dherbassy, Q.; Wencel-Delord, J. Cyclic Diaryl λ^3-Bromanes as Original Aryne Precursors. *Angew. Chem. Int. Edn.* **2021**, *60* (27), 14852−14857.
(235) Reinhard, D. L.; Heinen, F.; Stoesser, J.; Engelage, E.; Huber, S. M. Tuning the Halogen Bonding Strength of Cyclic Diaryliodonium Salts. *Helv. Chim. Acta* **2021**, *104* (2), No. e2000221.
(236) Hirschberg, M. E.; Barthen, P.; Frohn, H.-J.; Bläser, D.; Tobey, B.; Jansen, G. Interaction of the electrophilic bis(pentafluorophenyl)-iodonium cation [(C6F5)2I]+ with the ambident pseudohalogenide anions [SCN]− and [CN]−. *J. Fluorine Chem.* **2014**, *163*, 28−33.
(237) Clegg, W.; Harrington, R. W. CCDC 2206345: Experimental Crystal Structure Determination. *Cambridge Crystallographic Data Centre*. 2022. DOI: 10.5517/ccdc.csd.cc2d1wfs.
(238) Aliyarova, I. S.; Tupikina, E. Y.; Soldatova, N. S.; Ivanov, D. M.; Postnikov, P. S.; Yusubov, M.; Kukushkin, V. Y. Halogen Bonding Involving Gold Nucleophiles in Different Oxidation States. *Inorg. Chem.* **2022**, *61* (39), 15398−15407.
(239) Keil, H.; Sonnenberg, K.; Müller, C.; Herbst-Irmer, R.; Beckers, H.; Riedel, S.; Stalke, D. Insights into the Topology and the Formation of a Genuine ppσ Bond: Experimental and Computed Electron Densities in Monoanionic Trichlorine $[Cl_3]^-$. *Angew. Chem. Int. Edn.* **2021**, *60* (5), 2569−2573.
(240) Lee, S.; Chen, B.; Fredrickson, D. C.; DiSalvo, F. J.; Lobkovsky, E.; Adams, J. A. Crystal Structures of $(Pyrene)_{10}(I_3^-)_4(I_2)_{10}$ and $[1,3,6,8\text{-Tetrakis(methylthio)pyrene}]_3(I_3^-)_3(I_2)_7$: Structural Trends in Fused Aromatic Polyiodides. *Chem. Mater.* **2003**, *15* (7), 1420−1433.
(241) Braga, D.; Cojazzi, G.; Abati, A.; Maini, L.; Polito, M.; Scaccianoce, L.; Grepioni, F. Making and converting organometallic pseudo-polymorphs via non-solution methods. *J. Chem. Soc., Dalton Trans.* **2000**, No. 21, 3969−3975.
(242) Zhang, H.-Y.; Chen, X.-G.; Zhang, Z.-X.; Song, X.-J.; Zhang, T.; Pan, Q.; Zhang, Y.; Xiong, R.-G. Methylphosphonium Tin Bromide: A 3D Perovskite Molecular Ferroelectric Semiconductor. *Adv. Mater.* **2020**, *32* (47), No. 2005213.
(243) Greenacre, V. K.; Levason, W.; Powell, J.; Reid, G.; Smith, D. E. The reactions of MoOCl4 with neutral group 15 and 16 ligands and a re-investigation of some N-donor ligand complexes of $MoOCl_3$. *Polyhedron* **2021**, *204*, No. 115262.
(244) Szafrański, M. Effect of high pressure on the supramolecular structures of guanidinium based ferroelectrics. *CrystEngComm* **2014**, *16* (27), 6250−6256.
(245) Somisara, D. M. U. K.; Bühl, M.; Lebl, T.; Richardson, N. V.; Slawin, A. M. Z.; Woollins, J. D.; Kilian, P. 1,2-Diphosphaacenaphthene 1,2-Dications: Synthetic, Stereochemical and Computational Study of the Stabilising Role of Naphthalene-1,8-diyl Backbone. *Chem.-Eur. J.* **2011**, *17* (9), 2666−2677.
(246) Strasser, C. E.; Gabrielli, W. F.; Esterhuysen, C.; Schuster, O. B.; Nogai, S. D.; Cronje, S.; Raubenheimer, H. G. Preparation of tris(azolyl)phosphine gold(I) complexes: digold(I) coordination and variation in solid state intermolecular interactions. *New J. Chem.* **2008**, *32* (1), 138−150.

(247) Alzamil, N. O.; Al-Enzi, G. M.; Alamri, A. H.; Abdi, I.; BenAli, A. Synthesis, Crystal Structures and Characterization of Two Nonmetal Cation Tetrafluoroborates. *Crystals* **2020**, *10* (9), 812.
(248) Hoyer, S.; Seppelt, K. Phenyliodine(V) fluorides. *J. Fluorine Chem.* **2004**, *125* (6), 989−996.
(249) Alvarez, S. A cartography of the van der Waals territories. *Dalton Trans.* **2013**, *42* (24), 8617−8636.
(250) Burgenmeister, B.; Sonnenberg, K.; Riedel, S.; Krossing, I. From Square-Planar $[ICl_4]-$ to Novel Chloroiodates(III)? A Systematic Experimental and Theoretical Investigation of Their Ionic Liquids. *Chem.-Eur. J.* **2017**, *23* (47), 11312−11322.
(251) El Khalika, S. A.; El Mervat, E.; Dombrowskih, I.; Tebbeb, K.-F. Notizen: Untersuchungen an Polyhalogeniden, XXXIX. $[(H_3O)(18\text{-Krone-}6)]I_7$, eine Struktur-Neubestimmung/Studies on Polyhalides, XXXIX. Structure Refinement of $[(H_3O)(18\text{-crown-}6)]I_7$. *Zeit. Naturforsch. B* **1999**, *54* (1), 136−139.
(252) Mann, L.; Senges, G.; Sonnenberg, K.; Haller, H.; Riedel, S. Polybromide Dianions and Networks Stabilized by Fluorinated Bromo(triaryl)phosphonium Cations. *Eur. J. Inorg. Chem.* **2018**, *2018* (28), 3330−3337.
(253) Schmidt, B.; Sonnenberg, K.; Beckers, H.; Steinhauer, S.; Riedel, S. Synthesis and Characterization of Nonclassical Interhalides Based on Bromine Monochloride. *Angew. Chem. Int. Edn.* **2018**, *57* (29), 9141−9145.
(254) Haller, H.; Ellwanger, M.; Higelin, A.; Riedel, S. Structural Proof for a Higher Polybromide Monoanion: Investigation of [N(C3H7)4][Br9]. *Angew. Chem., Int. Ed.* **2011**, *50* (48), 11528−11532.
(255) Bartashevich, E.; Tsirelson, V. A comparative view on the potential acting on an electron in a molecule and the electrostatic potential through the typical halogen bonds. *J. Comput. Chem.* **2018**, *39* (10), 573−580.
(256) Troian-Gautier, L.; Turlington, M. D.; Wehlin, S. A. M.; Maurer, A. B.; Brady, M. D.; Swords, W. B.; Meyer, G. J. Halide Photoredox Chemistry. *Chem. Rev.* **2019**, *119* (7), 4628−4683.
(257) Sonnenberg, K.; Pröhm, P.; Schwarze, N.; Müller, C.; Beckers, H.; Riedel, S. Investigation of Large Polychloride Anions: $[Cl_{11}]^-$, $[Cl_{12}]^{2-}$, and $[Cl_{13}]^-$. *Angew. Chem., Int. Ed.* **2018**, *57* (29), 9136−9140.
(258) Liebing, P.; Pitts, C. R.; Reimann, M.; Trapp, N.; Rombach, D.; Bornemann, D.; Kaupp, M.; Togni, A. The Supramolecular Structural Chemistry of Pentafluorosulfanyl and Tetrafluorosulfanylene Compounds. *Chem.-Eur. J.* **2021**, *27* (19), 6086−6093.
(259) Cavallo, G.; Murray, J. S.; Politzer, P.; Pilati, T.; Ursini, M.; Resnati, G. Halogen bonding in hypervalent iodine and bromine derivatives: halonium salts. *IUCrJ.* **2017**, *4*, 411−419.
(260) Balthazor, T. M.; Godar, D. E.; Stults, B. R. Synthesis and structure of benziodazoles. *J. Org. Chem.* **1979**, *44* (9), 1447−1449.
(261) Ochiai, M.; Nakano, A.; Yoshimura, A.; Miyamoto, K.; Hayashi, S.; Nakanishi, W. Imido transfer of sulfonylimino-λ^3-bromane makes possible the synthesis of sulfonylimino-λ^3-iodanes. *Chem. Commun.* **2009**, No. 8, 959−961.
(262) Poeira, D. L.; Negrão, A. C. R.; Faustino, H.; Coelho, J. A. S.; Gomes, C. S. B.; Gois, P. M. P.; Marques, M. M. B. Hypervalent Iodine(III) Reagents with Transferable Primary Amines: Structure and Reactivity on the Electrophilic α-Amination of Stabilized Enolates. *Org. Lett.* **2022**, *24* (2), 776−781.
(263) Ammon, H. L.; Bhattacharjee, S. K.; Holden, J. R. Crystallographic studies of high-density organic compounds: 5-fluoro-2,4,6-trinitro-1,3-benzenediamine. *Acta Cryst. B* **1982**, *38* (6), 1851−1854.
(264) Kumar, V. J.; Wu, J.-Z.; Judd, M.; Rousset, E.; Korb, M.; Moggach, S. A.; Cox, N.; Low, P. J. The syntheses, structures and spectroelectrochemical properties of 6-oxo-verdazyl derivatives bearing surface anchoring groups. *J. Mater. Chem. C* **2022**, *10* (5), 1896−1915.
(265) Costa, L. D.; Guieu, S.; Faustino, M. d. A. F.; Tomé, A. C. Straightforward synthesis of thiazolo[5,4-*c*]isoquinolines from dithiooxamide and 2-halobenzaldehydes. *New J. Chem.* **2022**, *46* (8), 3602−3615.
(266) Eskandari, K.; Zariny, H. Halogen bonding: A lump−hole interaction. *Chem. Phys. Lett.* **2010**, *492* (1), 9−13.
(267) Duarte, D. J. R.; Peruchena, N. M.; Alkorta, I. Double Hole−Lump Interaction between Halogen Atoms. *J. Phys. Chem. A* **2015**, *119* (16), 3746−3752.
(268) Willett, R. D.; Awwadi, F.; Butcher, R.; Haddad, S.; Twamley, B. The Aryl Bromine−Halide Ion Synthon and Its Role in the Control of the Crystal Structures of Tetrahalocuprate(II) Ions. *Cryst. Growth & Design* **2003**, *3* (3), 301−311.
(269) Schneider, D.; Schier, A.; Schmidbaur, H. Governing the oxidative addition of iodine to gold(I) complexes by ligand tuning. *Dalton Trans.* **2004**, No. 13, 1995−2005.
(270) Adonin, S. A. Crystal structures of binuxlear chlorobismuthate xomplexes with 3-methylpyridinium and 4-iodipyridinium cations. *J. Struct. Chem.* **2021**, *62* (8), 1257−1262.
(271) Bussing, R.; Ott, I.; Jones, P. G. Crystal structures of the gold NHC complex bis(4-bromo-1,3-diethylimidazol-2-ylidene)gold(I) iodide and its 1:1 adduct with trans-bis(4-bromo-1,3-diethylimidazol-2-ylidene)diiodidogold(III) iodide. *Acta Cryst. E* **2021**, *77* (12), 1249−1252.
(272) Babu, R.; Bhargavi, G.; Rajasekharan, M. V. Polybromides of Transition Metal Chelates − Synthesis, Structure and Spectral Properties. *ChemistrySelect* **2021**, *6* (14), 3487−3499.
(273) Pfrunder, M. C.; Whittaker, J. J.; Parsons, S.; Moubaraki, B.; Murray, K. S.; Moggach, S. A.; Sharma, N.; Micallef, A. S.; Clegg, J. K.; McMurtrie, J. C. Controlling Spin Switching with Anionic Supramolecular Frameworks. *Chem. Mater.* **2020**, *32* (7), 3229−3234.
(274) Taipale, E.; Siepmann, M.; Truong, K.-N.; Rissanen, K. Iodine(I) and Silver(I) Complexes of Benzoimidazole and Pyridylcarbazole Derivatives. *Chem.-Eur. J.* **2021**, *27* (69), 17412−17419.
(275) Alcock, N. W.; Countryman, R. M. Secondary bonding. Part 1. Crystal and molecular structures of $(C_6H_5)_2$ IX (X = Cl, Br, or I). *J. Chem. Soc., Dalton Trans.* **1977**, No. 3, 217−219.
(276) Flörke, U. CCDC 1404492: Experimental Crystal Structure Determination. *Cambridge Crystallographic Data Centre*. 2015. DOI: 10.5517/cc1j4h6c.
(277) Suslonov, V. V.; Soldatova, N. S.; Ivanov, D. M.; Galmés, B.; Frontera, A.; Resnati, G.; Postnikov, P. S.; Kukushkin, V. Y.; Bokach, N. A. Diaryliodonium Tetrachloroplatinates(II): Recognition of a Trifurcated Metal-Involving μ_3-I···(Cl,Cl,Pt) Halogen Bond. *Cryst. Growth & Design* **2021**, *21* (9), 5360−5372.
(278) Marstokk, K.-M.; Stromme, K. O. The crystal structure of the molecular complex formed by acetonitrile and bromine in the mole ratio 2:1. *Acta Cryst. B* **1968**, *24* (5), 713−720.
(279) Ghiassi, K. B.; Bowles, F. L.; Chen, S. Y.; Olmstead, M. M.; Balch, A. L. Incorporation of the Similarly Sized Molecules, Diiodine and Carbon Disulfide, into Cocrystals Formed with the Fullerenes, C_{60} or C_{70}. *Cryst. Growth Des.* **2014**, *14* (10), 5131−5136.
(280) Jalali, M.; Ho, C. C.; Fuller, R. O.; Lucas, N. T.; Ariafard, A.; Bissember, A. C. Photochemical Activation of a Hydroxyquinone-Derived Phenyliodonium Ylide by Visible Light: Synthetic and Mechanistic Investigations. *J. Org. Chem.* **2021**, *86* (2), 1758−1768.
(281) Pomarański, P.; Roszkowski, P.; Maurin, J. K.; Czarnocki, Z. Regio-and atropselective synthesis of selected ortho-phenyl substituted arylpyridine derivatives. *J. Mol. Struct.* **2019**, *1177*, 564−570.
(282) Zhao, W.-W.; Shao, Y.-C.; Wang, A.-N.; Huang, J.-L.; He, C.-Y.; Cui, B.-D.; Wan, N.-W.; Chen, Y.-Z.; Han, W.-Y. Diazotrifluoroethyl Radical: A CF_3-Containing Building Block in [3 + 2] Cycloaddition. *Org. Lett.* **2021**, *23* (23), 9256−9261.
(283) Mix, A.; Lamm, J.-H.; Schwabedissen, J.; Gebel, E.; Stammler, H.-G.; Mitzel, N. W. Monitoring dynamic pre-crystallization aggregation processes in solution by VT-DOSY-NMR spectroscopy. *Chem. Commun.* **2022**, *58* (21), 3465−3468.
(284) Knop, O.; Cameron, T. S.; Bakshi, P. K.; Linden, A.; Roe, S. P. Crystal chemistry of tetraradial species. Part 5. Interaction between cation lone pairs and phenyl groups in tetraphenylborates: crystal structures of Me_3S^+,Et_3S_+,Me_3SO^+,Ph_2I_+, and 1-azoniapropellane tetraphenylborates. *Can. J. Chem.* **1994**, *72* (8), 1870−1881.

(285) Robidas, R.; Guérin, V.; Provençal, L.; Echeverria, M.; Legault, C. Y. Investigation of Iodonium Trifluoroborate Zwitterions as Bifunctional Arene Reagents. *Org. Lett.* **2017**, *19* (23), 6420−6423.
(286) Álvarez-Boo, P.; Casas, J. S.; Couce, M. D.; Fernández-Moreira, V.; Freijanes, E.; García-Martínez, E.; Sordo, J.; Vázquez-López, E. Formation of 3-Sulfanylcoumarins by SnPh3OH-Promoted Cyclization of 3-Aryl-2-Sulfanylpropenoic Acids. *Eur. J. Inorg. Chem.* **2005**, *2005* (21), 4425−4429.
(287) Jones, B. J.; Scopelliti, R.; Tomas, A.; Bloom, S. R.; Hodson, D. J.; Broichhagen, J. Potent Prearranged Positive Allosteric Modulators of the Glucagon-like Peptide-1 Receptor. *ChemistryOpen* **2017**, *6* (4), 501−505.
(288) Hübscher, J.; Seichter, W.; Weber, E. Intermolecular contacts in the crystal structures of specifically varied halogen and protonic group substituted azines. *CrystEngComm* **2017**, *19* (22), 3026−3036.
(289) Graening, T.; Bette, V.; Neudörfl, J.; Lex, J.; Schmalz, H.-G. Total Synthesis of (−)-Colchicine via a Rh-Triggered Cycloaddition Cascade. *Org. Lett.* **2005**, *7* (20), 4317−4320.
(290) Mamane, V.; Peluso, P.; Aubert, E.; Weiss, R.; Wenger, E.; Cossu, S.; Pale, P. Disubstituted Ferrocenyl Iodo- and Chalcogenoalkynes as Chiral Halogen and Chalcogen Bond Donors. *Organometallics* **2020**, *39* (21), 3936−3950.
(291) Demangeat, C.; Tang, Y.; Cielo, J. Z.; Dou, Y.; Kim, E.; Lee, H.-J.; D'Aléo, A.; Hu, B.; Attias, A. J. Necessary and sufficient condition for organic room-temperature phosphorescence from host-guest doped crystalline systems. *Adv. Opt. Mater.* **2023**, *11* (10), 2300289.
(292) Keith, T. A. *AIMAll*ver. 19.10.12; TK Gristmill Software: Overland Park, KS, 2019. http://aim.tkgristmill.com.
(293) Lu, T.; Chen, F. Multiwfn: A multifunctional wavefunction analyzer. *J. Comput. Chem.* **2012**, *33* (5), 580−592.
(294) Lu, T.; Chen, F. Quantitative analysis of molecular surface based on improved Marching Tetrahedra algorithm. *J. Mol. Graphics Model.* **2012**, *38*, 314−323.
(295) Frisch, M. J.; Trucks, G. W.; Schlegel, H. B.; Scuseria, G. E.; Robb, M. A.; Cheeseman, J. R.; Scalmani, G.; Barone, V.; Petersson, G. A.; Nakatsuji, H.; Li, X.; Caricato, M.; Marenich, A. V.; Bloino, J.; Janesko, B. G.; Gomperts, R.; Mennucci, B.; Hratchian, H. P.; Ortiz, J. V.; Izmaylov, A. F.; Sonnenberg, J. L.; Williams-Young, D.; Ding, F.; Lipparini, F.; Egidi, F.; Goings, J.; Peng, B.; Petrone, A.; Henderson, T.; Ranasinghe, D.; Zakrzewski, V. G.; Gao, J.; Rega, N.; Zheng, G.; Liang, W.; Hada, M.; Ehara, M.; Toyota, K.; Fukuda, R.; Hasegawa, J.; Ishida, M.; Nakajima, T.; Honda, Y.; Kitao, O.; Nakai, H.; Vreven, T.; Throssell, K.; Montgomery, J. A., Jr.; Peralta, J. E.; Ogliaro, F.; Bearpark, M. J.; Heyd, J. J.; Brothers, E. N.; Kudin, K. N.; Staroverov, V. N.; Keith, T. A.; Kobayashi, R.; Normand, J.; Raghavachari, K.; Rendell, A. P.; Burant, J. C.; Iyengar, S. S.; Tomasi, J.; Cossi, M.; Millam, J. M.; Klene, M.; Adamo, C.; Cammi, R.; Ochterski, J. W.; Martin, R. L.; Morokuma, K.; Farkas, O.; Foresman, J. B.; Fox, D. J. *Gaussian 16*, rev. C.01; Gaussian, Inc.: Wallingford, CT, 2016.
(296) Frisch, M. J.; Head-Gordon, M.; Pople, J. A. A direct MP2 gradient method. *Chem. Phys. Lett.* **1990**, *166* (3), 275−280.
(297) Head-Gordon, M.; Head-Gordon, T. Analytic MP2 frequencies without fifth-order storage. Theory and application to bifurcated hydrogen bonds in the water hexamer. *Chem. Phys. Lett.* **1994**, *220* (1), 122−128.
(298) Varadwaj, A.; Varadwaj, P. R.; Yamashita, K. Do surfaces of positive electrostatic potential on different halogen derivatives in molecules attract? like attracting like! *J. Comput. Chem.* **2018**, *39* (7), 343−350.
(299) Cremer, D.; Kraka, E. A Description of the Chemical Bond in Terms of Local Properties of Electron Density and Energy. *Croat. Chem. Acta* **1984**, *57* (6), 1259−1281.
(300) Shukla, R.; Chopra, D. Characterization of N—O non-covalent interactions involving σ-holes: "electrostatics" or "dispersion. *Phys. Chem. Chem. Phys.* **2016**, *18*, 29946−29954.
(301) Minkin, V. I. Glossary of terms used in theoretical organic chemistry. *Pure Appl. Chem.* **1999**, *71* (10), 1919−1981.
(302) Bartashevich, E. V.; Matveychuk, Y. V.; Mukhitdinova, S. E.; Sobalev, S. A.; Khrenova, M. G.; Tsirelson, V. G. The common trends for the halogen, chalcogen, and pnictogen bonds via sorting principles and local bonding properties. *Theor. Chem. Acc.* **2020**, *139*, 26.
(303) Thomas, S. P.; Dikundwar, A. G.; Sarkar, S.; Pavan, M. S.; Pal, R.; Hathwar, V. R.; Row, T. N. G. The Relevance of Experimental Charge Density Analysis in Unraveling Noncovalent Interactions in Molecular Crystals. *Molecules* **2022**, *27* (12), 3690.
(304) Sarkar, S.; Pavan, M. S.; Guru Row, T. N. Experimental validation of 'pnicogen bonding' in nitrogen by charge density analysis. *Phys. Chem. Chem. Phys.* **2015**, *17* (4), 2330−2334.
(305) Gibbs, G. V.; Tamada, O.; Boisen, M. B.; Hill, F. C. Laplacian and bond critical point properties of the electron density distributions of sulfide bonds: A comparison with oxide bonds. *Am. Mineral.* **1999**, *84* (3), 435−446.
(306) Parrish, R. M.; Hohenstein, E. G.; Sherrill, C. D. Tractability gains in symmetry-adapted perturbation theory including coupled double excitations: CCD+ST(CCD) dispersion with natural orbital truncations. *J. Chem. Phys.* **2013**, *139* (17), No. 174102.
(307) Parker, T. M.; Burns, L. A.; Parrish, R. M.; Ryno, A. G.; Sherrill, C. D. Levels of symmetry adapted perturbation theory (SAPT). I. Efficiency and performance for interaction energies. *J. Chem. Phys.* **2014**, *140*, No. 094106.
(308) Lao, K. U.; Schäffer, R.; Jansen, G.; Herbert, J. M. Accurate Description of Intermolecular Interactions Involving Ions Using Symmetry-Adapted Perturbation Theory. *J. Chem. Theory Comp.* **2015**, *11* (6), 2473−2486.
(309) Smith, D. G. A.; Burns, L. A.; Simmonett, A. C.; Parrish, R. M.; Schieber, M. C.; Galvelis, R.; Kraus, P.; Kruse, H.; Di Remigio, R.; Alenaizan, A.; James, A. M.; Lehtola, S.; Misiewicz, J. P.; Scheurer, M.; Shaw, R. A.; Schriber, J. B.; Xie, Y.; Glick, Z. L.; Sirianni, D. A.; O'Brien, J. S.; Waldrop, J. M.; Kumar, A.; Hohenstein, E. G.; Pritchard, B. P.; Brooks, B. R.; Schaefer, H. F., III; Sokolov, A. Y.; Patkowski, K.; DePrince, A. E., III; Bozkaya, U.; King, R. A.; Evangelista, F. A.; Turney, J. M.; Crawford, T. D.; Sherrill, C. D. PSI4 1.4: Open-source software for high-throughput quantum chemistry. *J. Chem. Phys.* **2020**, *152* (18), No. 184108.
(310) Boys, S. F.; Bernardi, F. The calculation of small molecular interactions by the differences of separate total energies. Some procedures with reduced errors. *Mol. Phys.* **1970**, *19* (4), 553−566.
(311) Metrangolo, P.; Murray, J. S.; Pilati, T.; Politzer, P.; Resnati, G.; Terraneo, G. The fluorine atom as a halogen bond donor, viz. a positive site. *CrystEngComm* **2011**, *13*, 6593−6596.
(312) Metrangolo, P.; Murray, J. S.; Pilati, T.; Politzer, P.; Resnati, G.; Terraneo, G. Fluorine-centered halogen bonding: A factor in recognition phenomena and reactivity. *Cryst. Growth Des.* **2011**, *11*, 4238−4246.
(313) Scheiner, S. F-Halogen Bond: Conditions for Its Existence. *J. Phys. Chem. A* **2020**, *124* (36), 7290−7299.
(314) Politzer, P.; Murray, J. S. σ-holes and π-holes: Similarities and differences. *J. Comput. Chem.* **2018**, *39* (9), 464−471.
(315) Ivlev, S. I.; Buchner, M. R.; Karttunen, A. J.; Kraus, F. Synthesis and characterization of the pyridine—bromine trifluoride (1/1) complex, [py•BrF3]. *J. Fluorine Chem.* **2018**, *215*, 17−24.
(316) Richardson, R. D.; Zayed, J. M.; Altermann, S.; Smith, D.; Wirth, T. Tetrafluoro-IBA and-IBX: Hypervalent Iodine Reagents. *Angew. Chem., Int. Ed.* **2007**, *46* (34), 6529−6532.
(317) Eskandari, K.; Lesani, M. Does fluorine participate in halogen bonding? *Chem.-Eur. J.* **2015**, *21*, 4739−4746.
(318) Schmid, J. R.; Pröhm, P.; Voßnacker, P.; Thiele, G.; Ellwanger, M.; Steinhauer, S.; Riedel, S. Soluble Fluoridobromates as Well-Behaved Strong Fluorination Reagents. *Eur. J. Inorg. Chem.* **2020**, *2020* (47), 4497−4500.
(319) Shaw, A. J. M.; Corbo, R.; Wilson, D. J. D.; Dutton, J. L. A 2,2′-bipyridine coordination complex of [ICl2]+. *Dalton Trans.* **2015**, *44* (34), 15083−15087.
(320) Miyamoto, K.; Saito, M.; Tsuji, S.; Takagi, T.; Shiro, M.; Uchiyama, M.; Ochiai, M. Benchtop-Stable Hypervalent Bromine(III) Compounds: Versatile Strategy and Platform for Air- and Moisture-Stable λ^3-Bromanes. *J. Am. Chem. Soc.* **2021**, *143* (25), 9327−9331.

(321) Minkwitz, R.; Hertel, T.; Preut, H. Reaktion von Chlornitrat mit CF_3I: Isolierung von Trifluormethylchloriodnitrat $CF_3I(Cl)ONO_2$ und Kristallstruktur von Trifluormethylioddinitrat $CF_3I(ONO_2)_2$. *Z. Anorg. Allg. Chem.* **1995**, *621* (9), 1552−1557.
(322) Bailly, F.; Barthen, P.; Breuer, W.; Frohn, H.-J.; Giesen, M.; Helber, J.; Henkel, G.; Priwitzer, A. Pentafluorphenylioddifluorid: alternative Darstellungsmethoden, Molekülstruktur und Eigenschaften. *Z. Anorg. Allg. Chem.* **2000**, *626* (6), 1406−1413.
(323) Thornberry, M. P.; Slebodnick, C.; Deck, P. A.; Fronczek, F. R. Structural and Electronic Effects of Pentafluorophenyl Substituents on Cyclopentadienyl Complexes of Fe, Co, Mn, and Re1. *Organometallics* **2000**, *19* (25), 5352−5369.
(324) Widner, D. L.; Knauf, Q. R.; Merucci, M. T.; Fritz, T. R.; Sauer, J. S.; Speetzen, E. D.; Bosch, E.; Bowling, N. P. Intramolecular Halogen Bonding Supported by an Aryldiyne Linker. *J. Org. Chem.* **2014**, *79* (13), 6269−6278.
(325) Togo, H.; Taguchi, R.; Yamaguchi, K.; Yokoyama, M. Reactivity of [bis(1-adamantylcarbonyloxy)iodo]arenes in substitution and addition reactions. *J. Chem. Soc., Perkin Trans. 1* **1995**, No. 17, 2135−2139.
(326) Schröckeneder, A.; Stichnoth, D.; Mayer, P.; Trauner, D. The crystal structure of the Dess−Martin periodinane. *Beilstein J. Org. Chem.* **2012**, *8*, 1523−1527.
(327) Huang, J.; Guo, F.; Guo, Z.; Chen, J.; Dai, B.; Yu, F. $NH_4IO_2F_2$ and $(NH_4)_3(IO_2F_2)_3{\cdot}H_2O$: A Series of Ammonium-Containing Fluoroiodates with Wide Band Gaps. *Inorg. Chem.* **2022**, *61* (30), 11803−11810.
(328) Seppelt, K. CCDC 1953176: Experimental Crystal Structure Determination. *Cambridge Crystallographic Data Centre*. 2019. DOI: 10.5517/ccdc.csd.cc23kfpt.
(329) Gerken, M.; Hazendonk, P.; Iuga, A.; Mack, J. P.; Mercier, H. P. A.; Schrobilgen, G. J. The solid-state $_{19}F$ NMR spectrum of $[N(CH_3)_4][IO_2F_2]$, a vibrational study of $[N(CH_3)_4][IO_3]$ and $[N(CH_3)_4][IO_3]{\cdot}2H_2O$, and the X-ray crystal structures of $[N(CH_3)_4][IO_2F_2]$ and $[N(CH_3)_4][IO_3]$. *J. Fluorine Chem.* **2006**, *127* (10), 1328−1338.
(330) Aliyarova, I. S.; Ivanov, D. M.; Soldatova, N. S.; Novikov, A. S.; Postnikov, P. S.; Yusubov, M. S.; Kukushkin, V. Y. Bifurcated Halogen Bonding Involving Diaryliodonium Cations as Iodine(III)-Based Double-σ-Hole Donors. *Cryst. Growth Des.* **2021**, *21* (2), 1136−1147.
(331) Bykowski, D.; McDonald, R.; Tykwinski, R. R. *ARKIVOC* **2003**, *2003*, 21−26.
(332) Ochiai, M.; Miyamoto, K.; Suefuji, T.; Shiro, M.; Sakamoto, S.; Yamaguchi, K. Synthesis and structure of supramolecular complexes between 1-alkynyl(phenyl)(tetrafluoroborato)-λ^3-iodanes and 18-crown-6. *Tetrahedron* **2003**, *59* (51), 10153−10158.
(333) Hassel, O. Structural Aspects of Interatomic Charge-Transfer Bonding. *NobelPrize.org*, 1969. https://www.nobelprize.org/prizes/chemistry/1969/hassel/lecture/ (accessed 2021-10-04).
(334) Zhang, Y.; Ma, N.; Wang, W. A new class of halogen bonds that avoids the σ-hole. *Chem. Phys. Lett.* **2012**, *532*, 27−30.
(335) Franchini, D.; Forni, A.; Genoni, A.; Pieraccini, S.; Gandini, E.; Sironi, M. The Origin of the σ-Hole in Halogen Atoms: a Valence Bond Perspective. *ChemistryOpen* **2020**, *9* (4), 445−450.

https://doi.org/10.1021/acs.cgd.4c00228
Cryst. Growth Des. 2024, 24, 5494−5525